

PROCESS IMPROVEMENTS IN BIOLOGICAL NUTRIENT REMOVAL
SYSTEMS FOR BETTER WASTEWATER TREATMENT
PERFORMANCE

A Dissertation

presented to

the Faculty of the Graduate School

at the University of Missouri-Columbia

In Partial Fulfillment

of the Requirements for the Degree

Doctor of Philosophy

by

SHENGNAN XU

Dr. Zhiqiang Hu, Dissertation Supervisor

JULY 2014

The undersigned, appointed by the dean of the Graduate School, have examined the dissertation entitled

**PROCESS IMPROVEMENTS IN BIOLOGICAL NUTRIENT REMOVAL
SYSTEMS FOR BETTER WASTEWATER TREATMENT
PERFORMANCE**

presented by Shengnan Xu,

a candidate for the degree of doctor of philosophy,

and hereby certify that, in their opinion, it is worthy of acceptance.

Professor Zhiqiang Hu

Professor Thomas Clevenger

Professor Matthew Bernards

Professor Allen Thompson

Professor Enos Inniss

ACKNOWLEDGMENTS

This dissertation would not have been possible without the guidance and the help of my advisor, all the committee members, my friends and my parents who contributed their valuable assistance throughout my PhD study.

First and foremost, I would like to express my deep appreciation and gratitude to my advisor, Dr. Zhiqiang Hu, for the continuous support of my PhD study and research, all the way from when I was first considering applying to the PhD program through to the completion of this thesis. I could not have imagined completing PhD research work without his patience, motivation and immense knowledge. I am truly fortunate to have had the opportunity to work with him.

Besides my advisor, I would like to thank the rest of my dissertation committee members, Dr. Thomas Clevenger, Dr. Matthew Bernards, Dr. Allen Thompson and Dr. Enos Inniss. I deeply appreciate their encouragement, insightful comments and thought-provoking suggestions.

I would like to thank all the group members, Dr. Yanyan Zhang, Dr. Yu Yang, Dr. Zihua Liang, Dr. Liang Zhu, Dr. Donglei Wu, for their presence every time when I need help for my PhD study and research. I would like to thank Dr. Shashikanth Gajaraj, Dr. Guangzhi Wang, Dr. Jiangzhong Zheng, and Dr. Atryee Sims for their helpful cooperation and discussion in the lab. Also I thank Minghao Sun, Qi Shen, Meng Xu, Qian Chen, Chiqian Zhang, Jialiang Guo, Tianyu Tang, Kevin Stark, and everybody for all the assistance and friendship I received from them. I am so grateful that all the people in our group are very nice and friendly to me and will remember all the fun and tears we had together.

I would also like to thank our department staff for their help. Last but not the least, my deep gratitude goes to my parents, my wonderful mother and father, for their innumerable sacrifices and unconditional support while I pursue the final degree.

TABLE OF CONTENTS

ACKNOWLEDGMENTS.....	II
TABLE OF CONTENTS.....	IV
LIST OF TABLES	IX
LIST OF FIGURES	X
ABSTRACT	XVII
1. INTRODUCTION.....	1
1.1. ANAEROBIC/ANOXIC/OXIC (A ² /O) AND REVERSE A ² /O PROCESSES IN BIOLOGICAL NUTRIENT REMOVAL.....	1
1.2. NZVI: ENVIRONMENTAL APPLICATIONS AND IMPLICATIONS	5
1.3. FILAMENTOUS SLUDGE BULKING CONTROL AND NZVI TOXICITY	9
1.4. TOXICITY AND BIODEGRADATION OF MELAMINE	13
1.5. ROLE OF SLUDGE ACCLIMATION AND HIGH SLUDGE CONCENTRATION OPERATION IN MBR SYSTEMS	15
1.6. HYPOTHESES AND RESEARCH OVERVIEW	17
2. EVALUATION OF ANAEROBIC/ANOXIC/OXIC (A²/O) AND REVERSE A²/O PROCESSES IN BIOLOGICAL NUTRIENT REMOVAL	19
2.1. OBJECTIVES	20
2.2. MATERIALS AND METHODS	20
2.2.1. <i>Bioreactor Setup and Operation.....</i>	<i>20</i>
2.2.2. <i>Sludge Phosphorus Content and P Release/Uptake Kinetics</i>	<i>22</i>
2.2.3. <i>Fluorescent Microscopy Analysis of Activated Sludge Including PAOs</i>	<i>23</i>

2.2.4.	<i>Bacterial Activity Measurement</i>	24
2.2.5.	<i>Analysis of Nitrifying Communities in the A²/O and Reverse A²/O Systems</i>	25
2.2.6.	<i>Chemical and Statistical Analysis</i>	27
2.3.	RESULTS AND DISCUSSION.....	27
2.3.1.	<i>BNR Performance</i>	27
2.3.2.	<i>Sludge P Content, PAO Distribution, and P Release/Uptake Kinetics</i>	38
2.3.3.	<i>Microbial Activities and Sludge Settling Characteristics</i>	43
2.3.4.	<i>Nitrifying Bacteria Community Structure</i>	44
2.3.5.	<i>Implications in Process Design and Control</i>	45
2.4.	CONCLUSIONS.....	48
3.	KINETICS OF NUTRIENT REMOVAL BY NANO ZERO-VALENT IRON UNDER DIFFERENT BIOCHEMICAL ENVIRONMENTS	50
3.1.	OBJECTIVES	51
3.2.	MATERIALS AND METHODS	51
3.2.1.	<i>NZVI Synthesis and Characterization</i>	51
3.2.2.	<i>Batch Systems</i>	52
3.2.3.	<i>Nitrate Reduction Kinetics</i>	54
3.2.4.	<i>Phosphorus Removal under Different Biochemical Environments</i>	55
3.2.5.	<i>Physical, Chemical and Statistical Analysis</i>	55
3.3.	RESULTS AND DISCUSSION.....	58
3.3.1.	<i>Nitrate Reduction to Ammonia by NZVI in Abiotic and Biotic Systems</i>	58
3.3.2.	<i>Phosphorus Removal by NZVI under Different Biochemical Conditions</i>	64

3.3.3.	<i>Applications and Implications of NZVI in Wastewater Treatment</i>	73
3.4.	CONCLUSIONS.....	74
4.	FILAMENTOUS SLUDGE BULKING CONTROL BY NANO ZERO-VALENT IRON IN ACTIVATED SLUDGE TREATMENT SYSTEMS.....	76
4.1.	OBJECTIVES	77
4.2.	MATERIALS AND METHODS	77
4.2.1.	<i>Nano Zero-Valent Iron Synthesis</i>	77
4.2.2.	<i>Bioreactor Set-Up and Operation</i>	77
4.2.3.	<i>Filamentous Bacterial DNA and Polymerase Chain Reaction Analysis</i>	79
4.2.4.	<i>Effect of NZVI Dosing on Nitrifying Bacterial Population and Nitrifying Activity</i>	86
4.2.5.	<i>Microtiter Assay and NZVI Dose Choice</i>	86
4.2.6.	<i>Microscopic, Chemical and Statistical Analysis</i>	88
4.3.	RESULTS AND DISCUSSION.....	89
4.3.1.	<i>Sludge Bulking Associated with Long SRT Operation and Bioreactor Performance</i>	89
4.3.2.	<i>Effectiveness of NZVI in Killing Filamentous Bacteria</i>	99
4.3.3.	<i>Impact of Sludge Bulking and NZVI Dosing on Nitrifying Bacterial Population and Activity</i>	105
4.3.4.	<i>Bioreactor Performance Recovery and Other Benefits Associated with NZVI Dosing</i>	110
4.4.	CONCLUSIONS.....	113
5.	FATE AND TOXICITY OF MELAMINE IN ACTIVATED SLUDGE TREATMENT SYSTEMS AFTER A LONG-TERM SLUDGE ADAPTATION	114
5.1.	OBJECTIVES	115
5.2.	MATERIALS AND METHODS	116

5.2.1.	<i>Bioreactor Setup and Operation</i>	116
5.2.2.	<i>Effect of Long-term Melamine Dosing on Bioreactor Performance</i>	117
5.2.3.	<i>Batch Melamine Degradation and Adsorption Study</i>	118
5.2.4.	<i>Melamine Toxicity Inferred from the Microtiter Assay</i>	119
5.2.5.	<i>Effect of Melamine on Nitrifying Community Structure and Population</i>	120
5.2.6.	<i>Chemical and Statistical Analysis</i>	121
5.3.	RESULTS AND DISCUSSION	121
5.3.1.	<i>Biodegradation of Melamine by Activated Sludge</i>	121
5.3.2.	<i>Bioreactor Performance before and after Melamine Exposure</i>	124
5.3.3.	<i>Toxicity of Melamine to Activated Sludge</i>	129
5.3.4.	<i>Bacteria Community Structure Changes after Continuous Melamine Dosing</i>	131
5.3.5.	<i>Implications of Melamine Biodegradation and Its Toxicity to Activated Sludge</i>	133
5.4.	CONCLUSIONS	137
6.	BIODEGRADATION OF MELAMINE IN A MEMBRANE BIOREACTOR WITH HIGH BIOMASS CONCENTRATION	139
6.1.	OBJECTIVES	140
6.2.	MATERIALS AND METHODS	141
6.2.1.	<i>MBR Setup and Operation</i>	141
6.2.2.	<i>Effect of Long-Term Melamine Dosing on Bioreactor Performance</i>	144
6.2.3.	<i>Batch Melamine Adsorption and Degradation Study</i>	144
6.2.4.	<i>Effect of Melamine on Nitrifying Community Structure and Microbial Activities</i>	146
6.2.5.	<i>Chemical and Statistical Analysis</i>	147

6.3.	RESULTS AND DISCUSSION.....	147
6.3.1.	<i>Biodegradation of Melamine in the MBR System.....</i>	<i>147</i>
6.3.2.	<i>Bioreactor Performance before and after Melamine Exposure</i>	<i>155</i>
6.3.3.	<i>Bacterial Activities before and after Melamine Dosing</i>	<i>160</i>
6.3.4.	<i>Bacterial Community Structure Changes after Melamine Dosing</i>	<i>162</i>
6.3.5.	<i>Implications of Melamine Biodegradation in MBR Operated at High Biomass Concentrations</i>	<i>163</i>
6.4.	CONCLUSIONS.....	165
7.	SUMMARY AND FUTURE RESEARCH DIRECTIONS	166
	APPENDIX	169
	BIBLIOGRAPHY	170
	VITA	188

LIST OF TABLES

Table 1. Primer used for specific AOB and NOB 16s rRNA gene amplification	26
Table 2. Composition of medium used in batch studies	53
Table 3. Primer used for filamentous bacteria detection	81
Table 4. Primer and DNA Concentrations used in q-PCR.....	83
Table 5. One-way ANOVA analysis of the effluent water quality in the MLE and CSTR systems before (phase I) and after melamine dosing (phase II).	129

LIST OF FIGURES

Figure 1. A schematic of the two biological nutrient removal processes: (A) A ² /O and (B) reverse A ² /O.....	3
Figure 2. Melamine Degradation Pathway	15
Figure 3. Influent (□) and effluent COD concentrations in the A ² /O (○) and reverse A ² /O (●) systems. The error bars represent the data range of duplicate samples.	28
Figure 4. Effluent NH ₄ ⁺ -N (A), NO ₂ ⁻ -N (B) and NO ₃ ⁻ -N (C) concentrations in the A ² /O (○) and reverse A ² /O (●) systems. The error bars represent the data range of duplicate samples.....	31
Figure 5. Influent (□) and effluent TN concentrations in the A ² /O (○) and reverse A ² /O (●) systems. The error bars represent the data range of duplicate samples.	32
Figure 6. Influent (□) and effluent TP concentrations in the A ² /O (○) and reverse A ² /O (●) systems. The error bars represent the data range of duplicate samples.	34
Figure 7. Influent (□) and effluent PO ₄ ³⁻ -P concentrations in the A ² /O (○) and reverse A ² /O (●) systems. The error bars represent the data range of duplicate samples.	35
Figure 8. The NO ₃ ⁻ -N concentration distribution (a) and the sludge P content (b) in different chambers of the A ² /O (□) and reverse A ² /O (■) systems. The error bars represent one standard error of the mean (n = 6).....	37
Figure 9. Light and fluorescent microscopy micrographs of the sludge taken from the A ² /O, reverse A ² /O, and control systems. The control was taken from a conventional activated sludge plant.....	40

Figure 10. P release from the sludge taken from the A²/O (○) and reverse A²/O (●) systems under anaerobic conditions, and P uptake by the sludge from the A²/O (Δ) and reverse A²/O (▲) systems under aerobic conditions. The error bars represent one standard error of the mean (n = 6). 42

Figure 11. Biomass concentrations of the A²/O (○) and reverse A²/O (●) systems. The error bars represent the data range of duplicate samples..... 44

Figure 12. Nitrifying bacterial community composition reflected by T-RFLP profiles targeting 16S rRNA genes of *Nitrosomonas* (A and B, 161 bp) and *Nitrospira* (C and D, 261 and 271 bp) in the A²/O (A and C) and reverse A²/O (B and D) systems. DNA samples were taken after 3 months of stable operation. 45

Figure 13. Nitrate removal in abiotic (▲ for NZVI and Δ for ZVI powder), biotic (● for NZVI and ○ for ZVI powder) and ZVI-free biological (◆) system. Error bars represent one standard deviation from the mean of triplicate samples..... 61

Figure 14. Ammonia generated in abiotic (▲ for NZVI and Δ for ZVI powder), biotic (● for NZVI and ○ for ZVI powder) and ZVI-free biological (◆) system. Error bars represent one standard deviation from the mean of triplicate samples..... 62

Figure 15. Observed nitrate removal by NZVI in abiotic (▲) and biotic (●) system and ZVI-free biological (◆) system. 63

Figure 16. Observed ammonia generation by NZVI in abiotic (▲) and biotic (●) system. 64

Figure 17. Abiotic phosphorus removal by dosing NZVI under anaerobic (◆), anoxic (○) and aerobic (Δ) conditions. Error bars represent one standard deviation from the mean of triplicate samples. 66

Figure 18. Observed abiotic phosphorus removal rate by dosing NZVI under anaerobic (◆), anoxic (○) and aerobic (Δ) conditions. Error bars represent one standard deviation from the mean of triplicate samples..... 67

Figure 19. pH in abiotic (□) and biotic (■) systems at 150 min of the batch studies. Error bars represent one standard deviation from the mean of triplicate samples. 68

Figure 20. Phosphorus removal by dosing NZVI under anaerobic (◆ and ◇), anoxic (● and ○) and aerobic (▲ and Δ) conditions. The markers with fill represent WWTP mixed liquor suspended solids (MLSS) sample and the ones without fill represent the sludge from a lab-scale EBPR process. Error bars represent one standard deviation from the mean of triplicate samples. 69

Figure 21. Observed biotic phosphorus removal rate by dosing NZVI under anaerobic ◆ and ◇), anoxic (● and ○) and aerobic (▲ and Δ) conditions. The markers with fill represent WWTP mixed liquor suspended solids (MLSS) sample and the ones without fill represent lab-scale RAAO process MLSS. Error bars represent one standard deviation from the mean of triplicate samples. 70

Figure 22. Particle size in abiotic (□) and biotic (■) systems at 150 min of the batch studies. Error bars represent one standard deviation from the mean of triplicate samples. 71

Figure 23. Zeta potential in abiotic (□) and biotic (■) systems at 150 min of the batch studies. Error bars represent one standard deviation from the mean of triplicate samples. 72

Figure 24. qPCR standard curves for Type 021N and total bacteria in the presence (◆) and absence (▲) of EDTA and MgCl₂ in PCR reactions. Error bars represent one standard deviation from the mean of triplicate samples. 85

Figure 25. Aerobic bacterial growth, as indicated by optical density measurements at 600 nm, in the groups treated with different NZVI concentrations: Control (◆), 20 mg/L (■), 100 mg/L (▲) and 200 mg/L (×). Activated sludge from the Columbia WWTP was used as a seed culture. The error bars represent one standard error of the mean (n = 8). 88

Figure 26. SVI values in Tank #1 before (○) and after (●) NZVI dosing on day 89 and SVI values in Tank #2 before (◇) and after (◆) after NZVI dosing on day 104. Two vertical hashed lines show the days of NZVI addition in Tanks #1 and #2, respectively. 91

Figure 27. Micrographs of light microscopy of activated sludge samples from Tank #1 (left panel) and Tank #2 (right panel) taken on day 80 and 100, respectively. 92

- Figure 28. Biomass concentrations in Tank #1 (○) and Tank #2 (◇) before NZVI dosing and in Tank #1 (●) and Tank #2 (◆) after NZVI dosing on day 89 and day 104, respectively. Two vertical hashed lines show the days of NZVI addition in Tanks #1 and #2, respectively. The SRT was increased from 10 to 20 day from day 61 onwards. Error bars represent the range of duplicate samples..... 93
- Figure 29. Effluent COD concentrations in Tank #1 (○) and Tank #2 (◇) before NZVI dosing and in Tank #1 (●) and Tank #2 (◆) after NZVI dosing on day 89 and day 104, respectively. Two vertical hashed lines show the days of NZVI addition in Tanks #1 and #2, respectively. Error bars represent the range of duplicate samples..... 95
- Figure 30. Effluent $\text{NH}_4^+\text{-N}$ (a), $\text{NO}_2^-\text{-N}$ (b) and $\text{NO}_3^-\text{-N}$ (c) concentrations in Tank #1 (○) and Tank #2 (◇) before NZVI dosing and in Tank #1 (●) and Tank #2 (◆) after NZVI dosing on day 89 and day 104, respectively. Error bars represent the range of duplicate samples..... 98
- Figure 31. Type 021N (A) and total bacterial population (B) dynamics in Tank #1 and Tank #2 . A single dose of NZVI at the final concentration of 100 mg Fe/L in the mixed liquor was applied on day 89 and day 104 in Tank #1 and Tank #2, respectively. Two vertical hashed lines show the days of NZVI addition in Tanks #1 and #2, respectively. Error bars represent one standard deviation from the mean of at least triplicate samples. 100
- Figure 32. Micrographs of light microscopy of activated sludge samples from Tank #1 (left panel) and Tank #2 (right panel) taken 1 h after NZVI dosing in the MLE systems with agglomerated NZVI structure shown in black..... 103
- Figure 33. The viability of bulking activated sludge before NZVI treatment. Under fluorescence microscopy, living cells were stained green and dead cells were stained red. 103
- Figure 34. The viability of activated sludge from Tank #1 (with sludge bulking and significant sludge loss already, left) and Tank #2 (with the early stages of bulking, right) after the NZVI treatment on day 90 and 105, respectively. Under fluorescence microscopy, living cells were stained green and dead cells were stained red..... 104

- Figure 35. Conventional PCR analysis of the sludge samples targeting genomic DNA (829 bp) of *Gordonia* spp. Lane 1, molecular mass marker (100 bp plus DNA ladder); Lane 2, DNA template from Tank #1 before NZVI dosing; Lane 3, DNA template from Tank #1 one day after NZVI dosing; Lane 4, DNA template from Tank #2 before NZVI dosing; Lane 5, DNA template from Tank #2 one day after NZVI dosing; Lane 6, negative control (no DNA template)..... 105
- Figure 36. Nitrifying bacterial community composition reflected by T-RFLP profiles targeting 16S rRNA genes of *Nitrosomonas* (a) and *Nitrospira* (b) in Tank #1 before and after NZVI dosing on day 89. 108
- Figure 37. Autotrophic SOUR in Tank #1 (○) and #2 (◇) before NZVI dosing and in Tank #1 (●) and #2 (◆) after NZVI dosing on day 89 and day 104 and day 104, respectively. Two vertical hashed lines show the days of NZVI addition in Tanks #1 and #2, respectively..... 109
- Figure 38. Effluent $\text{PO}_4^{3-}\text{-P}$ concentrations in Tank #1 (●) and Tank #2 (◆) right after NZVI dosing. Error bars represent one standard deviation from the mean of duplicate samples..... 112
- Figure 39. Influent (■) and effluent melamine concentrations in the CSTR (○) and MLE (●) systems after continuous melamine dosing starting on day 125. Error bars represent one standard deviation from the mean of triplicate samples..... 122
- Figure 40. Change in melamine concentration due to biodegradation (●) and adsorption (○) of melamine under anoxic conditions in batch studies. 123
- Figure 41. Change in melamine concentration due to biodegradation (●) and adsorption (○) of melamine under aerobic conditions in batch studies. 123
- Figure 42. Influent (■) and effluent COD concentrations in the CSTR (○) and MLE (●) systems before (Phase I) and after (Phase II) melamine dosing. Error bars represent the data range of duplicate samples..... 126
- Figure 43. Effluent $\text{NH}_4^+\text{-N}$ (a), $\text{NO}_2^-\text{-N}$ (b) and $\text{NO}_3^-\text{-N}$ (c) concentrations in the CSTR (○) and MLE (●) bioreactors before (Phase I) and after (Phase II) melamine dosing. Error bars represent the data range of duplicate samples. 128

- Figure 44. Change in autotrophic SOURs in the CSTR (○) and MLE (●) bioreactors before (Phase I) and after (Phase II) melamine dosing. Error bars represent the data range of duplicate samples..... 130
- Figure 45. Aerobic bacterial growth as indicated by optical density curves at 600 nm, with different substrate concentrations: 0.6 mM (or 75.6 mg/L) melamine only (■), 14 mM glucose only (◆), and a combination of 0.6 mM melamine and 14 mM glucose (○). Activated sludge from the CSTR before melamine dosing was used as a seed culture. Error bars represent one standard error of the mean (n=4). 131
- Figure 46. Ammonia-oxidizing bacterial community structure and abundance reflected by T-RFLP profiles targeting 16S rRNA genes of *Nitrosomonas* in the CSTR before melamine dosing (A), the CSTR after melamine dosing (B), the MLE before melamine dosing (C), and the MLE after melamine dosing (D). AU = arbitrary units. DNA samples were taken 1 month before melamine dosing and after 50 days of continuous melamine dosing 133
- Figure 47. Biomass concentrations in the CSTR (○) and MLE (●) bioreactors before (Phase I) and after (Phase II) melamine dosing. Error bars represent data range of duplicate samples..... 137
- Figure 48. A schematic of a bench-scale submerged MLE-MBR. P stands for a transmembrane pressure measurement device..... 143
- Figure 49. Change in the biomass concentration in the MBR bioreactors before (Start-up and Phase I) and after (Phase II) melamine dosing. Error bars represent data range of duplicate samples..... 148
- Figure 50. Influent (●) and effluent (○) melamine concentrations in the MBR system after continuous melamine dosing starting from day 85. Error bars represent one standard deviation of the mean (n = 3). 149
- Figure 51. Change in melamine concentration in the absence of readily biodegradable substrate under aerobic (○) and anoxic (●) conditions in the mixed liquor with an average biomass concentration of 10 g COD/L in batch studies: live cells (a) and dead cells (b). Error bars represent one standard error of the mean (n = 4). ... 151
- Figure 52. Change in melamine concentrations by unacclimated sludge of 2 g/L (●), acclimated sludge of 2 g/L (○), acclimated sludge of 2 g/L with ammonia substrate

	(20 mg/L) (Δ), and acclimated sludge of 10 g/L (\diamond) in batch studies. Error bars represent one standard error of the mean (n = 4).....	153
Figure 53.	Change in melamine concentrations with time at initial melamine concentrations of 2.5 mg/L (\circ), 5 mg/L (\square), 10 mg/L (Δ) and 20 mg/L (\diamond) in batch studies. Error bars represent one standard error of the mean (n = 4).	154
Figure 54.	Effluent COD concentrations in the MBR before (Start-up and Phase I) and after (Phase II) melamine dosing. Error bars represent the data range of duplicate samples.....	157
Figure 55.	Effluent NH_4^+ -N (a), NO_2^- -N (b) and NO_3^- -N (c) concentrations in the MBR before (Start-up and Phase I) and after (Phase II) melamine dosing. Error bars represent the data range of duplicate samples.....	160
Figure 56.	Changes in autotrophic (\circ) and heterotrophic (\bullet) SOURs in the MBR before (Phase I) and after (Phase II) melamine dosing. Error bars represent the data range of duplicate samples.....	161
Figure 57.	Nitrifying bacterial community composition reflected by T-RFLP profiles targeting 16S rRNA genes of <i>Nitrosomonas</i> (A), and <i>Nitrospria</i> (B) before (Phase I) and after (Phase II) melamine dosing	163

PROCESS IMPROVEMENTS IN BIOLOGICAL NUTRIENT REMOVAL SYSTEMS
FOR BETTER WASTEWATER TREATMENT PERFORMANCE

Shengnan Xu

Dr. Zhiqiang Hu, Dissertation Supervisor

ABSTRACT

Process improvements for better wastewater treatment performance are necessary with stringent discharge requirements. The main objective of this research is to develop new wastewater treatment technologies for improved nutrient removal and the degradation of recalcitrant organic nitrogen compounds. In this research, a reverse A²/O system demonstrated better phosphorus removal efficiency than the regular A²/O system by inverting the sequence of anaerobic and anoxic zones. Placing an anoxic stage before the anaerobic stage in the reverse A²/O process resulted in a lower oxidation-reduction potential in the anaerobic zone, which contributed to higher P uptake by bacteria under subsequent aerobic respiration.

With the development of emerging environmental nanotechnology, the effectiveness of nano zero-valent iron (NZVI) in nutrient removal was also determined under anaerobic, anoxic and aerobic conditions. The highest P removal efficiency (95% at the initial P concentration of 10 mg/L) by NZVI was observed under anoxic abiotic conditions.

Furthermore, new applications of NZVI as an antiseptic/antimicrobial material were extended to sludge bulking control. In two Modified Ludzack-Ettinger (MLE) activated sludge treatment systems, a single dose of NZVI at the final concentration of 100 mg Fe/L in the mixed liquor reduced the number of filamentous bacteria Type 021N by 2-3 log units (a reduction of 99.9 and 96.7% in MLE tank #1 and #2, respectively). Additional benefits of the use of NZVI such as improved P removal was also determined. The side effect of the use of NZVI depended on sludge bulking conditions and biomass concentration.

In the last part of this dissertation, process improvements to remove recalcitrant organic N compounds such as melamine were evaluated. Melamine is a nitrogen-rich (67% nitrogen by mass) heterocyclic aromatic compound that could significantly increase effluent total nitrogen concentrations. The degradation of melamine and its impact on activated sludge operation in conventional activated sludge (CAS) systems and MBRs with high biomass concentrations were compared. Melamine was dosed continuously in CAS and MBR systems at an influent concentration of 3 mg/L for about 100 days. Even after such a long period of sludge adaptation, melamine appeared not to be easily biodegradable in any of the CAS and MBR systems indicating that selective enrichment of special microbes (melamine degradation specialists) and the special enzymes responsible for melamine degradation cannot be induced through acclimation. However, a

significant reduction in toxicity of melamine to the activated sludge was observed in MBR systems, demonstrating the significance of MBR operation at high sludge concentrations.

CHAPTER 1

1. Introduction

1.1. Anaerobic/Anoxic/Oxic (A²/O) and Reverse A²/O Processes in Biological Nutrient Removal

Biological nutrient removal (BNR) is increasingly used in wastewater treatment for nitrogen and phosphorus reduction. Nitrogen removal relies on different groups of bacteria that are responsible for nitrification followed by denitrification, while phosphorus removal relies on the proliferation of phosphate-accumulating organisms (PAOs) through an anaerobic-aerobic sequence in activated sludge processes (Ersu et al., 2010, Ramphao et al., 2005). In enhanced biological phosphorus removal (EBPR), the PAOs use energy generated through the breakdown of Poly-P molecules to convert readily biodegradable organic matter to carbon compounds such as poly-hydroxyalkanoates (PHAs) under anaerobic conditions (Smolders et al., 1994). Under subsequent aerobic conditions, PAOs use the stored PHAs as an energy source to take up soluble P released under the anaerobic conditions plus the phosphate originally present in the wastewater due to the difference in energetics between anaerobic and aerobic metabolism (Grady et al., 2011).

The EBPR process must be integrated with nitrification and denitrification processes very well to achieve simultaneous nitrogen and phosphorus removal because both the EBPR and the denitrification processes compete for organic substrates. As a result, many BNR processes have been developed. These include, but are not limited to, the anaerobic/anoxic/oxic (A²/O) process, the five-stage Bardenpho process, the University of Cape Town (UCT) or modified UCT process, and the oxidation ditch process (Grady et al., 2011, Metcalf and Eddy, 2003). All of these treatment processes are capable of removing nutrients with moderate cost (Littleton et al., 2003, Peng and Ge, 2011, Ramphao et al., 2005, Solley and Armstrong, 2003). The A²/O process is comprised of three chambers in sequence—anaerobic, anoxic, and oxic (or aerobic) chambers (Figure 1)—and can be viewed as a combination of the Modified Ludzack-Ettinger (MLE) and the A/O processes for nitrogen and phosphorus removal, respectively (Grady et al., 2011). Studies have shown that the influent wastewater composition (chemical oxygen demand (COD), total N, and total P) and distribution (e.g., step feeding), and operating parameters such as hydraulic retention time (HRT), solids retention time (SRT), dissolved oxygen (DO), return activated sludge (RAS), and mixed liquor recirculation (MLR) flow rate have significant impacts on the performance of A²/O systems (Guerrero et al., 2011, Kim et al., 2013, Maurer and Gujer, 1998, Scheer and Seyfried, 1997, Van Veldhuizen et al., 1999).

Due to the competition for organic substrates between PAOs and denitrifiers, there is a concern about the adverse effects of the nitrate in the returning sludge on the growth of PAOs, which prefer to grow under alternating anaerobic and aerobic conditions (Guerrero et al., 2011, Hauduc et al., 2013, Lee et al., 2009, Oehmen et al., 2007). Additionally, even though they have the function of simultaneous N and P removal (Beun et al., 2000, Kishida et al., 2006), the denitrifying PAOs (DPAOs) have a lower P uptake performance than the regular PAOs (Hu, Wentzel, and Ekama, 2002).

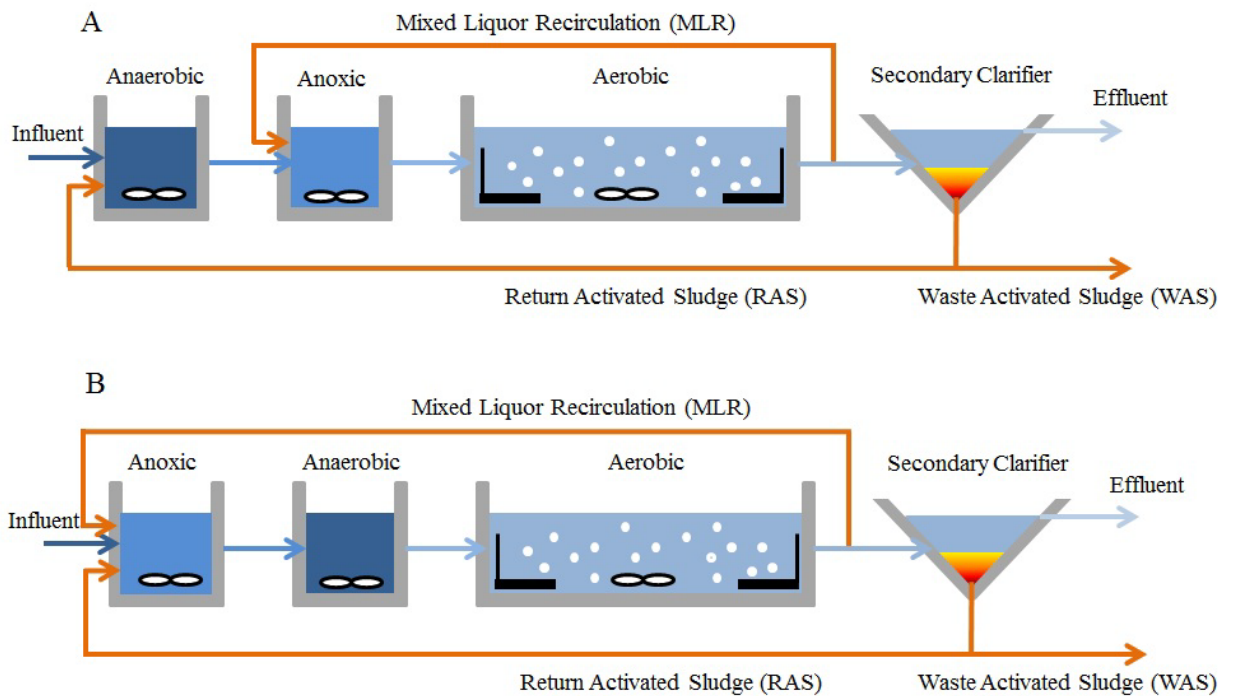


Figure 1. A schematic of the two biological nutrient removal processes: (A) A²/O and (B) reverse A²/O.

To overcome the inherent drawbacks of the A²/O process, a reverse A²/O process has been proposed for nutrient removal by placing an anoxic stage before the anaerobic stage (Figure 1) (Fu et al., 2004, Kang et al., 2011, Zhang and Gao, 1997, Zhou et al., 2011). It is claimed that the reverse A²/O process will result in more complete denitrification and improve P uptake by bacteria under aerobic conditions (Kang et al., 2011, Zhang and Gao, 1997). It is further claimed that by eliminating the MLR required in the A²/O process, the reverse A²/O process is easier to manage and can reduce energy consumption by about 20% (Kang et al., 2011). However, these claims may not be valid as the process performance is easily affected by wastewater strength and composition. Theoretically, the COD and nitrogen removal efficiencies would be similar for both A²/O and reverse A²/O processes if the HRT, the SRT, the aerobic and anoxic fractions of total volume, and the internal recycle flow rate are the same in both cases. The elimination of MLR may result in reduced nitrogen removal as denitrification becomes solely reliant on the flow of return activated sludge. Unfortunately, although there are quite a few publications advocating for reverse A²/O process in biological nutrient removal, there is still little information directly comparing the performance of A²/O and reverse A²/O processes under identical operating conditions.

1.2. NZVI: Environmental Applications and Implications

The application of nanotechnology offers great opportunities to improve contaminant removal and treatment performance (Qu et al., 2013, Tang and Lo, 2013). Among the nanoparticles, nano zero-valent iron (NZVI) underwent a period of uncertainty and scrutiny in applications due to its high reactivity (Tang and Lo, 2013). The application of NZVI is a complementary treatment of iron permeable reactive barriers (PRBs) for groundwater remediation (Hosseini et al., 2011, Huang and Cheng, 2012, Saeedi et al., 2013, Scherer et al., 2000, Shariatmadari et al., 2009, Yan et al., 2013). NZVI could be 25 times more reactive than its counterpart (bulk ZVI) because of its higher surface/volume ratio (Li et al., 2006, Nurmi et al., 2005) and faster delivery to deep contamination zones due to its smaller size (Vance, 2005). NZVI is also used in industrial wastewater treatment to remove heavy metals and recalcitrant organic compounds (Fang et al., 2011, Homhoul et al., 2011, Jagadevan et al., 2012, Ma and Zhang, 2008). On the other hand, NZVI has antimicrobial activity against a broad range of microorganisms, causing serious damage to the cell membrane and respiratory activity (Auffan et al., 2008, Kim et al., 2011, Kim et al., 2010). The mode of action of NZVI appears to be through reductive decomposition of protein functional groups and cell membrane due to strong reducing conditions at the

NZVI surface (Kim et al., 2010, Lee et al., 2008, Li et al., 2010). The antibacterial effect of NZVI may also involve the generation of intracellular reactive oxygen species (ROS) by dissociative recombination of H_3O^+ ($\text{H}_3\text{O}^+ + \text{e}^- \rightarrow \cdot\text{HO} + \text{H}_2$) catalyzed by $\text{Fe}^0/\text{Fe}(\text{II})$ (Kim et al., 2011, Zhaunerchyk et al., 2009).

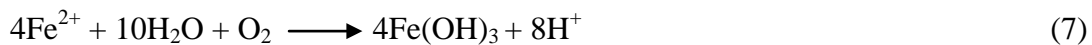
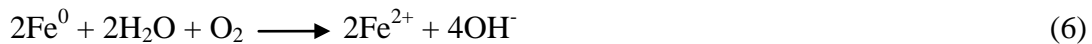
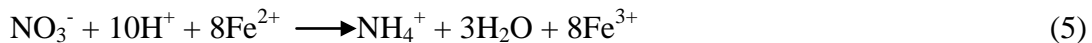
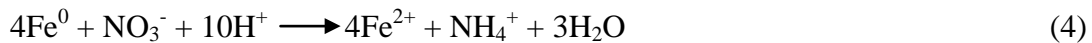
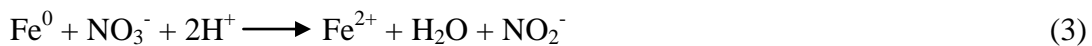
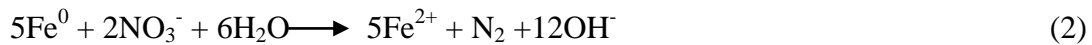
Despite recent progress in NZVI research, the applications and implications of NZVI in wastewater treatment plants (WWTPs) are less studied. Nowadays, many wastewater treatment systems are designed and operated under different biochemical environments for nutrient removal and resource recovery. With appropriate configuration of biochemical settings (e.g., activated sludge operation under anaerobic, anoxic and aerobic conditions), nutrient removal is achieved through nitrification/denitrification and enhanced biological phosphorus removal (EBPR). NZVI can also be used in wastewater treatment for nitrogen removal through chemical reduction of nitrate (Hwang et al., 2012, Shin and Cha, 2008) and chemical phosphate precipitation (Chang et al., 2008). The release of Fe^{2+} associated with the dissolution of NZVI helps sludge flocculation, and therefore, resulting in better sludge settling (Wilén et al., 2004). Furthermore, NZVI is promising for odor control in biosolids as the released ferrous ions can form stable complexes with malodorous sulfur compounds (Li et al., 2007). However, questions remain to be answered as how to

maximize nutrient removal in wastewater treatment facilities with different biochemical settings while minimizing the negative effects (e.g., microbial toxicity and excess production of $\text{NH}_4^+\text{-N}$ in treated wastewater) from the use of NZVI.

Earlier studies have shown that compared to that under anaerobic conditions, NZVI appears to have lower bactericidal activity under aerobic conditions (Li et al., 2010). This is because rapid oxidation of NZVI by oxygen can lead to the formation of different oxide layers, which are generally less toxic or non-toxic. As a result, partially oxidized NZVI particles are prevented from having direct contact with bacterial cells and are thus less toxic. It is also possible that under aerobic conditions, bacteria express enzymes that destroy ROS such as superoxide dismutase (Li et al., 2010).

On the other hand, under anoxic conditions, NZVI can remove nitrate through chemical reduction in both abiotic (free of activated sludge) and biotic systems, where the electrons required to reduce nitrate come directly from the dissolution of Fe^0 or indirectly through the corrosion products, Fe^{2+} and H_2 (Equation 1) (Stumm and Morgan, 1996). Biological denitrification could be therefore improved under the conditions of lack of organic carbon and molecular hydrogen because the Fe^{2+} released from NZVI dissolution can serve as an

electron donor for nitrate removal (Shin and Cha, 2008). The multiple pathways of nitrate reduction associated with the use of NZVI and its dissolution products are listed in Equations 2-5 (Choe et al., 2000, Ruangchainikom et al., 2006, Tyrovola et al., 2006). In addition to ammonia, nitrite, and nitrogen gas, the products of nitrate reduction by NZVI include other nitrogenous species such as NO and N₂O (Wang et al., 2006, Yang and Lee, 2005).



The dissolution of NZVI under anaerobic and aerobic conditions results in different pH changes due to the degree of hydrolysis of ferric ions (e.g., Equations 6-8 under aerobic conditions) (Ruangchainikom et al., 2006), which in turn affect the formation of iron (II, III) hydroxides and iron-phosphate complexes/precipitates (Stumm and Morgan, 1996, Wu et

al., 2013). NZVI has been therefore applied for the removal of phosphate (PO_4^{3-}) in water due to P precipitation and adsorption on the surface of NZVI particles and iron complexes (Almeelbi and Bezbaruah, 2012, Liu et al., 2013, Stumm and Morgan, 1996).

1.3. Filamentous Sludge Bulking Control and NZVI Toxicity

Sludge bulking, which is often caused by excessive growth of filamentous organisms in activated sludge (Jenkins et al., 2004), results in poor sludge settling, sludge loss from secondary clarifiers and deterioration of effluent water quality (Grady et al., 2011, Guo et al., 2012, Kappeler and Gujer, 1994, Nielsen et al., 2009). The kinetic selection theory is commonly used to explain sludge bulking and to explore engineering solutions to control bulking (Chudoba et al., 1973, Grady et al., 2011). Most filamentous bacteria are slowly growing organisms with lower maximum specific growth rate (μ_{max}) but higher affinity constant (K_s) than floc-forming bacteria (Grady et al., 2011). At low substrate concentrations (S) (i.e., $S \ll K_s$), filamentous bacteria may have higher growth rates, thus outcompeting floc-forming bacteria (e.g., *Zoogloea*) in activated sludge (Cenens et al., 2000). Nowadays, selectors are therefore commonly used by creating a substrate concentration gradient to improve sludge settling (Chudoba et al., 1973, Gray et al., 2010). Metabolic selection is another approach for filamentous sludge bulking control as most

filamentous bacteria cannot grow under anoxic or anaerobic conditions (Grady et al., 2011). Other theories and factors such as substrate diffusion limitation (Martins et al., 2003), intracellular polymer storage (Goel et al., 1998, Van Loosdrecht et al., 1997b), and the difference in decay rates between filaments and floc-forming bacteria (In and De Los Reyes III, 2005) have also been proposed. While an integrated framework combining kinetic selection and substrate diffusion limitation has been suggested for sludge bulking (Lou and De Los Reyes III, 2008), there is still no single mechanism that can fully explain the sludge bulking problems. In practice, the causes for filament growth in activated sludge treatment are complex and include factors such as low food-to-microorganisms (F/M), long solids retention time (SRT), low nutrients, low dissolved oxygen (DO), low pH or high sulfide levels (Grady et al., 2011, Jenkins et al., 2004, Wanner, 1994). Eikelboom type 021N (Type 021N), Type 1701, Type 0041, *Microthrix parvicella*, *Thiothrix* spp, *Gordonia* spp., among others, have been found to be responsible for most of the bulking and foaming events (Grady et al., 2011, Kanagawa et al., 2000, Madoni et al., 2000).

Practical control methods for filamentous sludge bulking include specific and non-specific methods (Kotay et al., 2011, Martins et al., 2004). Specific methods like the use of selectors are preferred as they eliminate the causes favorable for filamentous growth. In

order to apply the principles of kinetic selection and metabolic selection, approaches such as modifying process operating conditions and process configurations are necessary but can be costly (Martins et al., 2004). Non-specific methods can be a quick fix by adding toxicants (biocides) such as chlorine and hydrogen peroxide to improve sludge settleability (Guo et al., 2012, Jenkins et al., 2004). This approach is based on the fact that filaments protrude from the flocs are more susceptible to toxicant exposure, while most of floc-forming bacteria are embedded inside the flocs therefore protected from exposure to toxicants. Chlorination is the most widely applied method to control sludge bulking due to its low cost. Chlorine dose can be properly managed to control filamentous bulking without impairing nitrification performance (Jenkins et al., 2004). However, chlorination often causes side effects on wastewater treatment performance by deflocculating activated sludge resulting in poor effluent water quality (Mascarenhas et al., 2004, Wimmer and Love, 2004). There is also a concern about the development of chlorine-resistant filamentous bacteria in sludge (Guo et al., 2012, Séka et al., 2001b). Other types of toxicants such as cetyl trimethylammonium bromide (CTAB), ozone and hydrogen peroxide are generally too costly to use, not to mention the generation of harmful disinfection byproducts (DPBs), odor and chemical scum (Guo et al., 2012, Jenkins et al., 2004). Synthetic polymers and coagulants (e.g. lime, iron salts) may also be used to

improve sludge sedimentation through bridging between flocs (Agridiotis et al., 2007), but coagulation/flocculation does not kill filamentous bacteria.

Nanomaterials having antiseptic (antimicrobial) properties may have beneficial uses in wastewater treatment. Nano zero-valent iron (NZVI) is one of the most commonly used and studied engineered nanoparticles due to its broad applications (Lee et al., 2008, Shin and Cha, 2008). NZVI has been evaluated in wastewater treatment for nitrogen removal through chemical reduction of nitrate (Hwang et al., 2012, Shin and Cha, 2008) and phosphate removal through chemical precipitation (Chang et al., 2008). The associated release of Fe^{2+} due to oxidative dissolution of NZVI helps sludge flocculation and settling (Wilén et al., 2004). More importantly, NZVI is an effective biocide that can kill a broad range of microorganisms (Auffan et al., 2008, Kim et al., 2011, Kim et al., 2010) with its mode of action through reductive decomposition of cell membrane due to strong reducing conditions ($E_{\text{H}}^{\circ}(\text{Fe}^{2+}/\text{Fe}) = -0.447 \text{ V}$) at the NZVI surface (Kim et al., 2010, Lee et al., 2008). The antibacterial effect of NZVI may also involve the generation of intracellular reactive oxygen species (ROS) by dissociative recombination of H_3O^+ ($\text{H}_3\text{O}^+ + \text{e}^- \rightarrow \cdot\text{HO} + \text{H}_2$) catalyzed by $\text{Fe}^0/\text{Fe}(\text{II})$ (Zhaunerchyk et al., 2009). Remarkably, NZVI was also reported to be highly selective (Marsalek et al., 2012), with its EC_{50} on cyanobacteria

20-100 times lower than that on algae, daphnids, water plants and fishes. It is well established that the filaments have higher cell loss from biocide because a larger fraction of their population compared to floc formers is exposed to the bulk liquid (Jenkins et al., 2004).

1.4. Toxicity and Biodegradation of Melamine

Melamine ($C_3H_6N_6$), chemically known as 1, 3, 5-triazine-2, 4, 6-triamine, is a nitrogen-rich (67% nitrogen by mass) heterocyclic aromatic compound commonly used to make plastic for food containers and flame retardants (Costa and Camino, 1988, Salaün et al., 2011). Incidents of pet-food contamination by melamine and a 2008 Chinese milk scandal raise concerns about the impact of melamine on wastewater treatment operations and effluent water quality. With more stringent nutrient discharge limits for wastewater, it is important to understand the fate and toxicity of melamine in wastewater treatment systems.

Although it is not carcinogenic, melamine is well known to cause urinary stones and acute renal failure in human and animals. A combination of melamine and cyanuric acid (one of the melamine degradation byproducts) in a diet may lead to acute kidney failure (Dobson et

al., 2008, Puschner et al., 2007). Long-term exposure to melamine may also result in sperm DNA damage and abnormalities (Zhang et al., 2011). The toxicity of melamine to microorganisms is, however, rarely reported. Polyvinylalcohol (PVA) gel plate studies showed that melamine inhibited yeast growth at a concentration of 500 mg/L (Nishimura et al., 2002). Toxicity to activated sludge and nitrifying bacteria (*Nitrosomonas*) was not observed after a short-term (< 2 hours) exposure at melamine concentrations of 1,992 mg/L and 100 mg/L, respectively (Hockenbury and Grady Jr, 1977, UNEP). However, the impact on microbial growth after long-term activated sludge exposure to melamine is largely unknown.

To date, only a few soil bacteria have been isolated that are capable of degrading melamine via stepwise hydrolytic deamination reactions producing ammeline, ammelide, and cyanuric acid, sequentially (Boundy-Mills et al., 1997, Cook and Hütter, 1981, El-Sayed et al., 2006, Shelton et al., 1997). Melamine can also be hydrolyzed by melamine deaminase (TriA) from *Acidovorax avenae* subsp. *citrulli* strain NRRL B-12227 (Seffernick et al., 2001, Seffernick et al., 2000). Cyanuric acid is further subject to hydrolytic ring cleavage, producing CO₂ and NH₄⁺-N via hydrolysis of biuret and allophanate (Cheng et al., 2005, Cook, 1987, Nenner and Schulz, 1975).

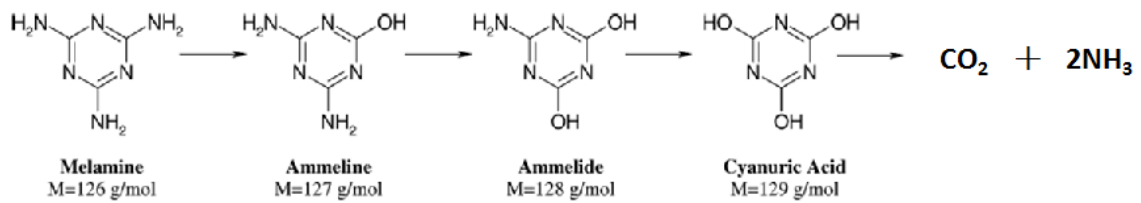


Figure 2. Melamine Degradation Pathway

1.5. Role of Sludge Acclimation and High Sludge Concentration Operation in MBR Systems

Sludge acclimation or adaptation generally improves degradation rates of recalcitrant organic compounds in the environment (Hu et al., 2005a, Hu et al., 2005b). Adaptations contribute to the fitness and plasticity of microorganisms in response to environmental stress and chemical exposure. There are several interrelated adaptation mechanisms including (i) selective enrichment of microorganisms, (ii) induction and/or depression of specific enzymes, and (iii) genetic changes resulting in new metabolic capabilities (Leahy and Colwell, 1990, Rittman and McCarty, 2001). Hence, a selection and concentration of specialized bacteria during acclimation improve biodegradation rates of synthetic organic chemicals such as nitrobenzoate and chlorophenol (Hu et al., 2005a, Hu et al., 2005b).

Membrane bioreactor (MBR) systems are excellent in solid-liquid separation and offer higher effluent quality than conventional activated sludge (CAS) systems (Ersu et al., 2010,

Metcalf and Eddy, 2003). Additional benefits can be achieved through MBR operation, such as higher volumetric loading rates and thus shorter hydraulic retention times (HRTs) for economical operation, and longer solid retention times (SRTs) and thus less sludge production (Bhatta et al., 2004, Metcalf and Eddy, 2003). The biomass concentration in MBR systems can therefore be 10 times that of the conventional activated sludge systems (Galil and Jacob, 2009), resulting in more efficient pollutant removal (Fleischer et al., 2005, Monclús et al., 2010). Although membrane fouling is still a big operational problem (Charcosset, 2006), MBR is increasingly used in wastewater treatment for wastewater reuse (Iversen et al., 2009, Juang et al., 2010, Mutamim et al., 2012, Rosenberger et al., 2006, Yoon et al., 2004).

For treating organic matter with low biodegradability, the MLSS must be high enough to increase the process of degradation (Mutamim et al., 2013). Compared with CAS, MBR operated at high biomass concentration could create more opportunities for the degradation of recalcitrant organic compounds. Highly diverse bacterial consortium with more slow growing microorganisms can be cultivated in MBR system to enhance the biodegradation of those compounds (Boonnorat et al., 2014).

1.6. Hypotheses and Research Overview

The main objective of this study was to develop new technologies for improved nutrient removal and the degradation of recalcitrant organic nitrogen, specifically through process reconfiguration, the use of emerging nanomaterials, and MBR operation at high biomass concentrations.

A few of the important questions need to be answered:

- a) *How will different sequences of anaerobic and anoxic processes affect nutrient removal in an enhanced biological phosphorus removal (EBPR) system?*
- b) *Is NZVI capable of removing nitrogen and phosphorus simultaneously? If so, what is the difference in removal efficiency under different biochemical environments?*
- c) *Will NZVI enhance or decrease denitrification because of its potential electron donor and antimicrobial characteristics?*
- d) *What is the possible mechanism of P removal by NZVI under different biochemical environments?*
- e) *Other than nutrient removal, will the use of NZVI be beneficial to sludge bulking control while minimizing its negative effect on floc-forming bacteria in activated sludge processes?*

f) Can recalcitrant organic nitrogenous compounds such as melamine be degraded after long-term activated sludge adaptation?

g) Will high biomass concentration in MBR help the removal of melamine?

With the above questions, comprehensive literature review, and preliminary data, we have proposed the following hypotheses:

Hypothesis 1: Improved N and P removal can be achieved in a reversed A²/O process following the sequence of anoxic-anaerobic-aerobic treatment.

Hypothesis 2: NZVI improves N and P removal in activated sludge treatment and the removal kinetics depend on the use of biochemical environments (e.g., under anaerobic, anoxic, and aerobic growth conditions).

Hypothesis 3: NZVI dosing is an effective method of sludge bulking control with minimal negative effect on activated sludge processes.

Hypothesis 4: The removal efficiency of recalcitrant organic nitrogen compounds such as melamine can be improved through a long-term sludge acclimation.

Hypothesis 5: MBR process with high biomass concentration helps degrade melamine.

CHAPTER 2

2. Evaluation of Anaerobic/Anoxic/Oxic (A²/O) and Reverse A²/O Processes in Biological Nutrient Removal*

A performance comparison between the conventional anaerobic/anoxic/oxic (A²/O) process and the anoxic/anaerobic/oxic (reverse A²/O) process was conducted in lab-scale at the hydraulic retention time of 0.75 d and solids retention time of 10 d for more than 200 days. Both processes demonstrated excellent removal efficiency for organic matter (> 96%) and total nitrogen (> 85%), with no significant difference in microbial activities, sludge phosphorus (P) content, sludge settling property, and nitrifying community (dominated by *Nitrosomonas* and *Nitrospira*). However, there was significant difference in P removal, with the total P removal efficiencies in the reverse A²/O and A²/O systems of $76 \pm 6\%$ and $70 \pm 6\%$, respectively. Placing an anoxic stage before the anaerobic stage in the reverse A²/O process resulted in a lower oxidation-reduction potential (ORP = -268 ± 45 mV) of

* A research paper based on this thesis chapter has been published: Full citation in Water Environment Research, *in press*.

the anaerobic zone, which contributed to higher P uptake by bacteria under subsequent aerobic respiration.

Objectives

The objective of this research was to comparatively evaluate the performance of A²/O and reverse A²/O processes under the same operating conditions. In this study, lasting more than 200 days, two lab-scale A²/O and reverse A²/O systems were operated in parallel at a HRT of 0.75 d and a target SRT of 10 d to investigate and compare their organic and nutrient removal efficiencies, P release and uptake kinetics, nitrifying bacterial community structure and activity, sludge P content, and sludge settling property.

2.2. Materials and Methods

2.2.1. Bioreactor Setup and Operation

The lab-scale A²/O and reverse A²/O bioreactors had total working volumes of 10.5 L each, with three separated chambers that were made of glass (Figure 1). The effective volumes of the anoxic, anaerobic and aerobic chambers were 1.8, 1.8, and 5.2 L, respectively. For each bioreactor, there was a separated settling zone with an effective volume of 1.7 L and the RAS was pumped into the first chamber at 100% of the influent flow rate. There was a mixed liquor recirculation flow that was about 200% of the influent flow rate from the

aerobic chamber to the anoxic chamber for both systems. Mixing was provided by magnetic stir-bars in each chamber while a fine bubble diffuser provided additional mixing and aeration in the aerobic (oxic) chamber. The DO was maintained at 3–4 mg/L in the aerobic chamber.

The medium-strength synthetic wastewater contained nonfat dry milk powder with a target COD concentration of 400 mg/L which contained 60 mg/L volatile fatty acids (VFAs), 40 mg/L total N (TN), 25 mg/L NH_4^+ -N, 10 mg/L total P (TP), and 8 mg/L PO_4^{3-} -P. The synthetic wastewater also contained the following macro- and micronutrients per liter: 44 mg MgSO_4 , 14 mg $\text{CaCl}_2 \cdot 2\text{H}_2\text{O}$, 2 mg $\text{FeCl}_2 \cdot 4\text{H}_2\text{O}$, 3.4 mg $\text{MnSO}_4 \cdot \text{H}_2\text{O}$, 1.2 mg $(\text{NH}_4)_6\text{Mo}_7\text{O}_{24} \cdot 4\text{H}_2\text{O}$, 0.8 mg CuSO_4 , 0.3 mg $\text{NiSO}_4 \cdot 6\text{H}_2\text{O}$, and 1.8 mg $\text{Zn}(\text{NO}_3)_2 \cdot 6\text{H}_2\text{O}$ (Sigma Aldrich, St. Louis, MO) (Liang et al., 2010a). The wastewater was prepared every 3 days and stored at room temperature (23 ± 1 °C) in a covered 130 L (volume) plastic storage bin.

The two bioreactors were operated at the same HRT of 0.75 d and target SRT of 10 d. At the beginning of bioreactor operation, a total of 4,000 mL activated sludge taken from the aeration basin of a local municipal wastewater treatment plant (Columbia, MO) was added

as an inoculum to each reactor. The bioreactors were operated for more than 200 days, during which time the influent (sampling from the storage bin) and effluent water quality (sampling from the settling zone) was carefully monitored twice a week.

2.2.2. Sludge Phosphorus Content and P Release/Uptake Kinetics

In addition to effluent water quality monitoring, batch experiments were conducted to determine the P content of the sludge from the A²/O and reverse A²/O systems. The sludge P content was calculated by subtracting the P concentration of the supernatant from the TP concentration of the mixed liquor suspended solids (MLSS), and then divided by the MLSS concentration. The sludge samples were taken from the anaerobic and aerobic chambers of the A²/O and reverse A²/O systems.

Batch studies were conducted to determine the phosphorus release and uptake kinetics of the sludge taken from the A²/O and reverse A²/O systems, and the maximum P release and uptake rates were calculated according to the procedures described elsewhere (Wachtmeister et al., 1997). Briefly, activated sludge samples taken from the aerobic chamber were centrifuged at 4,000 g for 5 min followed by three washing steps with distilled water to remove residual nutrients from the water. They were then resuspended to

a biomass concentration of about 2,000 mg COD/L. Sodium acetate was used as a soluble biodegradable substrate and it was added to a final concentration of 100 mg/L. After purging with nitrogen gas for 15 min, the mixed liquor in each serum bottle was tightly capped with a butyl rubber stopper and screw cap, and incubated on a shaker at 150 rpm for 240 min. For both the P release and uptake studies, the anaerobic condition was maintained for about 120 min before the mixed liquor was vigorously aerated for another 120 min. Aliquots of mixed liquor samples were taken at predetermined time intervals and filtered. The supernatant was collected for PO_4^{3-} -P analysis.

2.2.3. Fluorescent Microscopy Analysis of Activated Sludge Including PAOs

The fluorescent antibiotic tetracycline (TC) hydrochloride was proven to show highly polyphosphate-specific and stable fluorescence with a 15-times-lower unspecific background labeling than that of the DAPI (4',6'-Diamidino-2-Phenylindole) staining (Günther et al., 2009). Hence, the TC staining procedure was applied to determine the intracellular polyphosphate in the activated sludge from the A^2/O and reverse A^2/O systems. The cells in the mixed liquor taken from the aerobic chamber were fixed with 4% paraformaldehyde for 1 day. Aliquots (2 mL) of the fixed cell suspensions were centrifuged, washed with phosphate buffered saline (PBS) three times and resuspended in

PBS. The samples were stained with TC at a final concentration of 0.2 mM, and stored at 20 °C in the dark for 10 min before they were used for microscopic analysis. An activated sludge sample from a conventional activated sludge wastewater treatment plant served as the control. The treated cells were subjected to microscopy and image analysis (Axioskop [Zeiss] microscope, DXC-9100P camera, and Openlab 3.1.4. [Improvision] software) using light from a 100-W mercury arc lamp. The Zeiss filter set 02 (excitation G 365, BS 395, emission LP 420) was used for examining the green fluorescence of TC stained cells.

2.2.4. Bacterial Activity Measurement

Aliquots of the mixed liquor were taken from the aeration zone in the A²/O and reverse A²/O systems once a week to determine bacterial activity. This was assessed through the specific oxygen uptake rate (SOUR) measurements by extant respirometry (Hu, Chandran, Grasso, and Smets, 2002). Briefly, aliquots of 120 ml of biomass (for duplicate measures) were poured into two 50 ml respirometric bottles. After 3 min of aeration with pure oxygen gas, the respirometric bottles were tightly capped with no air space. MOPs (3-(N-morpholino) propanesulfonic acid) were added to a final concentration of 20 mM to maintain a constant pH of 7.5. At predetermined times, an aliquot of substrate (10 mg NH₄⁺-N/L or 20 mg/L COD in acetate) was injected with a 10-μL Hamilton syringe. A decrease of dissolved oxygen (DO) level in the respirometric bottles due to substrate oxidation was measured by the DO probe and continuously monitored at 4 Hz by an

interfaced computer. Oxygen uptake rates were calculated based on a linear regression analysis because zero-order reactions were observed for a long period of time. Specific oxygen uptake rate (SOUR) was calculated by dividing OUR by biomass concentration of each sample. At a minimum, all SOUR experiments were carried out in duplicate.

2.2.5. Analysis of Nitrifying Communities in the A²/O and Reverse A²/O Systems

To analyze the nitrifying community structure in the A²/O and reverse A²/O systems, three independent Terminal Restriction Fragment Length Polymorphism (T-RFLP) assays were conducted by targeting the 16S rRNA genes of ammonia-oxidizing bacteria (AOB) (Amann et al., 1990, Mobarry et al., 1996), and nitrite-oxidizing bacteria (NOB), including *Nitrospira* (Regan et al., 2002) and *Nitrobacter* (Wagner et al., 1995), was extracted from a 1.0 mL sample of mixed liquor taken directly from the aerobic chamber in each bioreactor using an Ultraclean Soil DNA Isolation Kit (Carlsbad, CA). The concentration and purity of DNA were analyzed with a NanoDrop instrument (ND-1000 NanoDrop Technologies, Wilmington, DE). All of the primers (Supporting Information, Table S1) were synthesized by Integrated DNA Technologies (Coralville, IA). A fluorescent dye, 6-FAM, was incorporated at the 5'-end of the labeled oligonucleotides.

Table 1. Primer used for specific AOB and NOB 16s rRNA gene amplification

Target	Primer	Sequence (5'-3')	References
Bacterial 16S rRNA	Eub338f	5'-(6-FAM)-ACTCCTACGGGAGGCAGC-3'	(Amann et al., 1990)
AOB 16S rRNA	Nso1225r	5'-CGCCATTGTATTACGTGTGA-3'	(Mobarry et al., 1996)
<i>Nitrobacter</i> 16S rRNA	NIT3r	5'-CCTGTGCTCCATGCTCCG-3'	(Wagner et al., 1995)
<i>Nitrospira</i> 16S rRNA	Ntspa685r	5'-CGGGAATTCCGCGCTC-3'	(Regan et al., 2002)

Polymerase chain reactions (PCRs) were conducted in a PCR DNA thermocycler (Eppendorf, Westbury, NY). The thermal profiles used for each PCR amplification have been described elsewhere (Siripong and Rittmann, 2007). The PCR amplification products were purified and digested with *MspI* restriction endonuclease (Promega, Madison, WI) at 37 °C for 3 hrs. After digestion, the DNA products were diluted 10 times and run through an ABI 3730 DNA Analyzer (Applied Biosystems, Carlsbad, CA) at the University of Missouri DNA Core Facility. An internal lane standard ranging from 20 to 600 bases (Genescan 600 LIZ) was added to each sample for precise sizing of each fragment by adjusting for lane-to-lane loading variation. All experiments were performed in triplicate per sample and all PCR runs included control reactions without the DNA template.

2.2.6. Chemical and Statistical Analysis

Wastewater influent and effluent samples were collected and used for COD, TN, ammonium-N, nitrite-N, nitrate-N, TP and orthophosphorus measurements following the standard methods (APHA, 2002). The biomass concentrations of the A²/O and reverse A²/O systems were measured in COD units, while oxidation-reduction potential (ORP) in each chamber was measured with an ORP meter (Fisher Scientific, Pittsburgh, PA). The sludge volume index (SVI) was calculated to describe the sludge settling characteristics according to the standard methods (APHA, 2002). One-way ANOVA analysis was conducted to assess the statistical significance of the differences among groups, with p values less than 0.05 indicating statistical significance.

2.3. Results and Discussion

2.3.1. BNR Performance

The start-up period in the A²/O and reverse A²/O systems lasted for about 40 days (>3 SRTs) before stable operation was observed. This is evidenced by consistently high effluent water quality as shown in Figure 3 and Figure 4. At an average influent COD concentration of 408 ± 17 mg/L, the effluent COD concentrations were 21 ± 12 mg/L and 17 ± 7 mg/L for the A²/O and reverse A²/O systems, respectively, with an average COD

removal efficiency of 95% and 96%, respectively. There was no significant difference in effluent COD concentration between the A²/O and reverse A²/O systems ($p = 0.11$).

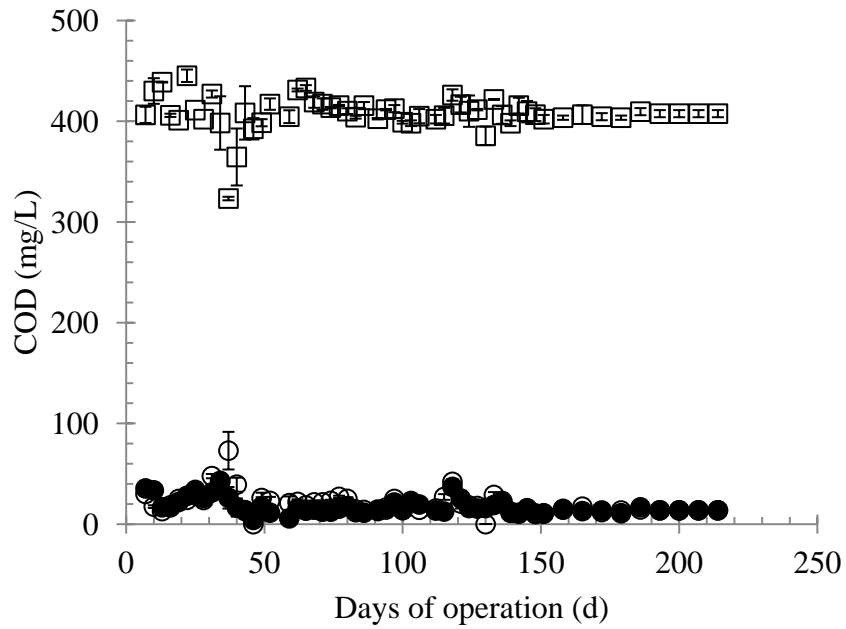
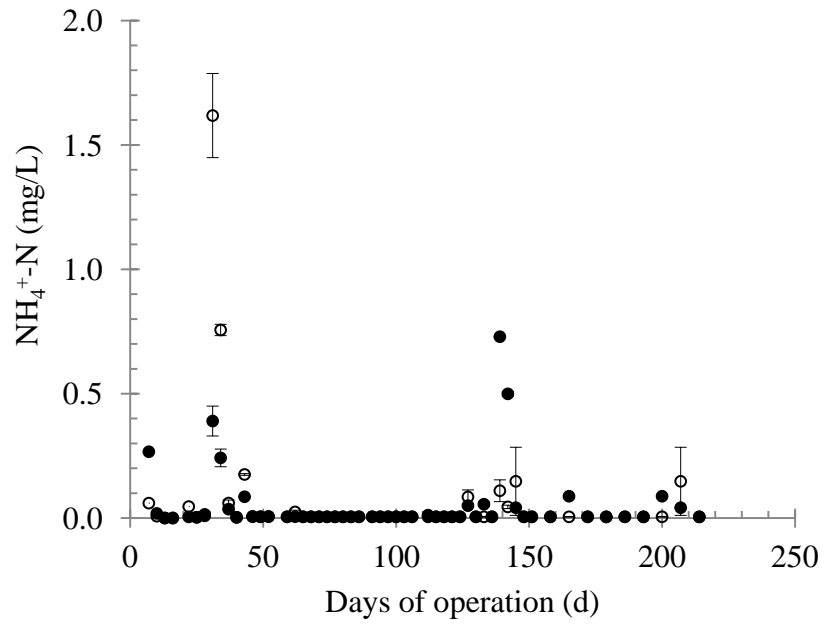
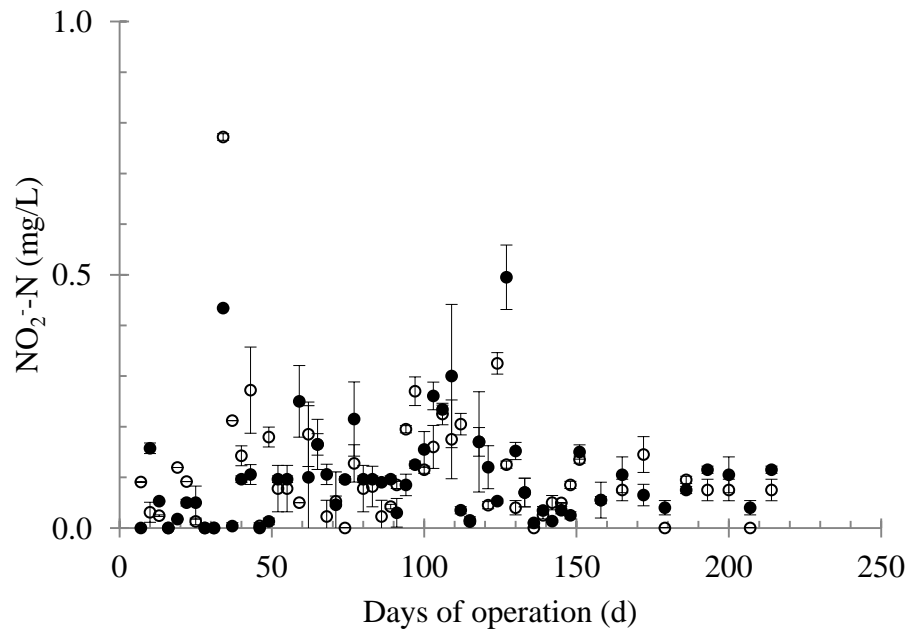


Figure 3. Influent (□) and effluent COD concentrations in the A²/O (○) and reverse A²/O (●) systems. The error bars represent the data range of duplicate samples.

(a)



(b)



(c)

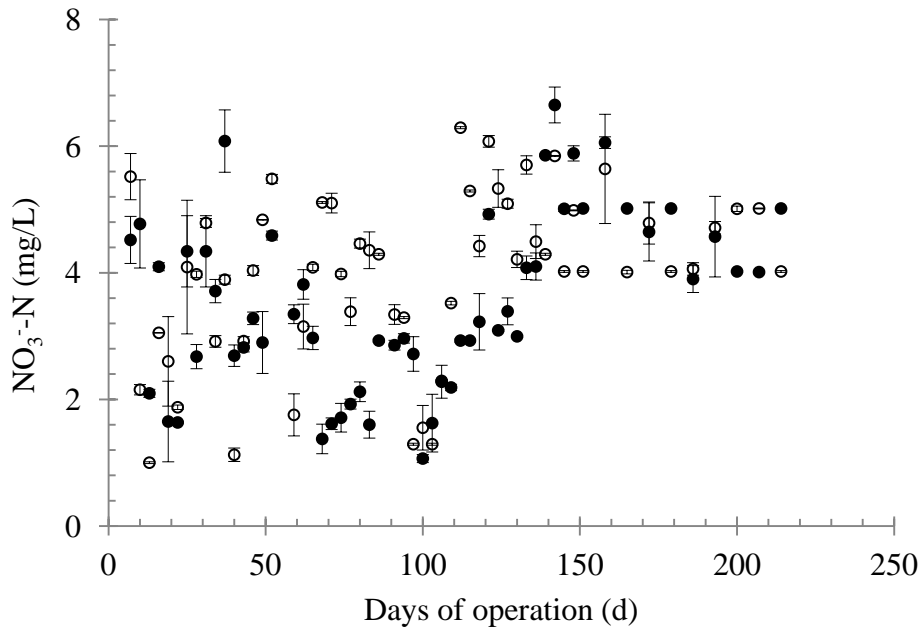


Figure 4. Effluent NH_4^+ -N (A), NO_2^- -N (B) and NO_3^- -N (C) concentrations in the A²/O (○) and reverse A²/O (●) systems. The error bars represent the data range of duplicate samples.

The average effluent TN concentration in the A²/O and reverse A²/O systems were 5.3 ± 1.4 mg/L and 4.9 ± 1.5 mg/L, respectively, as shown in Figure 5. This corresponds to average nitrogen removal efficiencies of $86 \pm 5\%$ and $87 \pm 4\%$, respectively. There was no significant difference in the effluent TN concentration between the A²/O and reverse A²/O systems ($p = 0.22$). There was also no significant difference in the effluent NH_4^+ -N ($p = 0.65$), NO_2^- -N ($p = 0.86$), and NO_3^- -N ($p = 0.10$) concentrations between the two BNR systems. With the exception of a short period of ammonia spike in the reverse A²/O system

on day 31 due to a sudden failure of aeration, the effluent $\text{NH}_4^+\text{-N}$ concentrations were 0.1 ± 0.3 mg/L, and 0.1 ± 0.1 mg/L for the A^2/O and reverse A^2/O systems, respectively, as shown in Figure 4. Correspondingly, the effluent $\text{NO}_2^-\text{-N}$ concentrations for the A^2/O and reverse A^2/O were 0.1 ± 0.1 mg/L and 0.1 ± 0.1 mg/L, respectively. The effluent $\text{NO}_3^-\text{-N}$ concentrations were 4.1 ± 1.2 mg/L and 3.6 ± 1.4 mg/L for the A^2/O and reverse A^2/O systems, respectively. These results illustrate that the alternating anoxic/oxic conditions offer equally high nitrogen removal efficiencies in the A^2/O and reverse A^2/O systems.

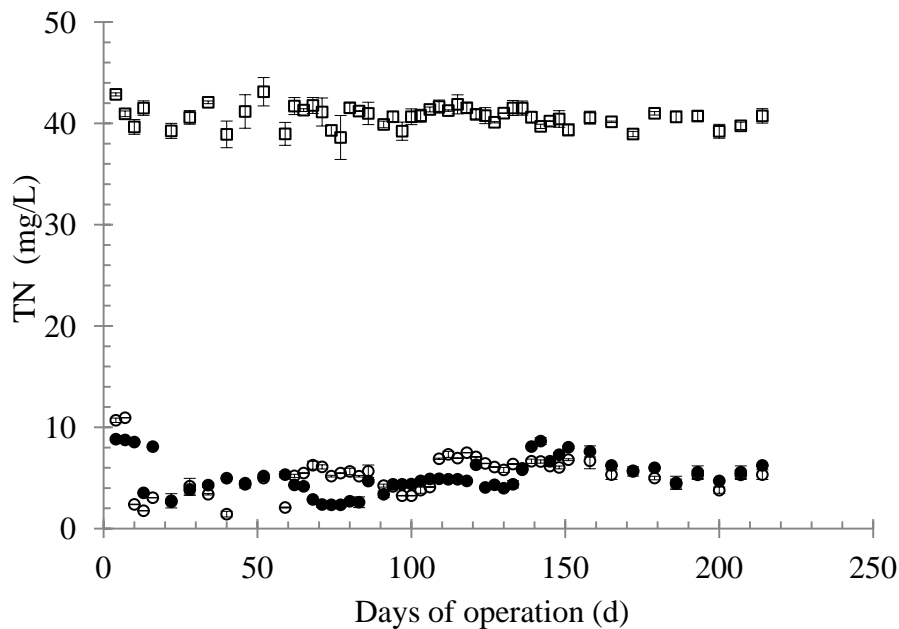


Figure 5. Influent (□) and effluent TN concentrations in the A^2/O (○) and reverse A^2/O (●) systems. The error bars represent the data range of duplicate samples.

In contrast, the effluent TP and $\text{PO}_4^{3-}\text{-P}$ data showed there was a significant difference in

the P removal performance between the A²/O and reverse A²/O systems. At an average influent TP concentration of 10.1 ± 0.2 mg/L, the effluent TP concentrations in the reverse A²/O and A²/O systems were 2.4 ± 0.6 mg/L and 2.9 ± 0.6 mg/L, respectively. The performance of these systems over time is shown in Figure 6. The average TP removal efficiency of the reverse A²/O system was $76 \pm 6\%$ (n = 46), which was significantly different (p = 0.0002) from that of the A²/O system ($70 \pm 6\%$, n = 46). In addition, at an average influent PO₄³⁻-P concentration of 8.1 ± 0.2 mg/L, the effluent PO₄³⁻-P concentrations in the reverse A²/O and A²/O systems were 1.1 ± 0.5 mg/L and 1.6 ± 0.5 mg/L, respectively (Figure 7). The average PO₄³⁻-P removal efficiencies were $86 \pm 6\%$ and $80 \pm 7\%$ in the reverse A²/O and A²/O systems, which was also statistically different (p < 0.001). The difference between the effluent TP and PO₄³⁻-P concentrations indicates the existence of refractory organic P from the feed and possibly produced in the EBPR process (e.g., acid hydrolysable P) (Gu et al., 2011).

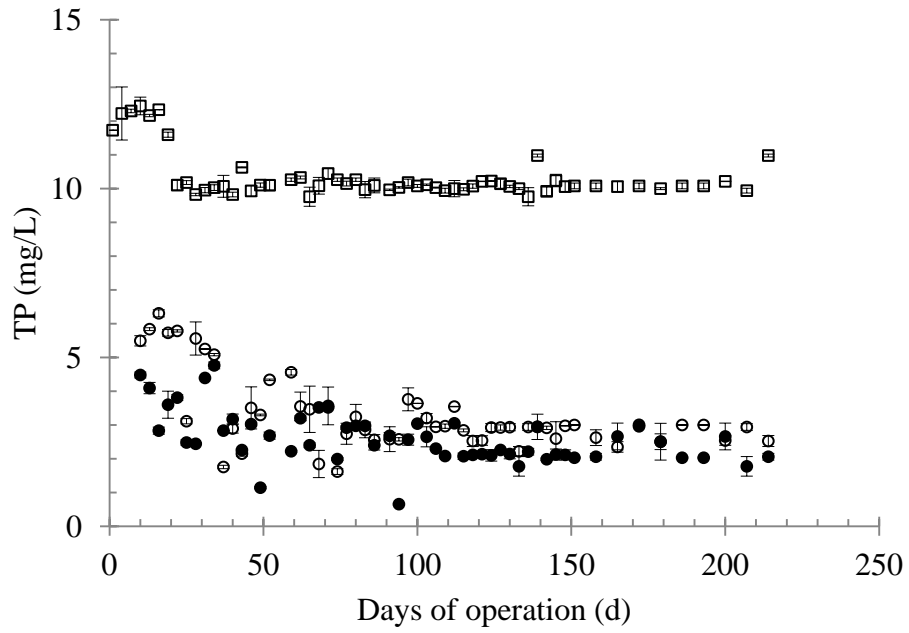


Figure 6. Influent (\square) and effluent TP concentrations in the A²/O (\circ) and reverse A²/O (\bullet) systems. The error bars represent the data range of duplicate samples.

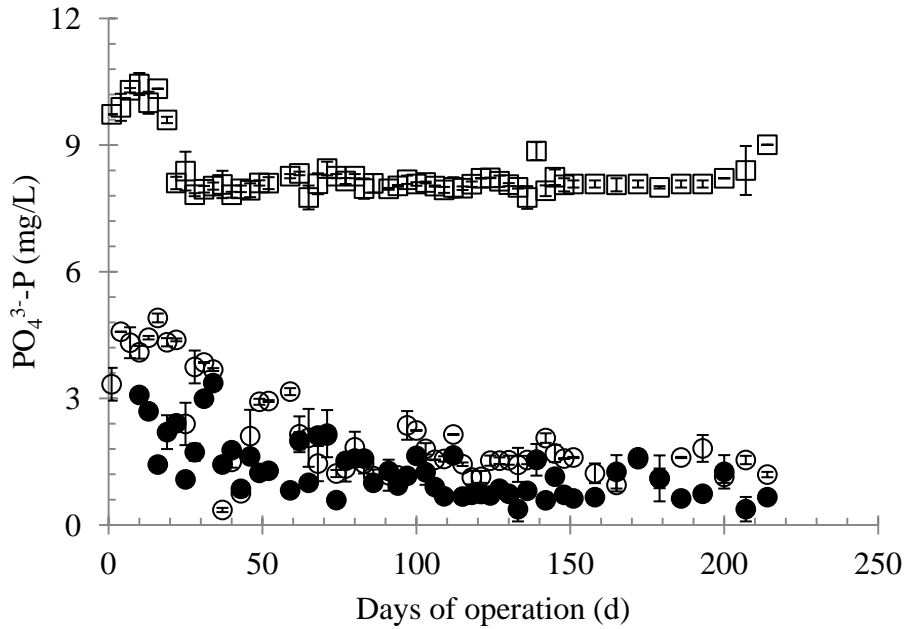


Figure 7. Influent (□) and effluent PO₄³⁻⁻P concentrations in the A²/O (○) and reverse A²/O (●) systems. The error bars represent the data range of duplicate samples.

Considering the extreme importance of maintaining a strictly anaerobic condition for enhanced biological P removal, the NO₃⁻-N concentration and ORP value in each chamber of the A²/O and reverse A²/O systems was determined. As can be seen in Figure 8a, there was a significant difference in the NO₃⁻-N concentration in the anaerobic chamber between the A²/O and reverse A²/O systems ($p = 0.04$). The higher NO₃⁻-N concentration in the anaerobic chamber of the A²/O system was due to NO₃⁻-N carried over from the RAS flow. In the reverse A²/O system, because of the reverse sequence of anaerobic and anoxic chambers, almost complete deletion of NO₃⁻-N was achieved through the two-stage

(anoxic followed by anaerobic) denitrification process. This favors the growth of PAOs that prefer to grow under alternating anaerobic and aerobic conditions. Earlier studies have shown the deleterious impact of NO_3^- -N on the P-release under anaerobic conditions (Guerrero et al., 2012, Lee et al., 2009), which could also affect P uptake and removal under aerobic conditions.

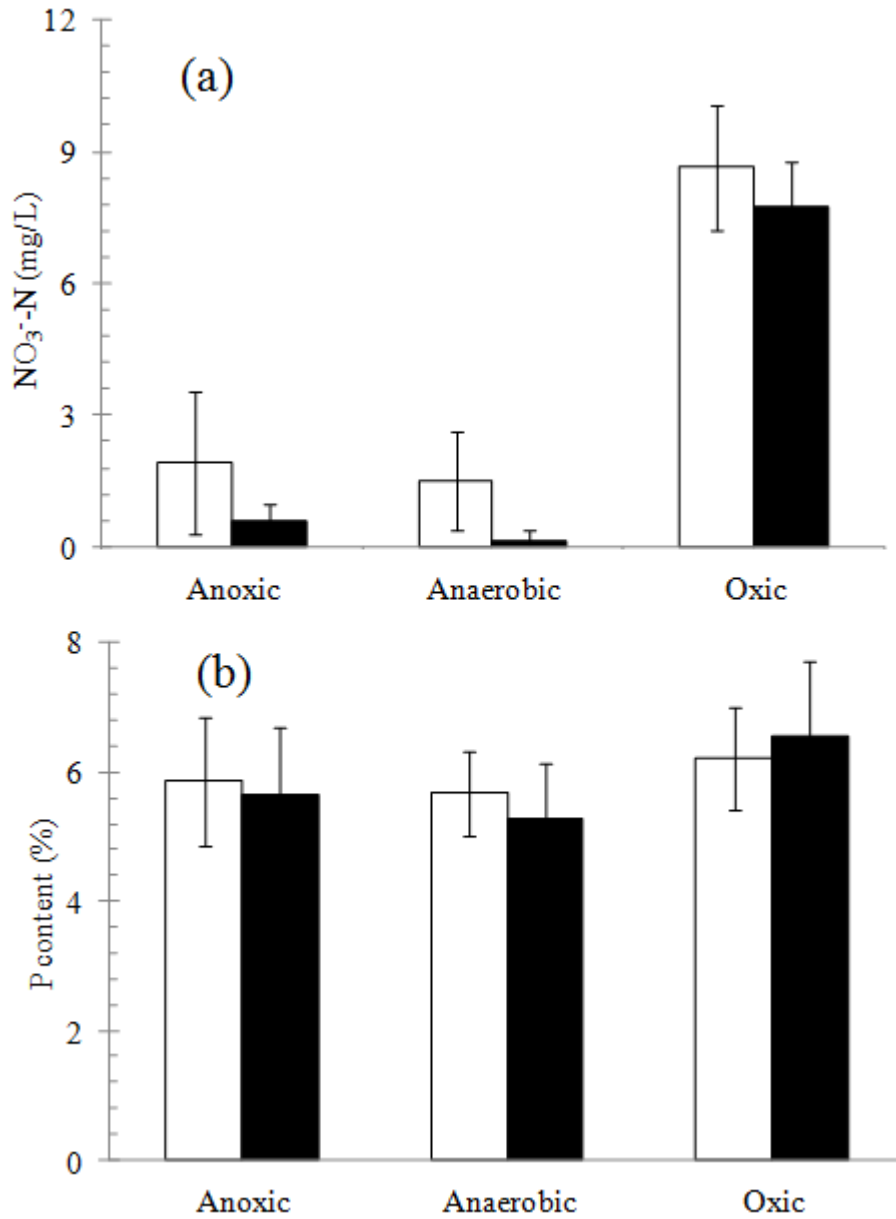


Figure 8. The NO₃⁻-N concentration distribution (a) and the sludge P content (b) in different chambers of the A²/O (□) and reverse A²/O (■) systems. The error bars represent one standard error of the mean (n = 6).

The ORP results were consistent with the nitrate distribution in different chambers and provided additional information about the biochemical environment in the A²/O and reverse A²/O processes. In the A²/O system, the ORP values for the anaerobic, anoxic, and aerobic (oxic) chambers were -170 ± 24 mV, -100 ± 39 mV, and 109 ± 23 mV, respectively. In comparison, the ORP values for the anaerobic, anoxic, and aerobic (oxic) chambers in the reverse A²/O system were -268 ± 45 mV, -145 ± 34 mV, and 152 ± 58 mV, respectively. The larger ORP change between the anaerobic chamber and aerobic chamber (420 ± 145 mV) in the reverse A²/O system may provide a better metabolic stimulus for PAOs to release and uptake P more efficiently. In the A²/O system, the presence of greater levels of NO₃⁻-N in the anaerobic chamber results in a smaller ORP difference between the anaerobic chamber and aerobic chamber (279 ± 67 mV). Therefore, it appears that the reverse A²/O process, with the anaerobic chamber followed directly by the aerobic chamber, could create a more favorable metabolic environment for P release and uptake by PAOs.

2.3.2. Sludge P Content, PAO Distribution, and P Release/Uptake Kinetics

As shown in Figure 8b, the P contents of the sludge collected from the anoxic, anaerobic and aerobic chambers of the A²/O system were $5.9 \pm 1.0\%$, $5.7 \pm 0.7\%$, and $6.2 \pm 0.8\%$,

respectively. In comparison, the P contents were $5.6 \pm 1.1\%$, $5.3 \pm 0.9\%$, and $6.5 \pm 1.1\%$ for the sludge from the anoxic, anaerobic and aerobic chambers in the reverse A²/O system, respectively. The difference in sludge P content between the sludge taken from the anaerobic and aerobic chambers was significant in both processes ($p = 0.03$ for A²/O and $p = 0.02$ for reverse A²/O). This can be explained by the fact that PAOs are able to uptake PO₄³⁻-P under aerobic conditions and release PO₄³⁻-P under anaerobic conditions, while the sludge was continuously recycled throughout the different chambers. Although the difference in sludge P content in different chambers between the two systems were not significant (p values > 0.05), the difference in P content between the sludge taken from the anaerobic zone and aerobic zone of the reverse A²/O system was higher than that of A²/O system ($p = 0.037$). This may be attributed to the lower ORP in the anaerobic chamber of the reverse A²/O system that can result in more PO₄³⁻-P release (Schon et al., 1993). While the P content per cell dry weight in the EBPR process can be higher (e.g., 12%) (Hauduc et al., 2013), an average sludge P content of 6% indicated the growth and enrichment of PAOs in the activated sludge for the A²/O and reverse A²/O systems because P content in regular activated sludge is between 1 and 3% (Van Loosdrecht et al., 1997a).

Light microscopy and fluorescent microscopy micrographs support the P measurement data for the A²/O and reverse A²/O processes. Although it was not quantified, the fraction of the PAOs in the sludge of the A²/O and reverse A²/O systems appears to be at a similar level (Figure 9). The presence of PAOs is suggested by Poly-P granules that were detected upon binding to TC in living cells taken from the sludge of the A²/O and reverse A²/O systems. These granules appear as bright (greenish) spots within the blue auto fluorescence caused by the sludge flocs. In contrast, there were no visible Poly-P granules in the activated sludge taken from a traditional wastewater treatment plant.

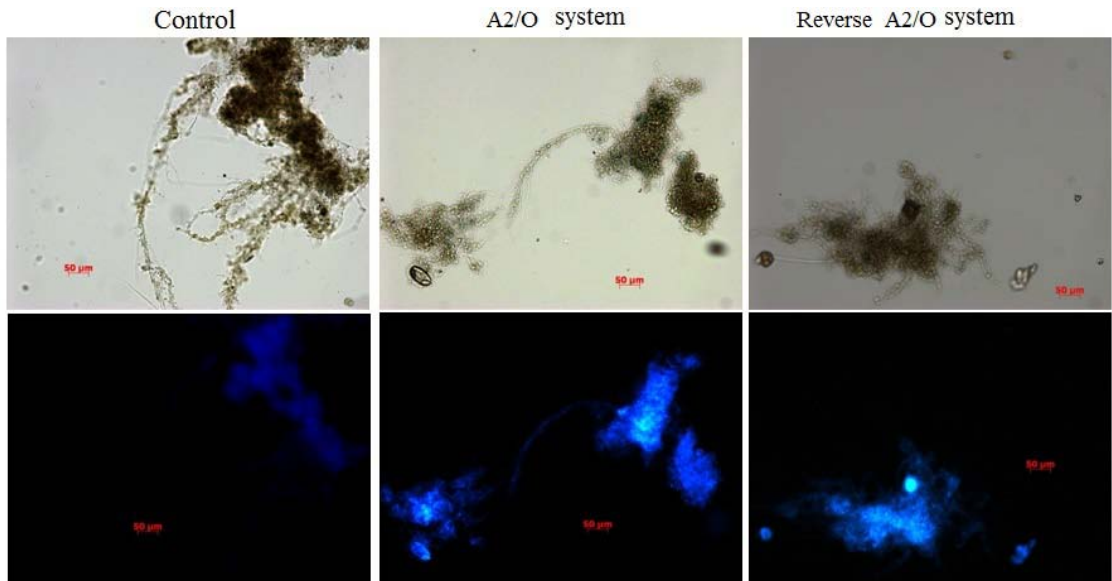


Figure 9. Light and fluorescent microscopy micrographs of the sludge taken from the A²/O, reverse A²/O, and control systems. The control was taken from a conventional activated sludge plant.

Batch studies were conducted to further investigate the P release and uptake by the sludge from the A²/O and reverse A²/O systems. Under anaerobic conditions, the sludge from the A²/O and reverse A²/O systems exhibited the same P release behavior as shown in Figure 10. The maximum P release rates were 0.22 ± 0.02 and 0.21 ± 0.02 mg P/mg MLSS/d for the the A²/O and reverse A²/O systems, respectively, with no significant difference ($p = 0.79$). These values are lower than those in the full-scale study (0.60~0.79 mg P/mg MLSS/d) because of the difference in substrate concentration and process operation (Qi et al., 2012). The maximum P concentrations in the aqueous solutions were both observed at 120 min for sludge taken from the A²/O and reverse A²/O processes. Remarkably, after 120 min, the PAOs started uptaking P even under anaerobic conditions, although the uptake was slow. This was probably due to the complete depletion of readily biodegradable COD (in the form of acetate) after 120 min, resulting in the PAOs using intracellularly stored PHAs as an energy and carbon source to uptake P for cell maintenance purposes. Although the phenomenon of P uptake under anaerobic conditions has not been reported before, there have been studies demonstrating P release under aerobic conditions (Ahn et al., 2002, Guisasola et al., 2004, Pijuan et al., 2005). The function of P release and uptake may therefore be changed in the presence or absence of external carbon sources regardless of anaerobic or aerobic conditions (Pijuan et al., 2005, Vargas et al., 2009). Under aerobic

conditions, phosphorus uptake began, and all the $\text{PO}_4^{3-}\text{-P}$ released during anaerobic phase was taken up within 80 min (Figure 8). The sludge from the A^2/O and reverse A^2/O systems exhibited the same P uptake behaviors, as well. The maximum phosphorus uptake rate were 0.32 and 0.31 mg P/mg MLSS/d for the the A^2/O and reverse A^2/O systems, with no significant difference ($p = 0.8$).

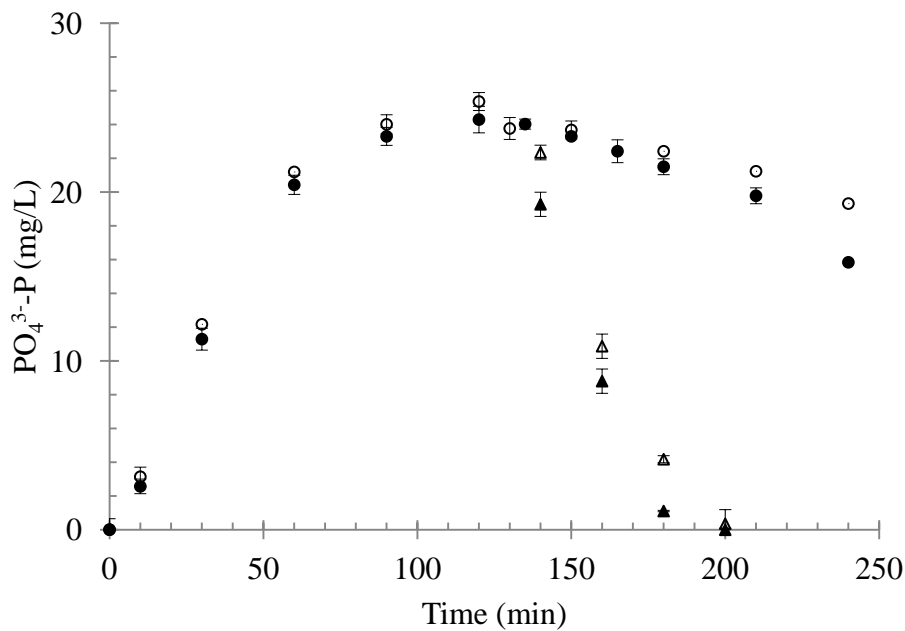


Figure 10. P release from the sludge taken from the A^2/O (\circ) and reverse A^2/O (\bullet) systems under anaerobic conditions, and P uptake by the sludge from the A^2/O (Δ) and reverse A^2/O (\blacktriangle) systems under aerobic conditions. The error bars represent one standard error of the mean ($n = 6$).

2.3.3. Microbial Activities and Sludge Settling Characteristics

The heterotrophic SOUR values were 32.7 ± 8.9 and 31.8 ± 11.6 mg O₂/g MLSS/h (n = 28) for the A²/O and reverse A²/O sludge, respectively. The autotrophic SOURs of the sludge from the A²/O and reverse A²/O were 29.2 ± 7.2 and 29.1 ± 6.4 mg O₂/g MLSS/h (n = 28), respectively. There were no significant differences in the heterotrophic (p = 0.88) and autotrophic (p = 0.97) activities between the A²/O and reverse A²/O systems. The results indicate that the change in sequence of the anaerobic and anoxic zones does not affect the regular microbial growth, as long as the appropriate SRTs were maintained in the BNR systems. Indeed, under the target SRT of 10 days, the biomass concentrations in the A²/O and reverse A²/O systems were maintained at 1550 ± 258 and 1638 ± 315 mg COD/L, respectively, with no significant differences (p = 0.12; Figure 11). The average SVI values for the A²/O and reverse A²/O systems were 129 mL/g and 122 mL/g, respectively, indicating excellent sludge settling characteristics.

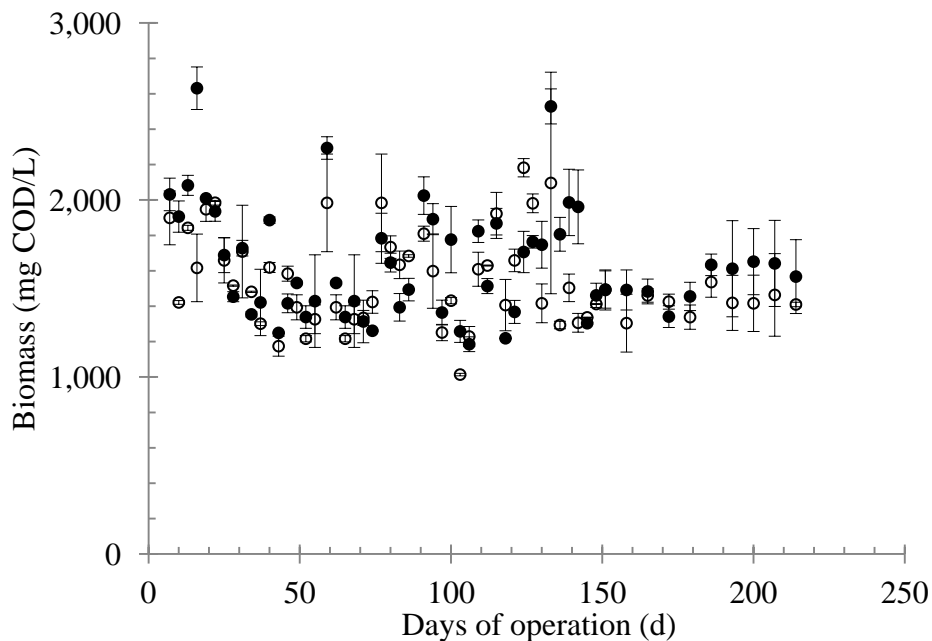


Figure 11. Biomass concentrations of the A²/O (○) and reverse A²/O (●) systems. The error bars represent the data range of duplicate samples.

2.3.4. Nitrifying Bacteria Community Structure

The T-RFLP analysis specifically targeting the AOB and NOB indicates that the AOB genera primarily consisted of *Nitrosomonas* spp. and the NOB genera contained *Nitrospira* spp. in both the A²/O and reverse A²/O systems. The peak heights in Figure 12 represent the relative abundance of each species in the A²/O and reverse A²/O systems (Regan et al., 2002). Both systems had almost the same AOB and NOB populations (p values > 0.05), while *Nitrobacter* spp. (NOB) was not detected in either the A²/O or reverse A²/O systems.

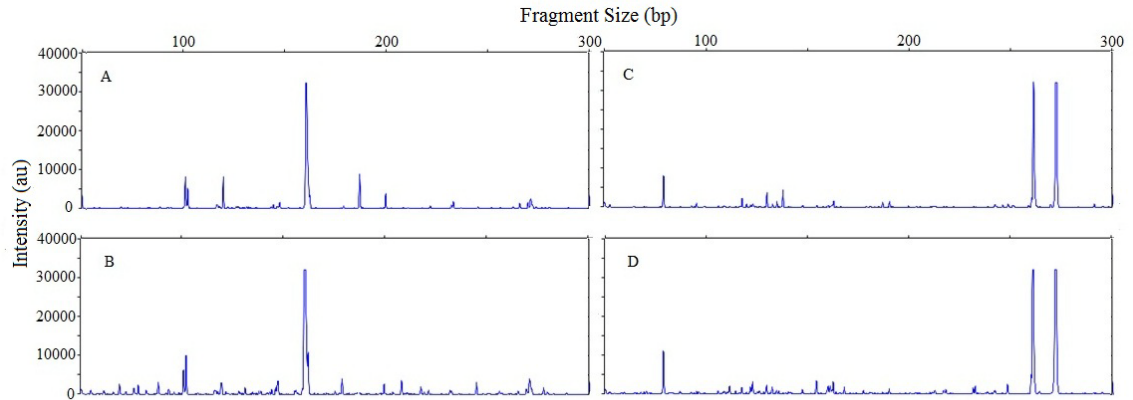


Figure 12. Nitrifying bacterial community composition reflected by T-RFLP profiles targeting 16S rRNA genes of *Nitrosomonas* (A and B, 161 bp) and *Nitrospria* (C and D, 261 and 271 bp) in the A²/O (A and C) and reverse A²/O (B and D) systems. DNA samples were taken after 3 months of stable operation.

2.3.5. Implications in Process Design and Control

By directly comparing the conventional A²/O process to the reverse A²/O process with identical operating conditions several insights and observations can be made. First of all, for both the A²/O and reverse A²/O processes, ordinary heterotrophic organisms (OHOs, including denitrifying bacteria), nitrifying bacteria, and PAOs are the three primary groups of microorganisms in the activated sludge. The different requirements for SRT between PAOs and nitrifying bacteria, along with system instability, demonstrate the challenges with simultaneous N and P removal in wastewater treatment (Gu et al., 2008). For instance, due to the slow growth of nitrifying bacteria, a longer SRT (> 8~15 d) is required for efficient and reliable N removal while a shorter SRT (< 5 d) is preferred for phosphorus

removal through wastage of high P content sludge (Onnis-Hayden et al., 2011). Competition for organic substrates between the PAOs and denitrifiers also exists when the carbon source is limited (Chiu and Chung, 2000, Kishida et al., 2004). In this study, the COD/N of 10 indicated that a sufficient carbon source was provided for the denitrifiers and the 10-d SRT was also sufficient to support the growth of nitrifiers. Therefore, the nitrogen removal was not affected by the change in sequence of the anaerobic and anoxic zones. This study confirmed that the sludge biomass concentration, the COD, and nitrogen removal efficiencies were similar for both treatment schemes under the same reactor conditions (i.e., with identical HRT, SRT, the aerobic and anoxic fractions of total volume, and the internal recycle flow rate in both cases). The expected advantage of the reverse A²/O for improved nitrogen removal was therefore not observed, as also evidenced by the similar microbial activity and nitrifying assemblages in both the A²/O and reverse A²/O systems.

Second, according to the experimental results, slightly higher phosphorus removal efficiency was observed in the reverse A²/O although the phosphorus release and uptake rates as well as the P content in the sludge were the same in both cases. In the reverse A²/O process, P release occurred in both the anoxic and anaerobic compartments, which could

result in a more efficient P release (Qi et al., 2012). More importantly, the direct anaerobic and aerobic sequence accompanied with the lower ORP in the anaerobic zone of the reverse A²/O could lead to more efficient phosphorus release under anaerobic conditions and subsequently higher P uptake efficiency under aerobic respiration. Third, the same sludge recycle and internal recirculation destination allows microorganisms to participate in a more complete anaerobic/aerobic metabolic pathway, giving rise to a "group effect" for enhanced BNR (Zhou et al., 2011). The shorter, effective, anaerobic HRT in the reverse A²/O system, due to the difference in MLR destination between the A²/O and reverse A²/O (Figure 1), could also affect P removal because of possible differences in VFA utilization mechanisms (Hauduc et al., 2013). This opens up new questions related to the competition between PAO and glycogen-accumulating organisms (GAOs). The phosphate to COD ratio we used in the study is 0.02, which is a critical value affecting the growth competition between PAOs and GAOs. When an influent contains lower than 0.02 g PO₄³⁻-P/g COD, the ability of uptaking phosphate by PAOs could be impacted adversely (Grady et al., 2011). Future work is needed to quantify PAOs and GAOs in both treatment schemes in order to determine the effect of the first anoxic zone on the proliferation of PAOs and GAOs. More study on the values and distribution of ORP in the anaerobic and aerobic zones could help elucidate their effect on P removal efficiency. In addition, how influent

wastewater containing low readily biodegradable BOD, or with low C/N ratio, would affect P removal in the A²/O and reverse A²/O systems remains to be studied and compared with each other. This is because reverse A²/O might not be working properly since all biodegradable BOD can be easily consumed by denitrifiers in the anoxic tank first.

Finally, from the engineering point of view, a lower energy consumption and operating cost may be achieved by combining the MLR with RAS flow, which also facilitates operation and maintenance (Kang et al., 2011). Chemical precipitation and biosorption of phosphorus are generally insignificant compared to EBPR in activated sludge wastewater treatment (Carlsson et al., 1997). To achieve more complete P removal, however, the ratios of the RAS and MLR flows should be optimized to maximize the growth of PAOs.

2.4. Conclusions

Both the A²/O and reverse A²/O systems showed excellent organic matter and total N removal. It was validated that the COD and nitrogen removal efficiencies were similar for both A²/O and reverse A²/O processes because the HRT, the SRT, the aerobic and anoxic fractions of total volume, and the internal recycle flow rate were the same in both cases. Placing an anoxic stage before the anaerobic stage in the reverse A²/O process, however,

resulted in a lower oxidation-reduction potential in the anaerobic zone, which contributed to higher P uptake by bacteria under subsequent aerobic respiration. The reverse A²/O process appears to be a better choice because of its higher P removal performance, and for its potentially simpler design for full-scale operation.

CHAPTER 3

3. Kinetics of Nutrient Removal by Nano Zero-Valent Iron under Different Biochemical Environments *

The effectiveness of nano zero-valent iron (NZVI, an average size of 55 nm at the concentration of 200 mg Fe/L) in nutrient removal was determined under anaerobic, anoxic and aerobic conditions. Compared to the rate of reduction of NO_3^- -N to NH_4^+ -N by NZVI alone, the presence of activated sludge increased the rate of complete reduction by 300%. About 31% of NO_3^- -N was converted to NH_4^+ -N through NZVI-facilitated dissimilatory nitrate reduction to ammonium while 56% of NO_3^- -N was removed by heterotrophic denitrification. The presence of sludge reduced the rates of phosphorus removal by NZVI, with the first-order reaction rate constants of 0.06 h^{-1} , 0.42 h^{-1} and 0.18 h^{-1} under anaerobic, anoxic and aerobic conditions, respectively. The highest P removal efficiency (95%) by NZVI was observed under anoxic abiotic conditions whereas the efficiency

* A research paper based on this thesis chapter has been published: Full citation in Water Environment Research, *in press*.

dropped to 31% under anaerobic biotic conditions, which was attributed to significant sludge-facilitated NZVI agglomeration.

3.1. Objectives

It becomes evident that NZVI has dual functions as both a reducing agent and a complexing agent/adsorbent for nitrate and phosphate removal, respectively. The objective of this study was to systematically determine the capability of NZVI in simultaneously removing nitrogen and phosphorus under different biochemical conditions while minimizing its negative effects on activated sludge wastewater treatment performance.

3.2. Materials and Methods

3.2.1. NZVI Synthesis and Characterization

NZVI particles were synthesized by the sodium borohydride reduction method ($2\text{Fe}^{2+} + \text{BH}_4^- + 3\text{H}_2\text{O} \rightarrow 2\text{Fe}^0 + \text{H}_2\text{BO}_3^- + 4\text{H}^+ + 2\text{H}_2$) (He et al., 2007). The diluted carboxymethyl cellulose (CMC, Sigma-Aldrich, St. Louis, MO) solution (0.2%, w/w) served as a capping agent (Lin et al., 2010). Briefly, 160 mL of the CMC solution was sparged with nitrogen for at least 20 min before use. Then 40 mL of freshly prepared $\text{FeCl}_2 \cdot 4\text{H}_2\text{O}$ (0.25 M) was gradually added to the CMC solution under nitrogen gas protection. Finally, a total of 50

mL freshly prepared NaBH_4 (0.4 M, Sigma-Aldrich) solution was added dropwise to the CMC solution that was magnetically stirred at 1,100 rpm at room temperature (24 ± 2 °C). Nitrogen sparging was continued for another 10 min to remove hydrogen gas. The final concentration of NZVI in the solution was 0.04 M. The NZVI stock suspension was purged with nitrogen gas throughout the synthesis process to ensure that only nano- Fe^0 was formed (Lee et al., 2008, Li et al., 2010). The NZVI particles had an average size of 55 ± 11 nm as reported in our recent study (Yang et al., 2013).

3.2.2. Batch Systems

A series of batch studies were conducted to determine the rates of nitrogen and phosphorus removal in abiotic or biotic systems. Synthetic wastewater containing sodium acetate with target concentrations of 400 mg/L chemical oxygen demand (COD), 25 mg/L NH_4^+ -N, and 10 mg/L PO_4^{3-} -P was used in each batch reactor under aerobic and anaerobic conditions. In addition, nitrate was added at a final concentration of 40 mg/L NO_3^- -N under anoxic conditions only. The synthetic wastewater also contained the following macro- and micronutrients per liter: 41 mg MgSO_4 , 14 mg $\text{CaCl}_2 \cdot 2\text{H}_2\text{O}$, 2 mg $\text{FeCl}_2 \cdot 4\text{H}_2\text{O}$, 3.4 mg $\text{MnSO}_4 \cdot \text{H}_2\text{O}$, 1.2 mg $(\text{NH}_4)_6\text{Mo}_7\text{O}_{24} \cdot 4\text{H}_2\text{O}$, 0.8 mg CuSO_4 , 0.3 mg $\text{NiSO}_4 \cdot 6\text{H}_2\text{O}$, and 1.8 mg $\text{Zn}(\text{NO}_3)_2 \cdot 6\text{H}_2\text{O}$ (Liang et al., 2010a) (Table 2). The activated sludge seed was taken

from the aeration basin at the Columbia Regional Wastewater Treatment Plant (WWTP) (Columbia, MO) and the sludge concentration was adjusted to about 2000 mg/L in each batch biotic test.

Table 2. Composition of medium used in batch studies

Medium composition	Final concentration		
	mg/L	Cations (mM)	Anions (mM)
CH ₃ COONa	512	6.24 Na ⁺	6.24 CH ₃ COO ⁻
Na ₂ HPO ₄	45.8	0.64 Na ⁺	0.32 HPO ₄ ²⁻
NH ₄ Cl	95.5	1.79 NH ₄ ⁺	1.79 Cl ⁻
NaNO ₃ *	242.9	2.86 Na ⁺	2.86 NO ₃ ⁻
MgSO ₄	41	0.34 Mg ²⁺	0.34SO ₄ ²⁻
CaCl ₂ ·2H ₂ O	14	0.096 Ca ²⁺	0.192 Cl ⁻
FeCl ₂ ·4H ₂ O	2	0.01 Fe ²⁺	0.02 Cl ⁻
MnSO ₄ ·H ₂ O	3.4	0.02 Mn ²⁺	0.02 SO ₄ ²⁻
(NH ₄) ₆ Mo ₇ O ₂₄ ·4H ₂ O	1.2	0.006 NH ₄ ⁺	0.001 Mo ₇ O ₂₄ ⁶⁻
CuSO ₄	0.8	0.01 Cu ²⁺	0.01 SO ₄ ²⁻
Zn(NO ₃) ₂ ·6H ₂ O	1.8	0.01 Zn ²⁺	0.02 NO ₃ ⁻
Ni(NO ₃) ₂ ·6H ₂ O	0.3	0.001 Ni ²⁺	0.002 NO ₃ ⁻

* Only present in anoxic batch reactors.

All the batch systems were set up in triplicate. Each anoxic or anaerobic study was conducted in a 160 mL serum bottle containing 130 mL of solution or mixed liquor and 30 mL of headspace. The bottles were sealed with both rubber stopper and aluminum caps and further covered by parafilm. The tests were initiated using a Lab-Line Orbit

Environ-Shaker (Model 3527, Lab-Line Instruments, IL) at 200 rpm to ensure complete mixing. In aerobic studies, aeration was provided through air bubbling in the solution/mixed liquor to provide 2~4 mg/L of dissolved oxygen (DO).

3.2.3. Nitrate Reduction Kinetics

To investigate the NO_3^- -N reduction kinetics under anoxic conditions, both ZVI powder (with an average size of 44 μm , Sigma-Aldrich) and NZVI were applied at a final concentration of 200 mg Fe/L according to the preliminary experimental data to compare their reactivity. In both abiotic and biotic systems, the liquid in batch reactors was purged with N_2 for 5 min to completely remove the oxygen from the solution before ZVI powder or NZVI was added. Aliquots (5 mL) of mixed liquor were collected at predetermined time intervals for nitrate and ammonia concentration measurements. To determine the rate constant of nitrate reduction, a surface-area-normalized kinetic model is used for heterogeneous reactions between reducible pollutants (e.g., nitrate) and metallic particles by fitting to the experimental data (Liou et al., 2007).

3.2.4. Phosphorus Removal under Different Biochemical Environments

Phosphorus removal was studied under anaerobic, anoxic and aerobic conditions in the presence or absence of activated sludge. In anaerobic and anoxic studies, the solution or mixed liquor was purged with N₂ gas for 5 min before NZVI was added at the final concentration of 200 mg Fe/L. Besides the seed sludge taken from the Columbia WWTP, the activated sludge from a lab-scale EBPR process was also used for comparison. To prevent the release of phosphorus in the batch assays under anaerobic conditions, the EBPR sludge was pretreated by incubating under anaerobic conditions for 120 min in order to release all the intracellular polyphosphate according to the procedure described elsewhere (Wachtmeister et al., 1997). Aliquots (5 mL) of mixed liquor were collected at predetermined time intervals for phosphate measurements.

3.2.5. Physical, Chemical and Statistical Analysis

The concentrations of NO₃⁻-N, NO₂⁻-N, NH₄⁺-N, and PO₄³⁻-P in the solution or mixed liquor were determined following the standard methods, specifically including ultraviolet spectrophotometry for NO₃⁻-N, a colorimetric method for NO₂⁻-N, nessler's method for NH₄⁺-N and ascorbic acid method for PO₄³⁻-P (APHA, 2002). The mixed liquor was filtered through a 0.22 μm syringe filter before chemical analysis. To avoid oxygen

exposure for the samples taken from anoxic and ananerobic batch studies, all sampling work was conducted in an anoxic glove box containing 5% H₂ and 95% N₂ (Coy Laboratory Producte Inc., MI). The pH of the solution was measured using a pH meter (Excel XL 15, Fisher Scietific, PA).

N₂O concentrations in the headspace were determined by gas chromatography (GC, Shimadzu 2014, Japan) equipped with a Poropak Q column (Restek, PA) and an electron capture detector (ECD) with helium as the carrier gas at a flow rate of 14 mL/min and temperatures of the column, injector and detector at 50 °C, 50 °C and 290 °C, respectively (Sims et al., 2013).

Particle size and zeta potential of NZVI in the mixed liquor were analyzed by ZEN3600 Zetasizer Nano-ZS (Malvern Instruments Inc, Westborough, MA) after taking the mixed liquor at the end of batch study.

Linear regression was performed to determine the first-order rate constants of phosphate removal, nitrate reduction and ammonia production under different biochemical

environments. ANOVA analysis was performed to assess significant difference between groups, with a p value of < 0.05 indicating statistical significance.

3.3. Results and Discussion

3.3.1. Nitrate Reduction to Ammonia by NZVI in Abiotic and Biotic Systems

As expected, NZVI was more reactive than ZVI powder in abiotic nitrate reduction. At the concentration of 200 mg Fe/L, NZVI and ZVI powder reduced $27 \pm 2\%$ and $2 \pm 0\%$ of NO_3^- -N, respectively, in 150 min when biological denitrification was complete (Figure 13). Meanwhile, ammonia (NH_4^+) was produced (Figure 14) and there was no nitrite (NO_2^-) or N_2O detected during the reaction period (data not shown). From the amount of NH_4^+ -N generation (Figure 14), only 13% of NO_3^- -N was reduced completely to NH_4^+ -N by NZVI in abiotic systems indicating the formation of other nitrate reduction products (e.g., N_2) (Yang and Lee, 2005). By contrast, the conversion of NO_3^- -N to NH_4^+ -N by ZVI powder was negligible (Figures 13 and 14), in agreement with previous studies (Huang et al., 1998, Yang and Lee, 2005). Because the rate of nitrate reduction was proportional to the surface area of Fe^0 (Huang and Zhang, 2002), NZVI having higher specific surface areas resulted in higher degree of chemical reduction of nitrate (Yang and Lee, 2005) than ZVI powder.

Nitrate reduction in biotic systems (in the presence of activated sludge) was significantly higher ($p < 0.001$) than in abiotic systems (Figure 13). During the 150-min reaction period, while NO_3^- -N was almost completely removed in biotic systems containing NZVI or ZVI

powder, about 44% of NO_3^- -N was converted to NH_4^+ -N by NZVI (Figure 14), a significant increase from only 13% under abiotic conditions. Remarkably, there was no conversion of NO_3^- -N to NH_4^+ -N by ZVI powder in the presence of activated sludge.

Since bacterial denitrification reduces NO_3^- -N as well, it is necessary to compare the overall nitrate reduction kinetics in the presence and absence of ZVI. Compared to the control (without ZVI), ZVI powder appeared to have no effect on denitrification (Figure 13) during the 150-min study period. In contrast, NZVI reduced the overall bacteria-facilitated nitrate reduction processes, which was attributed to the high reactivity and toxicity of NZVI to denitrifying organisms in activated sludge. NZVI is a known antimicrobial agent and especially effective against anaerobic organisms (Li et al., 2010). A direct contact of NZVI with the bacterial surface can result in a significant reduction in redox potential thus disrupting cell integrity (Xiu et al., 2010) while the reaction of dissolved Fe^{2+} with intracellular oxygen or hydrogen peroxide may induce ROS, further damaging the cells (Li et al., 2010, Marsalek et al., 2012).

The profiles of nitrate reduction (Figure 13) and ammonia production (Figure 14) indicated denitrifying bacteria in the sludge still play a significant role in dissimilatory nitrate

reduction regardless the presence of ZVI. NZVI particles may facilitate the microbial dissimilatory reduction of nitrate to ammonia (Hansen et al., 1996, Nielsen and Nielsen, 1998) because of significant reduction in redox potential of the cell membrane after the direct contact of nanoparticles with bacteria (Xiu et al., 2010). A process known as dissimilatory nitrate reduction to ammonium or DNRA, is also possibly activated for microorganisms that have the *nrfA* gene, which encodes a periplasmic nitrite reductase catalyzing the conversion of nitrite to ammonia (Smith et al., 2007). The presence of NZVI therefore resulted in the extension of microbial dissimilatory reduction of nitrate from regular denitrification (nitrate reduction to N_2) to DNRA, a more complete reduction of NO_3^- -N towards the formation of NH_4^+ -N. Based on the difference between the portions of nitrate reduction (Figure 13) and ammonia generation (Figure 14) in the biotic systems, it was estimated that 56% of NO_3^- -N was removed by bacteria through regular denitrification while 31% (after subtracting the 13% reduction by NZVI alone) of NO_3^- -N was completely reduced to NH_4^+ -N due to DNRA.

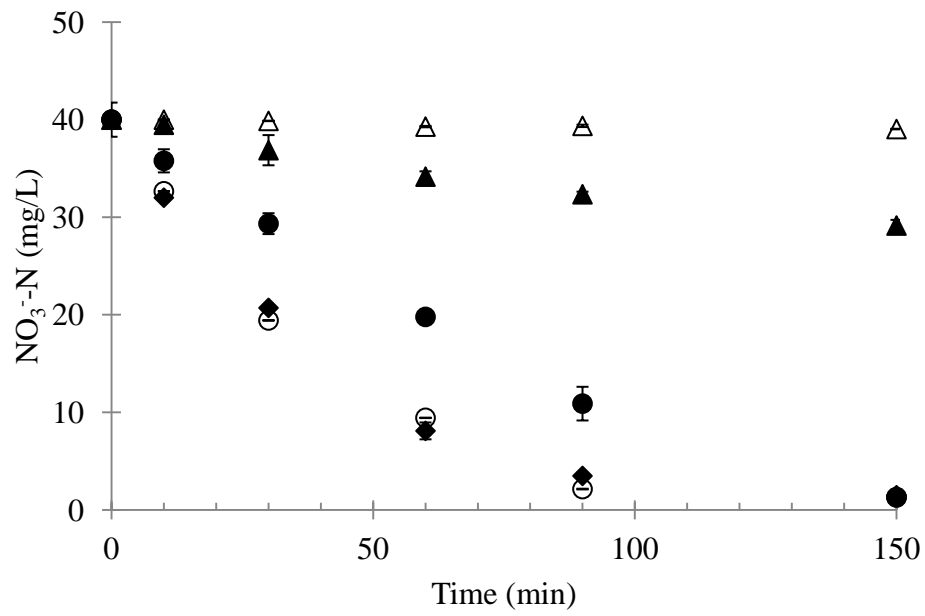


Figure 13. Nitrate removal in abiotic (▲ for NZVI and △ for ZVI powder), biotic (● for NZVI and ○ for ZVI powder) and ZVI-free biological (◆) system. Error bars represent one standard deviation from the mean of triplicate samples.

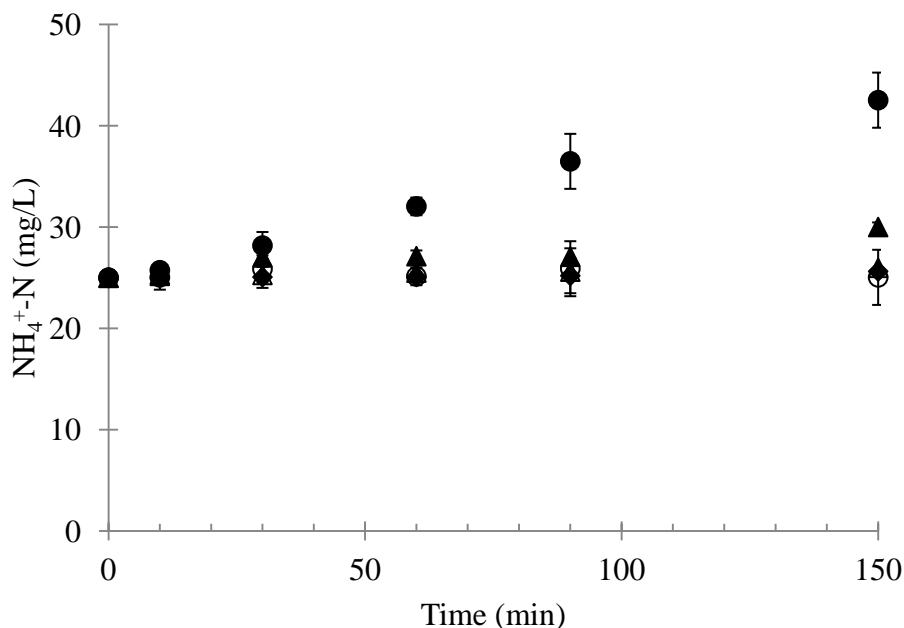


Figure 14. Ammonia generated in abiotic (▲ for NZVI and △ for ZVI powder), biotic (● for NZVI and ○ for ZVI powder) and ZVI-free biological (◆) system. Error bars represent one standard deviation from the mean of triplicate samples.

Nitrate reduction by NZVI has been described as a pseudo-first order reaction (Choe et al., 2000, Hwang et al., 2011, Tyrovola et al., 2006, Yang and Lee, 2005, Zhang et al., 2010) in abiotic systems, where the reaction rate and nitrate removal efficiency depend on factors such as initial nitrate concentration, NZVI dosage, particle size, and aqueous pH. Based on this study and previous studies (Shin and Cha, 2008), it appeared that the complete reduction of nitrate to ammonia by NZVI also followed a first-order reaction in the biotic systems. By comparing the difference of ammonia production rate between abiotic and

biotic systems (Figure 16), bacterial catalysis increased the rate of reduction of NO_3^- -N to NH_4^+ -N by 300%.

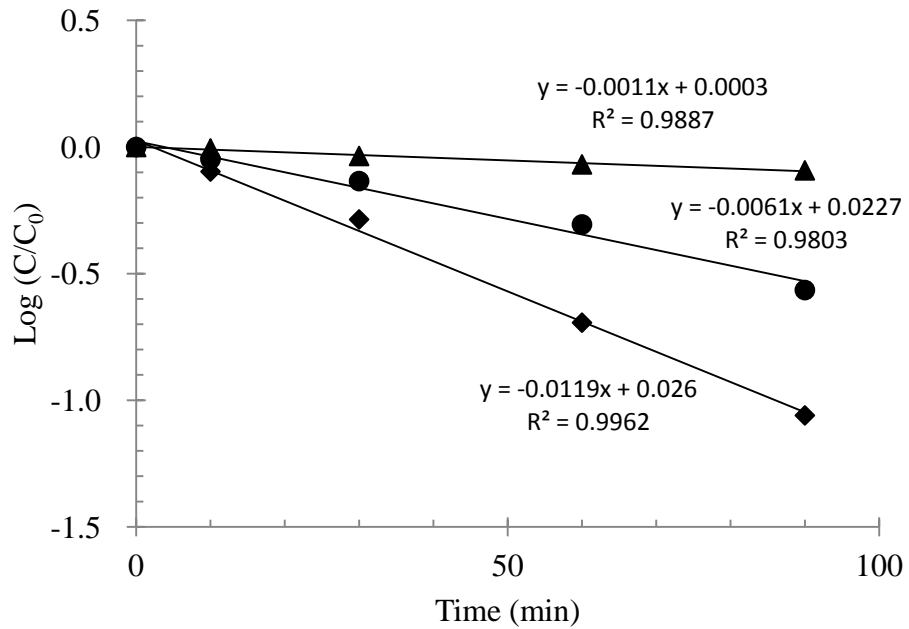


Figure 15. Observed nitrate removal by NZVI in abiotic (▲) and biotic (●) system and ZVI-free biological (◆) system.

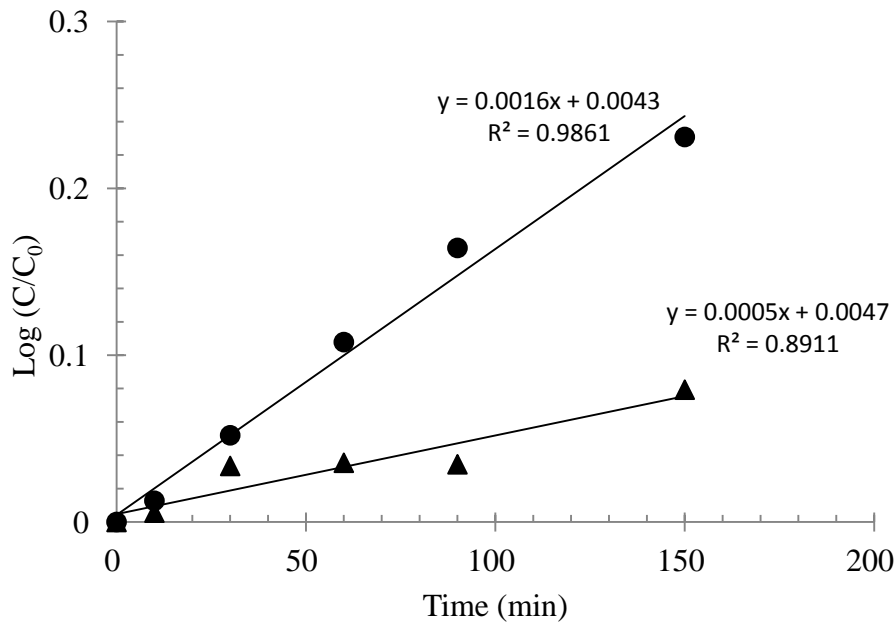


Figure 16. Observed ammonia generation by NZVI in abiotic (▲) and biotic (●) system.

3.3.2. Phosphorus Removal by NZVI under Different Biochemical Conditions

In abiotic systems, at the NZVI concentration of 200 mg/L and initial $\text{PO}_4^{3-}\text{-P}$ concentration of 10 mg/L, the overall $\text{PO}_4^{3-}\text{-P}$ removal efficiency was highest ($95 \pm 1\%$) under anoxic conditions, followed by $83 \pm 3\%$ under anaerobic conditions and then lowest ($76 \pm 4\%$) under aerobic conditions (Figure 17). The P removal by NZVI appeared to follow a first order reaction as well (Figure 18). The first-order P removal rate constants by NZVI under anaerobic and anoxic conditions were 0.3 h^{-1} and 0.6 h^{-1} , respectively.

Under aerobic conditions, the abiotic P removal kinetics may be divided into two stages (Figure 18). In the first 10 min, phosphorus was removed rapidly by NZVI while thereafter the removal rate was much slower ($p = 0.001$). The oxidation of NZVI by oxygen at neutral pH produces a rapid burst of oxidized iron species (e.g., Fe^{3+} , Fe_2O_3 and $\text{Fe}(\text{OH})_3$) (Greenlee et al., 2012, Kim et al., 2011, Ruangchainikom et al., 2006). In another study, NZVI exposed to oxygen-saturated water showed a rapid (< 24 h) loss of Fe^0 and evolved both magnetite and maghemite ($\gamma\text{-Fe}_2\text{O}_3$) within the oxide layer (Reinsch et al., 2010). Both Fe^{2+} and Fe^{3+} can react with phosphate to form iron (II, III) phosphate precipitates (Gunnars et al., 2002, Stumm and Morgan, 1996) while the freshly produced iron oxides and hydroxides are excellent materials for P adsorption on oxide surfaces by forming inner sphere complexes (Tyrovola et al., 2006). Hence, phosphorus removal was very fast initially. Thereafter, however, the rapid passivation of NZVI due to oxygen exposure (Kim et al., 2011, Reinsch et al., 2010) might result in slower rates of phosphorus removal.

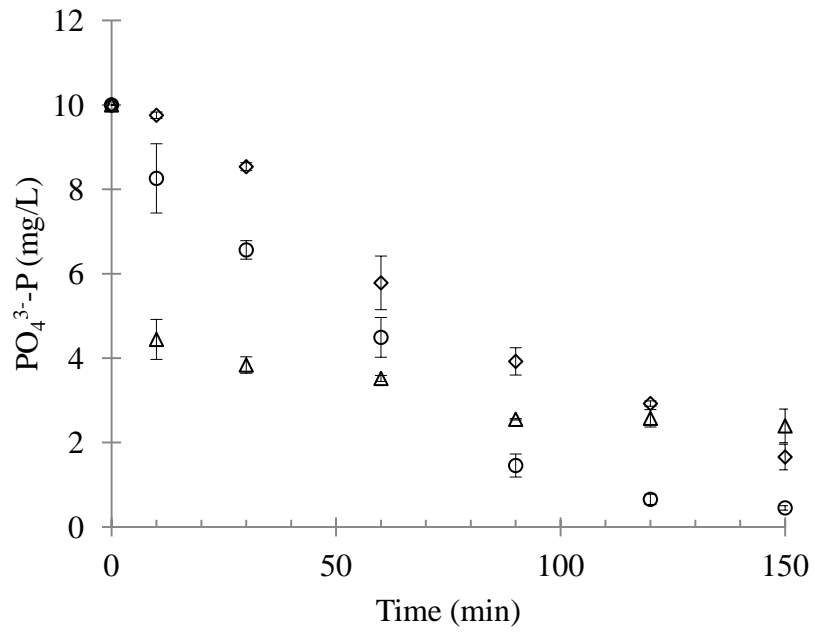


Figure 17. Abiotic phosphorus removal by dosing NZVI under anaerobic (\diamond), anoxic (\circ) and aerobic (Δ) conditions. Error bars represent one standard deviation from the mean of triplicate samples.

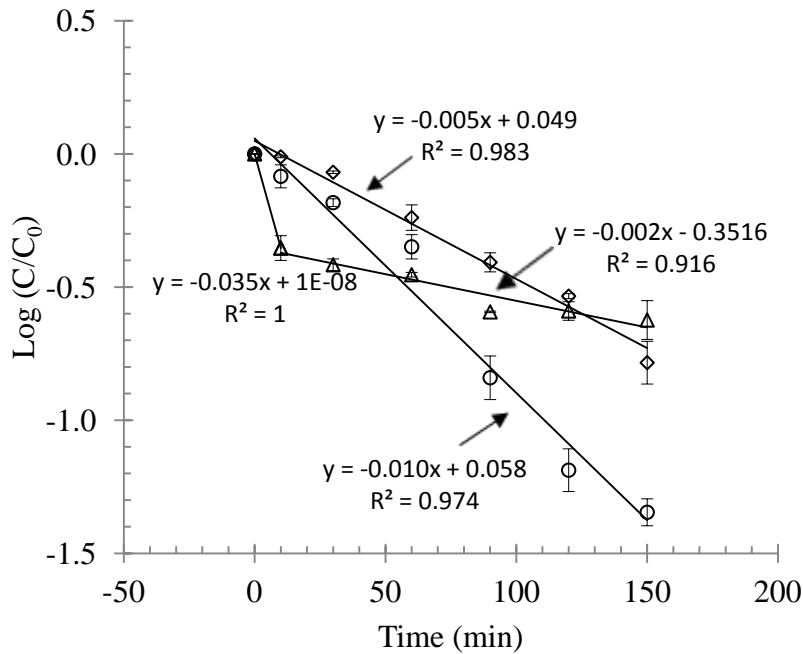


Figure 18. Observed abiotic phosphorus removal rate by dosing NZVI under anaerobic (◇), anoxic (○) and aerobic (△) conditions. Error bars represent one standard deviation from the mean of triplicate samples.

Compared to oxygen, nitrate also passivated the NZVI surface, but at a much slower rate (Reinsch et al., 2010), which could improve phosphorus removal because the iron (hydr)oxides produced by the dissolution of NZVI have a higher affinity for phosphate (Almeelbi and Bezbaruah, 2012). Other factors such as pH might affect the P removal efficiency as well. Compared to that under anaerobic or aerobic conditions (Figure 19), there was a significant pH increase due to the nitrate reduction by NZVI (also shown in Equation 4) ($p = 0.039$). In contrast, the pH was lowest under aerobic conditions due to rapid hydrolysis of iron salts which released H^+ (also indicated from Equation 7) (Stumm

and Morgan, 1996). Higher pH could facilitate the formation of Fe oxide/hydroxide and iron (II, III) phosphate complexes/precipitates thus resulting in highest P removal under anaerobic conditions.

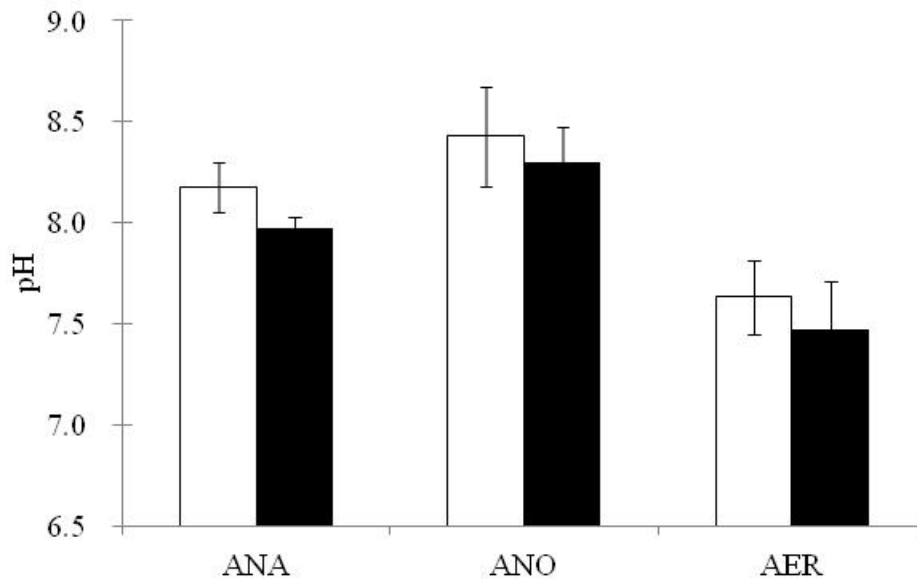


Figure 19. pH in abiotic (□) and biotic (■) systems at 150 min of the batch studies. Error bars represent one standard deviation from the mean of triplicate samples.

In biotic systems, the overall phosphorus removal efficiencies were $31 \pm 1\%$, $91 \pm 0\%$, and $66 \pm 1\%$ under anaerobic, anoxic and aerobic conditions, respectively. While the phosphorus removal kinetics followed the first-order reaction under all conditions, phosphorus removal by NZVI decreased in the presence of activated sludge, with the first-order reaction rate constants of 0.06 h^{-1} , 0.42 h^{-1} and 0.18 h^{-1} under anaerobic, anoxic

and aerobic conditions, respectively, corresponding to reductions by about 80%, 30% and 50%, respectively (Figure 20 and 21). While there was no significant difference in phosphorus removal between different activated sludge sources (Figure 20), the initial fast phosphorus removal stage was not observed under aerobic biotic conditions, indicating the microbial effect on the process of phosphorus removal by NZVI.

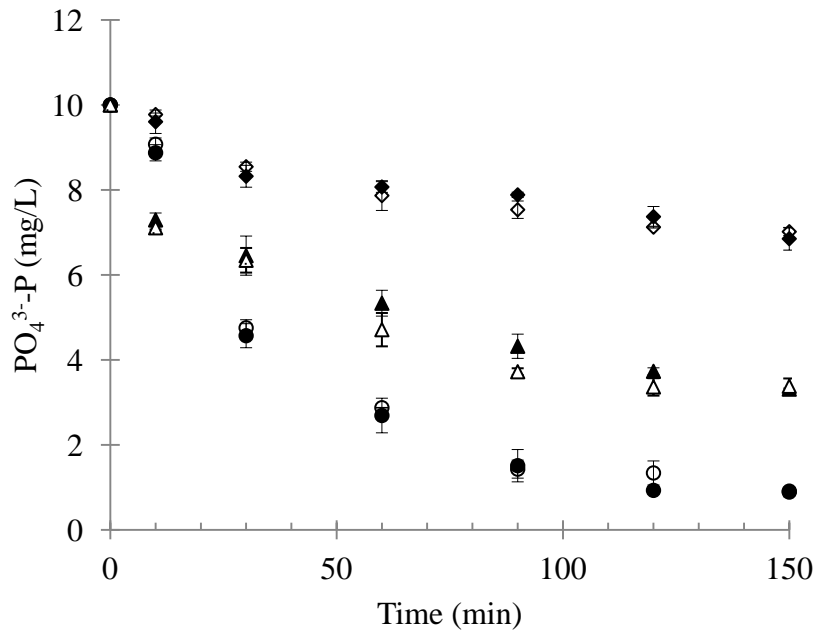


Figure 20. Phosphorus removal by dosing NZVI under anaerobic (◆ and ◇), anoxic (● and ○) and aerobic (▲ and △) conditions. The markers with fill represent WWTP mixed liquor suspended solids (MLSS) sample and the ones without fill represent the sludge from a lab-scale EBPR process. Error bars represent one standard deviation from the mean of triplicate samples.

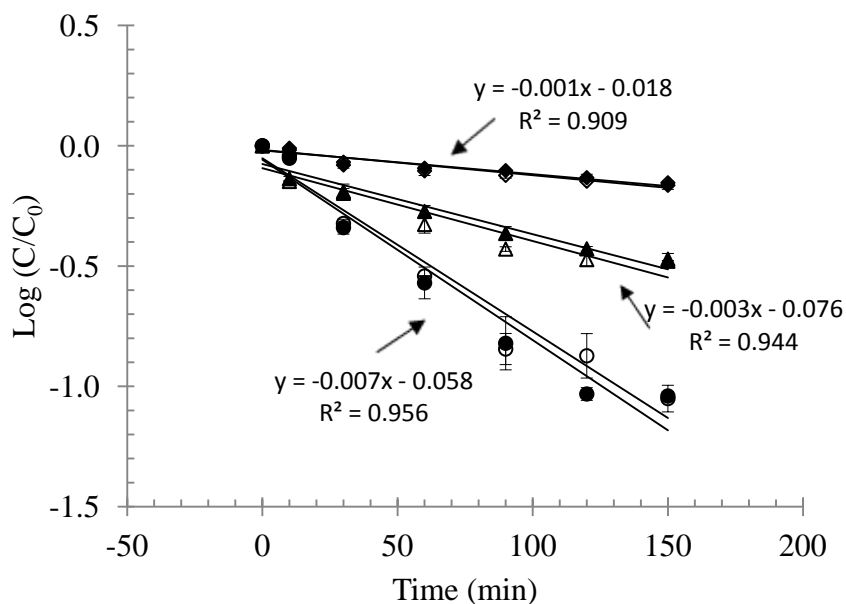


Figure 21. Observed biotic phosphorus removal rate by dosing NZVI under anaerobic (◆ and ◇), anoxic (● and ○) and aerobic (▲ and △) conditions. The markers with fill represent WWTP mixed liquor suspended solids (MLSS) sample and the ones without fill represent lab-scale Reverse A²/O process MLSS. Error bars represent one standard deviation from the mean of triplicate samples.

Indeed, the presence of activated sludge resulted in agglomeration of NZVI. In abiotic systems, the average NZVI particle sizes were $0.7 \pm 0.1 \mu\text{m}$, $0.6 \pm 0.0 \mu\text{m}$ and $0.5 \pm 0.0 \mu\text{m}$ under anaerobic, anoxic and aerobic conditions, respectively, suggesting agglomeration of NZVI in synthetic wastewater. In the presence of activated sludge in biotic systems, more significant NZVI agglomeration occurred with average particle sizes of $25.7 \pm 4.7 \mu\text{m}$, $1.4 \pm 0.1 \mu\text{m}$ and $0.6 \pm 0.0 \mu\text{m}$ under anaerobic, anoxic and aerobic conditions, respectively (Figure 22). Similar results have been reported regarding bacteria-facilitated

agglomeration of metallic nanoparticles such as NZVI (Yang et al., 2013) and silver nanoparticles (Choi et al., 2010) while the microbially derived extracellular proteins such as those rich in cysteine play an important role in rapid particle agglomeration (Moreau et al., 2007). The lowest phosphorus removal (31%) was observed under anaerobic biotic conditions, which was correlated to the most significant NZVI agglomeration ($p < 0.001$) due to the magnetic properties of iron (Phenrat et al., 2010).

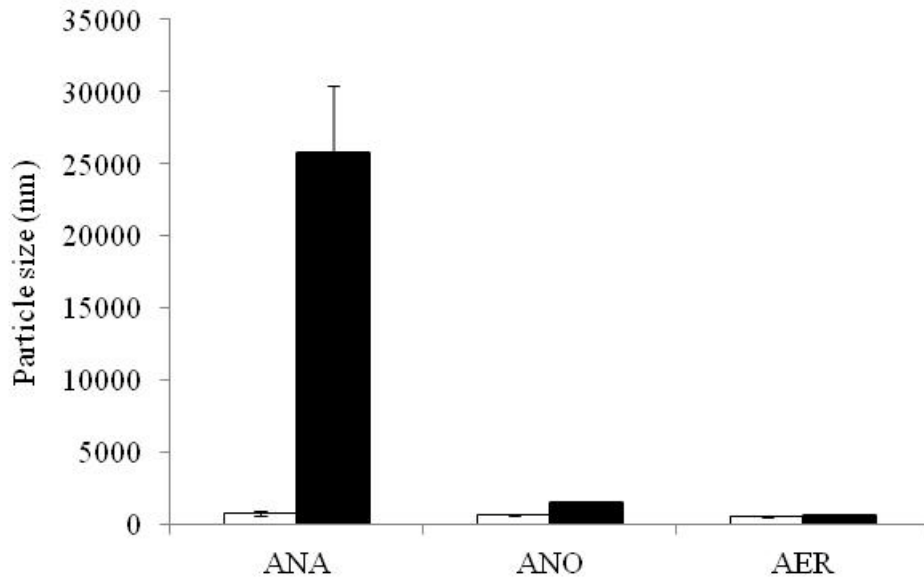


Figure 22. Particle size in abiotic (□) and biotic (■) systems at 150 min of the batch studies. Error bars represent one standard deviation from the mean of triplicate samples.

Since NZVI agglomeration is promoted by the magnetic properties of iron, it is plausible that the surface passivation caused by nitrate or DO will reduce the content of Fe^0 of NZVI

to mitigate NZVI agglomeration. The iron oxide shell formed on the NZVI surface could be responsible for the less agglomeration of NZVI particles. The formation of iron species with less magnetic (magnetite (Fe_3O_4)) or nonmagnetic (hematite (Fe_2O_3)) properties (Reinsch et al., 2010) from NZVI dissolution in the presence of oxygen might contribute to less significant particle agglomeration under aerobic conditions than under anoxic conditions. Meanwhile, the zeta potential of NZVI in all the systems remained relatively constant (Figure 23) and was consistent with the value reported earlier (around -30 mV) (Zhang and Elliott, 2006), further indicating the role of magnetic properties of NZVI in particle agglomeration.

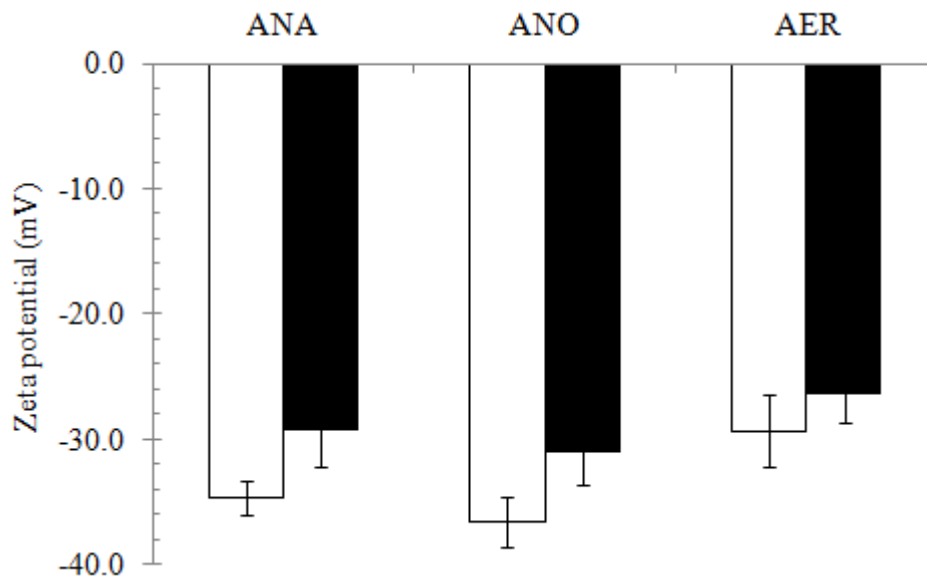


Figure 23. Zeta potential in abiotic (□) and biotic (■) systems at 150 min of the batch studies. Error bars represent one standard deviation from the mean of triplicate samples.

Yet the phosphorus removal efficiency under anoxic conditions was still higher than under aerobic conditions indicating the particle agglomeration was not the sole factor affecting P removal by NZVI. In fact, the significant increase in water pH (8.4 ± 0.2 , Figure 5) due to denitrification and dissimilatory nitrate reduction to ammonium under anoxic conditions could enhance iron phosphate precipitates (e.g., $\text{Fe}_3(\text{PO}_4)_2$, FePO_4 , and $\text{Fe}_x(\text{OH})_y(\text{PO}_4)_3$) (Stumm and Morgan, 1996) and the formation of iron oxides/hydroxides for P adsorption, thus improving phosphorus removal.

3.3.3. Applications and Implications of NZVI in Wastewater Treatment

There are several applications and implications of this study regarding the effectiveness and safe use of NZVI in biological wastewater treatment. Unlike its application for *in situ* groundwater remediation, NZVI is more commonly exposed to nitrate and dissolved oxygen in wastewater treatment. Such biochemical environments, particularly under anoxic conditions, are actually preferred for phosphorus removal by NZVI (Figure 20). Both nitrate and dissolved oxygen passivate the particle surface, thereby encapsulating the Fe^0 and decreasing NZVI reactivity (Reinsch et al., 2010) while reducing particle aggregation (Figure 22). It is therefore possible to dose NZVI in anoxic or aerobic zone to

improve phosphorus removal through precipitation and adsorption by iron oxides/hydroxides along with activated sludge flocs. On the other hand, unlike ZVI powder, NZVI facilitated dissimilatory nitrate reduction to ammonium (Figure 14), which is unwanted in secondary wastewater effluent. NZVI also exhibited inhibition to denitrification by denitrifying microorganisms (Figure 13). Nevertheless, benefits of the use of NZVI can prevail over the risk in wastewater treatment. For instance, our on-going work indicates that it could be used for sludge bulking control through selectively killing filamentous species in activated sludge treatment systems (data not shown). NZVI is also promising in biosolids treatment for odor control (Li et al., 2007). By considering its advantages and disadvantages, NZVI may be used to address urgent wastewater treatment problems such as P removal and sludge bulking control, but it is important to identify and select the appropriate dose of NZVI before use.

3.4. Conclusions

The kinetics of simultaneous nitrogen and phosphorus removal by NZVI under different biochemical conditions were determined. The rate of NO_3^- -N reduction in biotic systems was significantly higher than in abiotic systems (by NZVI alone). Unlike ZVI powder, bacterial catalytic nitrate reduction by NZVI resulted in the accumulation of ammonia.

About 31% of NO_3^- -N was converted to NH_4^+ -N through NZVI-facilitated dissimilatory nitrate reduction to ammonium (DNRA) while 56% of NO_3^- -N was removed by heterotrophic denitrification. Phosphorus removal by NZVI followed a first-order reaction, with the highest removal efficiencies observed under anoxic abiotic conditions, most likely due to P adsorption by Fe oxide/hydroxide associated with NZVI dissolution and iron phosphate complexes/precipitates at relatively higher pH values. The P removal rate was the lowest under anaerobic biotic conditions, which was attributed to the most significant NZVI agglomeration in the presence of sludge.

CHAPTER 4

4. Filamentous Sludge Bulking Control by Nano Zero-Valent Iron in Activated Sludge Treatment Systems

Sludge bulking causes loss of biomass in the effluent and deterioration of effluent water quality. This study explored the use of nano zero-valent iron (NZVI with an average particle size of 55 ± 11 nm) for sludge bulking control. In two Modified Ludzack-Ettinger (MLE) activated sludge treatment systems, a single dose of NZVI at the final concentration of 100 mg Fe/L in the mixed liquor reduced the number of filamentous bacteria Type 021N by 2-3 log units (a reduction of 99.9 and 96.7% in MLE tank #1 and #2, respectively). The side effect of the use of NZVI depended on sludge bulking conditions and biomass concentration. In the system with sludge bulking and significant sludge loss already (average biomass concentration = $1,022 \pm 159$ COD mg/L or at the ratio of 0.098 g Fe/g biomass COD), the use of NZVI increased effluent COD, NH_4^+ -N and NO_2^- -N concentrations, as also evident with loss of nitrifying populations and nitrifying activities. This resulted in more than 40 days to have the full recovery of the activated sludge system. In contrast, in the system with the early stages of bulking and the biomass concentration of

1,799 ± 113 COD mg/L (at the ratio of 0.056 g Fe/g biomass COD), the effluent water quality and overall bioreactor performance were only slightly affected for a few days.

4.1. Objectives

Because both filaments and NZVI have high surface/volume ratios, it is hypothesized that filamentous bacteria are more susceptible to NZVI exposure than floc-forming bacteria.

The main objective of this research was to explore the use of NZVI for sludge bulking control and to determine the side effect of the use of NZVI, which is likely related to sludge bulking conditions and biomass concentration (or NZVI/biomass ratio) in activated sludge wastewater treatment systems.

4.2. Materials and Methods

4.2.1. Nano Zero-Valent Iron Synthesis

The synthesis method of NZVI can be seen in 3.2.1.

4.2.2. Bioreactor Set-Up and Operation

Replicate lab-scale activated sludge systems (Tanks #1 and #2) employing a Modified Ludzack-Ettinger (MLE) process were used in this study. The MLE process was chosen so

that the approach of metabolic selection was applied in sludge bulking control while filamentous species such as type 021N would not be affected (Grady et al., 2011). Each system had a working volume of 7.4 L and consisted of anoxic and aerobic chambers separated by a glass baffle. The effective volumes of the anoxic, aerobic, and internal settling chambers were 1.9, 3.8 and 1.7 L, respectively. The feed flow rate was set at 7.2 L/d resulting in an average hydraulic retention time (HRT) of 0.8 d. There was recirculation at a flow rate equal to the influent flow rate from the aerobic chamber to the anoxic chamber in each MLE tank. For each bioreactor, a fine bubble diffuser in conjunction with the use of a magnetic stirrer provided mixing and aeration in the aeration chamber to maintain DO concentrations of 2-4 mg/L and only a magnetic stirrer was used to provide mixing in the anoxic chamber. Both bioreactors were inoculated with activated sludge obtained from the Columbia WWTP (Columbia, MO) and fed with synthetic wastewater. The synthetic wastewater (pH = 6.9 ± 0.1) prepared with tap water mainly contained nonfat dry milk powder with a target chemical oxygen demand (COD) concentration of 400 mg/L, 40 mg/L total nitrogen, 25 mg/L NH₄⁺-N and 8 mg/L PO₄³⁻-P. It also contained the following macro- and micronutrients per liter: 44 mg MgSO₄, 14 mg CaCl₂·2H₂O, 2 mg FeCl₂·4H₂O, 3.4 mg MnSO₄·H₂O, 1.2 mg (NH₄)₆Mo₇O₂₄·4H₂O, 0.8 mg CuSO₄, 0.3 mg NiSO₄·6 H₂O, and 1.8 mg Zn(NO₃)₂·6H₂O (Liang et al., 2010b). The

wastewater was prepared every 3 days and stored at room temperature (23 ± 1 °C) in a covered 130 L (volume) plastic storage bin.

The bioreactors were operated and monitored for 150 days after the start-up period, and divided into two phases. Phase I lasted for the first 60 days at the target SRT of 10 d by wasting the mixed liquor directly from the aerobic chamber. Phase II started from day 61 onwards at a long SRT (20 days) associated with high bulking potential. To determine bulking conditions, the sludge volume index (SVI) was regularly monitored following the standard methods (APHA, 2002) with modification (by taking 100-mL of the waste sludge). Through SVI measurements and microscopic observations, an instantaneous dose of NZVI in the anoxic chamber at the final concentration of 100 mg Fe/L in the entire mixed liquor was applied for sludge bulking control on day 89 and day 104 for Tank #1 and #2, respectively.

4.2.3. Filamentous Bacterial DNA and Polymerase Chain Reaction Analysis

Bacterial DNA samples were collected from each bioreactor before and after NZVI dosing at a predetermined time. Total genomic DNA was extracted from the mixed liquor taken from the aeration chamber using a MoBio Ultraclean™ Soil DNA Isolation Kit (MioBio

Laboratories, Inc., Carlsbad, CA). An average of 0.5 g biomass was collected in DNA extraction. The DNA was quantified by Nanodrop ND 1000 (NanoDrop Technologies, Wilmington, NC, USA) and its purity was analyzed by measuring the 260/280 nm absorbance ratio. The extracted DNA samples were stored at -20°C before use.

A broad range of filamentous bacteria including *Microthrix parvicella*, Eikelboom type 021N, *Gordonia* spp., *Thiothrix eikelboomii* were detected in the MLE systems by conventional polymerase chain reaction (PCR) methods as described elsewhere (Dumonceaux et al., 2006, Kumari et al., 2009, Vervaeren et al., 2005a). All primers were synthesized by Integrated DNA Technologies (Coralville, IA) and their detailed sequence information is available in Table 3.

Table 3. Primer used for filamentous bacteria detection

Target	Primer	Sequence (5'-3')	References
Most 021 N group strains	21Nf	CGTAGGCGGCTCTTTAAGTCRGAT	(Vervaeren et al., 2005b)
Most 021 N group strains	21Nr	CCGACGGCTAGTTGACATCGTTTA	(Vervaeren et al., 2005b)
<i>Gordonia</i> spp.	G268f	CGACCTGAGAGGGTGATCG	(Nielsen et al., 2004)
<i>Gordonia</i> spp	G1096r	ATAACCCGCTGGCAATACAG	(Nielsen et al., 2004)
<i>Candidatus Microthrix parvicella</i>	M1f	GGTGTGGGGAGAACTCAACTC	(Kumari et al., 2009)
<i>Candidatus Microthrix parvicella</i>	M2r	GACCCCGAAGGACACCG	(Kumari et al., 2009)
<i>T.eikelboomii</i> AP3	Cpn60 49/50f	ATAATAATGCGATTGCTCAAG	(Dumonceaux et al., 2006)
<i>T.eikelboomii</i> AP3	Cpn60 49/50r	ACGACTAAAGTGGCTAAGG	(Dumonceaux et al., 2006)
Bacterial 16S rRNA	1055f	ATGGCTGTCGTCAGCT	(Harms et al., 2003)
Bacterial 16S rRNA	1392r	ACGGGCGGTGTGTAC	(Harms et al., 2003)

For quantitative microbial analysis, Type 021N was selected as a representative filamentous species through quantitative real-time PCR (qPCR) analysis. Type 021N stands for a large group of filamentous bacteria and their growth is strongly related to an unbalanced influent composition, low molecular weight organic substrates and low oxygen concentrations in the aeration tanks (Gaval and Pernelle, 2003, Jenkins et al., 2004, Martins et al., 2004). The bacteria have also been shown to be present at moderate to high SRT (Martins et al., 2004). The qPCR assays were performed with the ABI 7500 Real time PCR System and the 7500 SDS system software (version 1.4, Applied Biosystems, CA), according to the protocols described previously with modification (Vervaeren et al.,

2005a). To avoid PCR inhibition, NZVI/iron ions in the DNA samples were removed with EDTA following a method described previously (Teng et al., 2008). PCR reactions were carried out in MicroAmp optical reaction plates (Applied Biosystems, Branchburg, NJ) containing 1 μL of each forward primer and reverse primer (stock concentration of 10 μM), 12.5 μL of SYBR Green PCR master Mix (Applied Biosystems, CA), 1.25 μL EDTA (10 mM), 0.5 μL MgCl_2 (25 mM), 3.75 μL of PCR water, and 5 μL sample DNA (a total of 4.3–11.6 ng DNA) in a 25 μL total volume. The qPCR reactions were performed starting at 50 $^\circ\text{C}$ for 2 min, followed by an initial denaturation at 95 $^\circ\text{C}$ for 10 min, and then 40 cycles of 95 $^\circ\text{C}$ for 15 s and 62 $^\circ\text{C}$ for 1 min. The dissociation step at 95 $^\circ\text{C}$ for 15 s and 60 $^\circ\text{C}$ for 1 min was added at the end to check the specificity of the PCR results (Table 4). For comparison purposes, qPCR was also applied to quantify total bacterial 16S rRNA gene copy number using primers 1055f and 1392r (Table 3). To reduce potential false-positive signals in total bacterial count, TaqMan-based detection was applied and the TaqMan probe 16S Taq1115 (6-FAM)-CAACGAGCGCAACCC-(TAMRA) was modified from the 1114f primer. The PCR Mix had a total volume of 25 μL consisting of 12.5 μL of TaqMan Universal PCR Master Mix (Applied Biosystems, CA), 1 μL of each forward primer and reverse primer (stock concentration of 20 μM), 0.5 μL of TaqMan probe, 1.25 μL EDTA (10 mM), 0.5 μL MgCl_2 (25 mM), 3.25 μL of PCR water, and 5 μL sample DNA.

The program for 16S rRNA gene amplification was set as follows: 10 min at 95 °C, 45 cycles of 30 s at 95 °C, 60 s at 50 °C, and 45 s at 72 °C.

Table 4. Primer and DNA Concentrations used in q-PCR

Methods	Component in one well	Stock Conc.	Volume per rxn ($\mu\text{L}/\text{well}$)	Final Conc in a 25- μL PCR rxn
SYBR Green ¹	F/ R Primer	10 μM	1	0.4 μM
	DNA Template (with 100 time dilution)	0.9-2.3 ng/ μL	5	0.2-0.5 ng/ μL
	SYBR PCR Mix	X	12.5	0.5 X
	PCR grade water		3.75	
	EDTA	10 mM	1.25	0.5 mM
	MgCl ₂	25 mM	0.5	0.5 mM
	Taqman Probe ²	F/ R Primer	10 μM	1
	Probe	10 μM	0.5	0.2 μM
	DNA Template (with 100 time dilution)	0.9-2.3 ng/ μL	5	0.2-0.5 ng/ μL
	Tapman PCR Mix	X	12.5	0.5 X
	PCR grade water		3.25	
	EDTA	10 mM	1.25	0.5 mM
	MgCl ₂	25 mM	0.5	0.5 mM

¹SYBR green method was for Type 021N and total PCR volume was 25 μL .

²Taqman probe method was used for total bacteria determination and total PCR volume was 25 μL .

The copy numbers of 16S rRNA genes of Type 021N and total bacteria in all the samples were determined at least in triplicate. Standard curves (mean cycle threshold (Ct) value of

triplicate assays versus log of cell number/PCR reaction) were constructed through serial dilutions of plasmid DNA carrying a cloned 16S rRNA gene of Type 021N or total bacteria using a TOPO[®] TA Cloning[®] kit (Invitrogen, CA). The PCR amplification efficiencies for Type 021N and total bacteria were 92.4% and 94.8%, respectively (Figure 24). The standard curves of the PCR assay without EDTA and MgCl₂ served as control to determine the effect of EDTA and MgCl₂ on PCR amplification efficiencies (Figure 24). The quantified 16S rRNA copy numbers were converted to cell numbers, according to the genomic information (available at <http://www.microbesonline.org>), with the assumption that Type 021N cell contains one 16S rRNA gene copy and total bacterial cell contains an average of 3.6 16S rRNA gene copies (Harms et al., 2003).

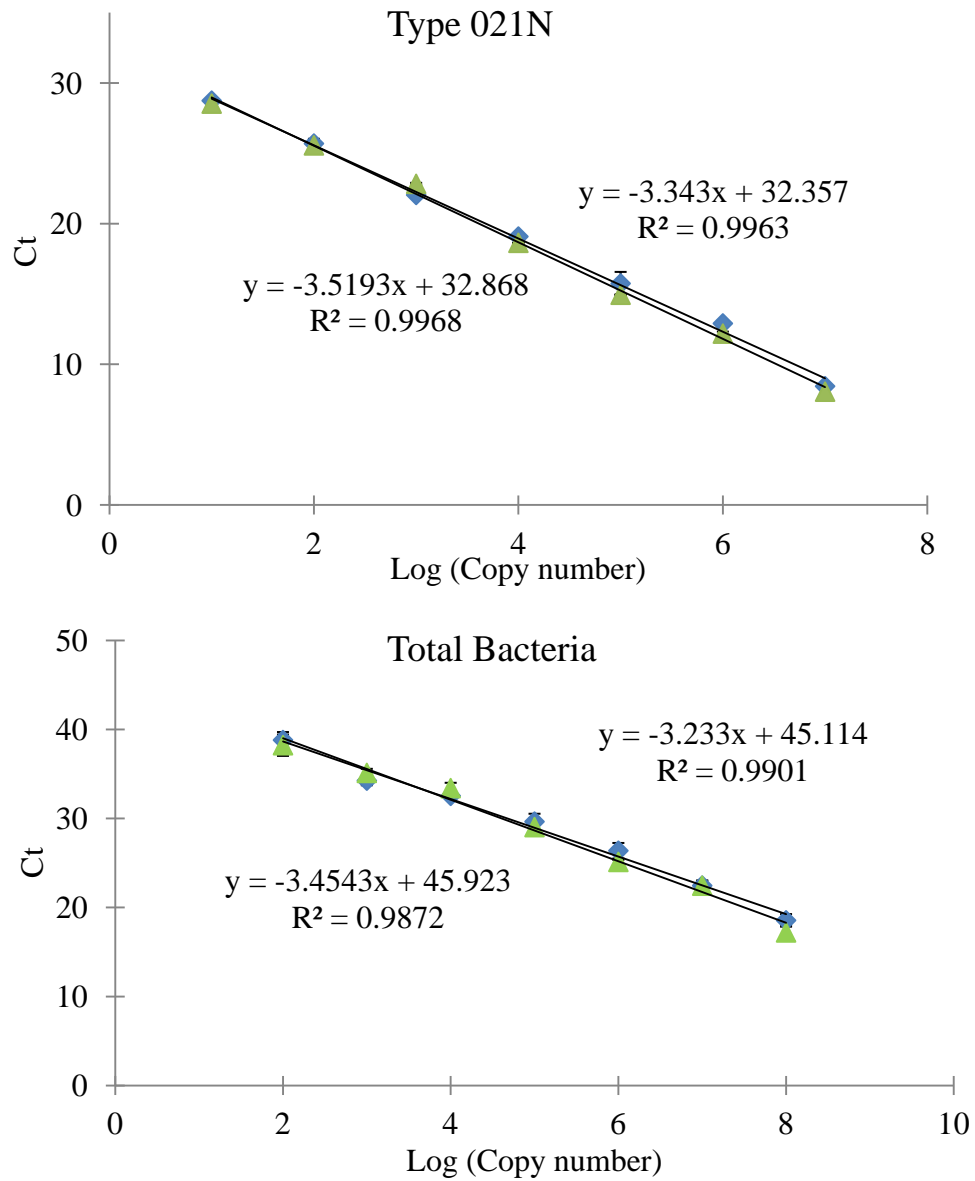


Figure 24. qPCR standard curves for Type 021N and total bacteria in the presence (◆) and absence (▲) of EDTA and MgCl₂ in PCR reactions. Error bars represent one standard deviation from the mean of triplicate samples.

4.2.4. Effect of NZVI Dosing on Nitrifying Bacterial Population and Nitrifying Activity

The side effect of NZVI dosing in activated sludge treatment systems was inferred from its effect on the growth of sensitive nitrifying bacteria, which include ammonia-oxidizing bacteria (AOB) and nitrite-oxidizing bacteria (NOB). To analyze the impact of NZVI on the nitrifying population, the collected DNA samples were analyzed by Terminal Restriction Fragment Length Polymorphism (T-RFLP) with details provided in 2.2.5.

To determine the change in nitrifying bacterial activity, aliquots of mixed liquor were periodically taken from the aeration chamber to determine the specific oxygen uptake rates (SOUR), with detailed procedures described in 2.2.4.

4.2.5. Microtiter Assay and NZVI Dose Choice

A turbidimetric microtiter assay was applied to evaluate the toxicity of NZVI on the growth of active sludge bacteria (at the concentration of about 2000 mg/L of biomass COD) at different concentrations (20, 100 and 200 mg Fe/L). Activated sludge samples from the Columbia WWTPs were washed with 1 × phosphate buffered saline (PBS) three times to remove the residue organic matter and nutrients before use. Aliquots (20 µL) of sludge samples in 8 replicates were added to the microplate wells followed by the addition of 180

μL sterile basal mineral medium in each well. The absorbance of cell culture in each microwell was measured at 600 nm every 1 hour for about 48 h by a microreader (VICTOR3, PerkinElmer, Shelton, USA). Activated sludge sample with no NZVI treatment served as control.

Figure 25 shows bacterial growth curves in the presence of NZVI using a microtiter assay. Compared with the control having the specific bacterial growth rate of $2.36 \pm 0.37 \text{ d}^{-1}$, the presence of NZVI at 20, 100 and 200 mg/L reduced the specific growth rates to $2.16 \pm 0.52 \text{ d}^{-1}$, $1.61 \pm 0.28 \text{ d}^{-1}$ and $1.59 \pm 0.43 \text{ d}^{-1}$, respectively. By increasing the NZVI concentration from 20 to 100 mg/L, the reduction in bacterial growth was increased from 8% to 32%. However, further reduction was not observed when NZVI concentration was increased to 200 mg/L. Therefore, an instantaneous, one-time dose of NZVI at the final concentration of 100 mg Fe/L in the mixed liquor was applied in the MLE bioreactors for sludge bulking control.

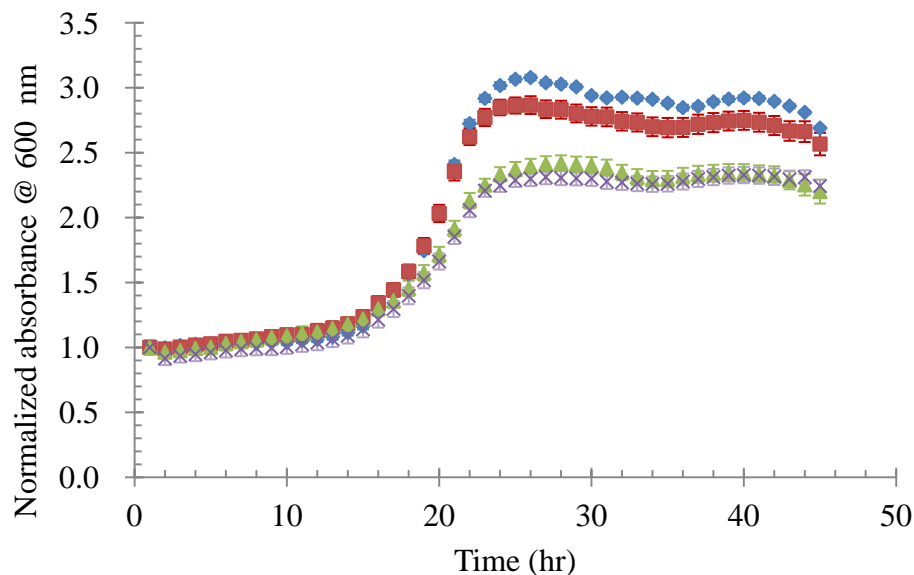


Figure 25. Aerobic bacterial growth, as indicated by optical density measurements at 600 nm, in the groups treated with different NZVI concentrations: Control (◆), 20 mg/L (■), 100 mg/L (▲) and 200 mg/L (×). Activated sludge from the Columbia WWTP was used as a seed culture. The error bars represent one standard error of the mean (n = 8).

4.2.6. Microscopic, Chemical and Statistical Analysis

Activated sludge in the aeration chamber was periodically subjected to light microscopic examination (Axioskop Zeiss microscope). One day after NZVI dosing into each MLE bioreactor, the activated sludge samples were subjected to live/dead analysis after fluorescent staining with the LIVE/DEAD® BacLight™ bacterial viability kit (Invitrogen Co., Carlsbad, CA), according to the work reported elsewhere (Hu et al., 2003). A

laser-scanning confocal microscope (Zeiss LSM 510 META) was used for fluorescence imaging of bacterial cells.

The influent and effluent water quality parameters such as COD, $\text{NH}_4^+\text{-N}$, $\text{NO}_2^-\text{-N}$, $\text{NO}_3^-\text{-N}$, and orthophosphorus in the MLEs were measured in duplicate following the standard methods (APHA, 2002). Biomass concentration was measured in COD units (Contreras et al., 2002, Münch and Pollard, 1997). One-way ANOVA analysis was conducted to assess the significance of the difference among groups, with $p < 0.05$ indicating statistical significance.

4.3. Results and Discussion

4.3.1. Sludge Bulking Associated with Long SRT Operation and Bioreactor Performance

Both MLE bioreactors were initially operated at the SRT of 10 d for about two months. The SRT increased to 20 days from day 61 onwards. As long SRT operation often favors filamentous bacterial growth (Grady et al., 2011) while short SRTs (< 5.7 d) suppress the growth of filamentous bacteria (*Microthrix parvicella*) (Noutsopoulos et al., 2006), an increase in SRT from 10 to 20 d encouraged sludge bulking as indicated from the SVI measurements and confirmed by light microscopy (Figures 26 and 27). In Tank #1, the SVI

value increased from < 100 mL/g at the SRT of 10 d to 333 mL/g after about 20 days of operation at the SRT of 20 d. For comparison, the SVI increase was slower in Tank #2, where the SVI increased from < 100 mL/g at the SRT of 10 d to 210 mL/g after about 40 days of operation at the SRT of 20 d (Figure 26). Though SVI values above 150 mL/g indicate sludge bulking (Metcalf and Eddy, 2003), the different trends in SVI change suggest the uncertainty and complex sludge bulking mechanisms involved in each bioreactor, even though the two tanks were identical and operated at the same HRT and SRT.

Correspondingly, the degree of loss of sludge differed between the two bioreactors during sludge bulking. At the SRT of 10 d with no evidence of sludge bulking, the average biomass COD concentrations in Tank #1 and #2 were $2,332 \pm 255$ mg/L and $2,269 \pm 235$ mg/L, respectively (Figure 28). There was no significant difference in the biomass concentration between the two bioreactors ($p = 0.67$). At the SRT of 20 d, due to sludge loss in the effluent associated with bulking, the biomass COD concentration in Tank #1 gradually reduced to $1,022 \pm 159$ mg/L on day 89. For comparison, in Tank #2, the biomass COD concentration was only reduced to $1,799 \pm 113$ mg/L on day 104 (after about 40 days of operation at an average SRT of 20 d). The SVI data (Figure 26) and microscopic

observation (Figure 27) also confirmed that sludge in Tank #1 was already bulking, resulting in sludge loss, while sludge in Tank #2 was in the early stages of bulking.

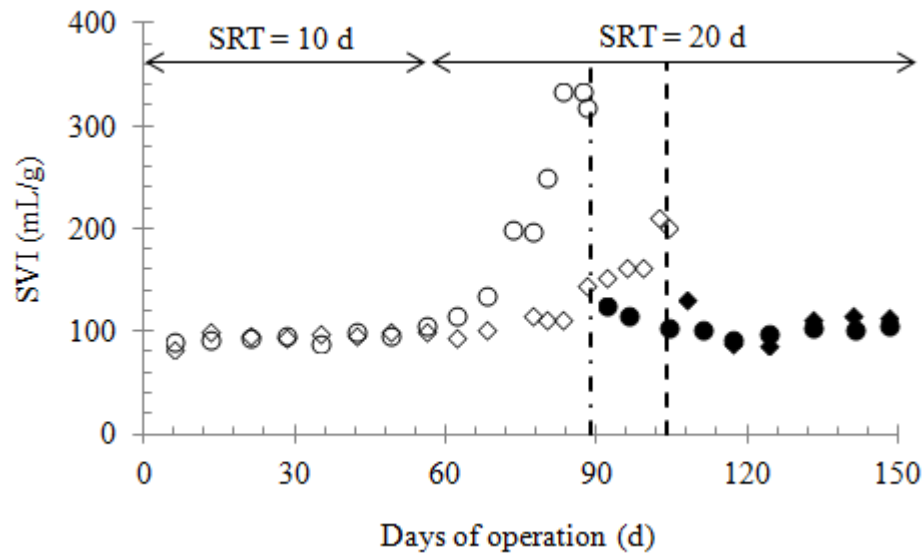


Figure 26. SVI values in Tank #1 before (○) and after (●) NZVI dosing on day 89 and SVI values in Tank #2 before (◇) and after (◆) after NZVI dosing on day 104. Two vertical hashed lines show the days of NZVI addition in Tanks #1 and #2, respectively.

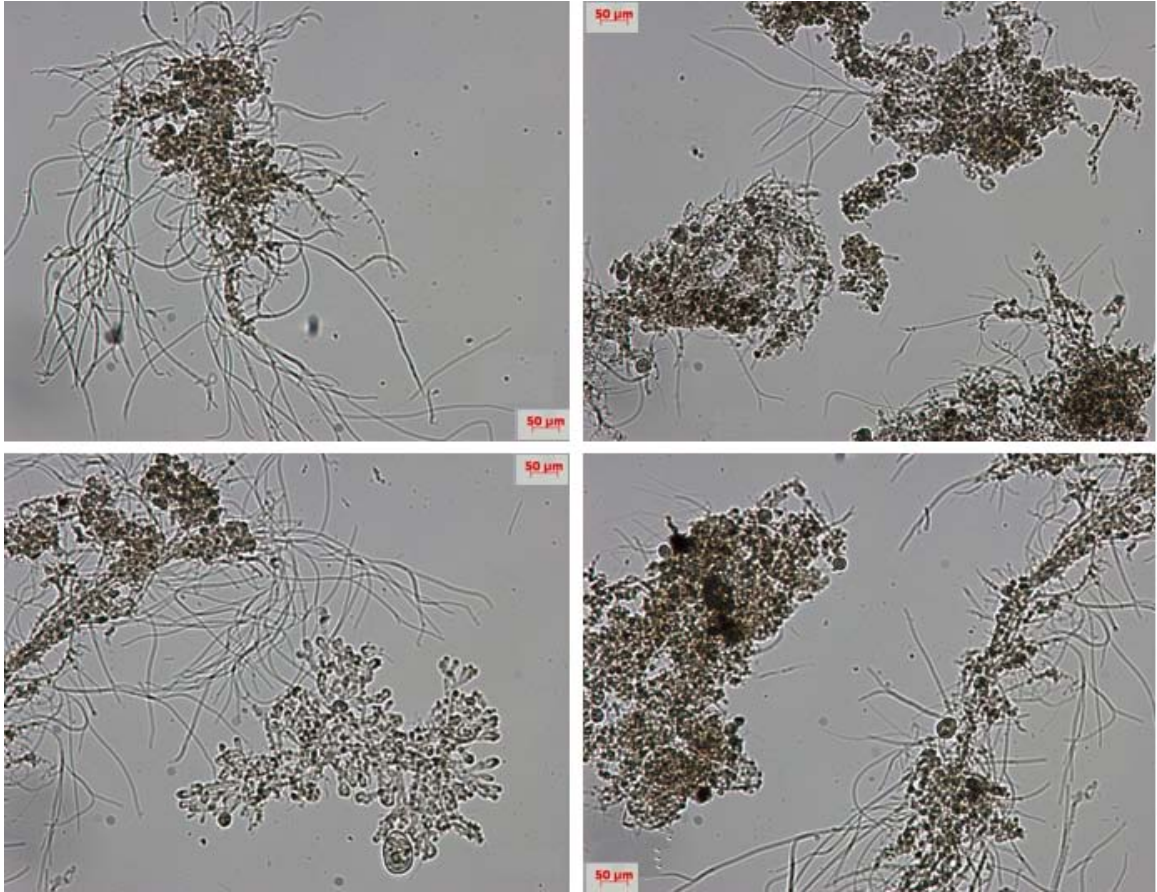


Figure 27. Micrographs of light microscopy of activated sludge samples from Tank #1 (left panel) and Tank #2 (right panel) taken on day 80 and 100, respectively.

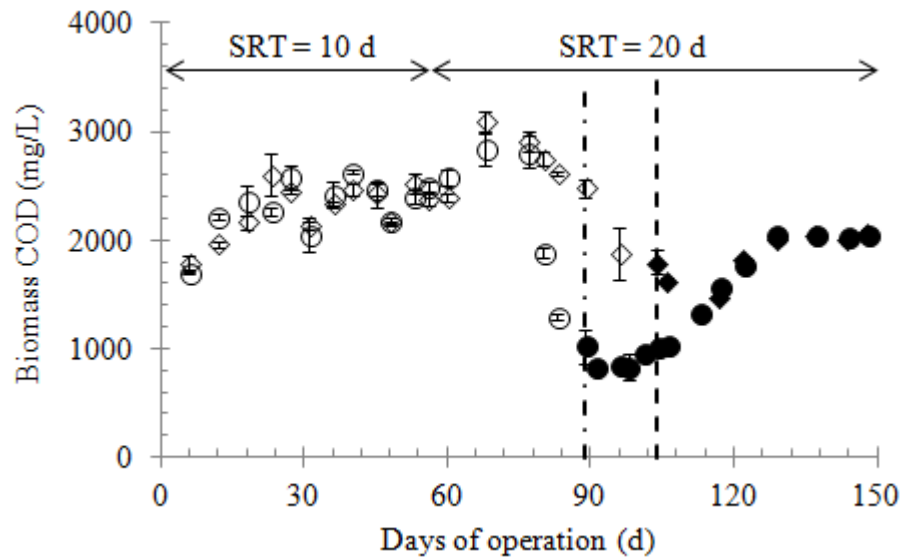


Figure 28. Biomass concentrations in Tank #1 (\circ) and Tank #2 (\diamond) before NZVI dosing and in Tank #1 (\bullet) and Tank #2 (\blacklozenge) after NZVI dosing on day 89 and day 104, respectively. Two vertical hashed lines show the days of NZVI addition in Tanks #1 and #2, respectively. The SRT was increased from 10 to 20 day from day 61 onwards. Error bars represent the range of duplicate samples.

Figures 29 and 30 demonstrate that sludge bulking affected effluent water quality. At the SRT of 10 d (with no sludge bulking) and influent COD concentration of 403 ± 47 mg/L, the effluent COD concentrations from Tank #1 and #2 were 21 ± 5 mg/L and 20 ± 5 mg/L, respectively, resulting in a similar average removal efficiency of 95% (Figure 29). There were also no significant differences in effluent $\text{NH}_4^+\text{-N}$ ($p = 0.75$), $\text{NO}_2^-\text{-N}$ ($p = 0.73$) or $\text{NO}_3^-\text{-N}$ ($p = 0.66$) concentrations between the two MLE bioreactors. The effluent $\text{NH}_4^+\text{-N}$ concentrations from Tank #1 and #2 were 0.4 ± 0.1 mg/L and 0.4 ± 0.2 mg/L, respectively, with removal efficiencies of 98% and 99%, respectively, indicating almost complete

nitrification (Figure 30A). Correspondingly, the effluent NO_2^- -N concentrations from Tank #1 and #2 were 0.4 ± 0.6 mg/L and 0.5 ± 0.7 mg/L, respectively, and the effluent NO_3^- -N concentrations were 20.2 ± 1.9 mg/L and 20.4 ± 1.9 mg/L, respectively.

As the SRT was increased to 20 days from day 61 onwards, the average effluent COD concentrations before NZVI dosing in Tank #1 and #2 increased to 40 ± 13 mg/L and 37 ± 7 mg/L, respectively (Figure 29). This was mainly attributed to the loss of sludge in the effluent due to sludge bulking. Meanwhile, the average effluent NH_4^+ -N and NO_2^- -N concentrations in Tank #1 increased significantly to 1.2 ± 1.4 mg/L and 1.9 ± 1.6 mg/L, respectively, while the effluent NO_3^- -N concentration decreased to 15.9 ± 6.3 mg/L. The much higher effluent NH_4^+ -N and NO_2^- -N concentrations in Tank #1 were linked to its more serious sludge bulking and biomass loss in the effluent, suggesting that nitrifying bacteria are more easily washed out and susceptible to perturbation associated with filamentous sludge bulking. For comparison, with the sludge in the early stages of bulking in Tank #2, the average effluent NH_4^+ -N and NO_2^- -N concentrations before NZVI dosing remained relatively low at 0.5 ± 0.2 mg/L and 0.4 ± 0.2 mg/L, respectively.

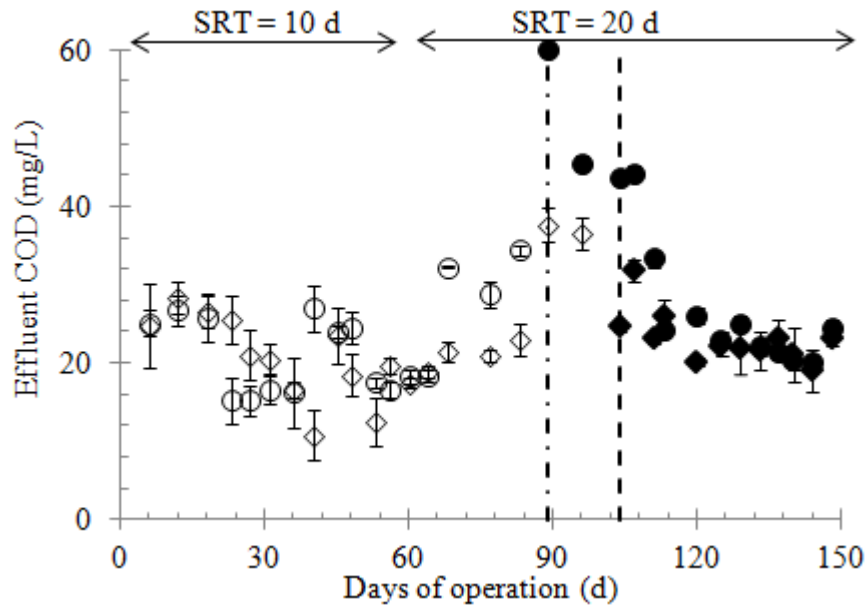
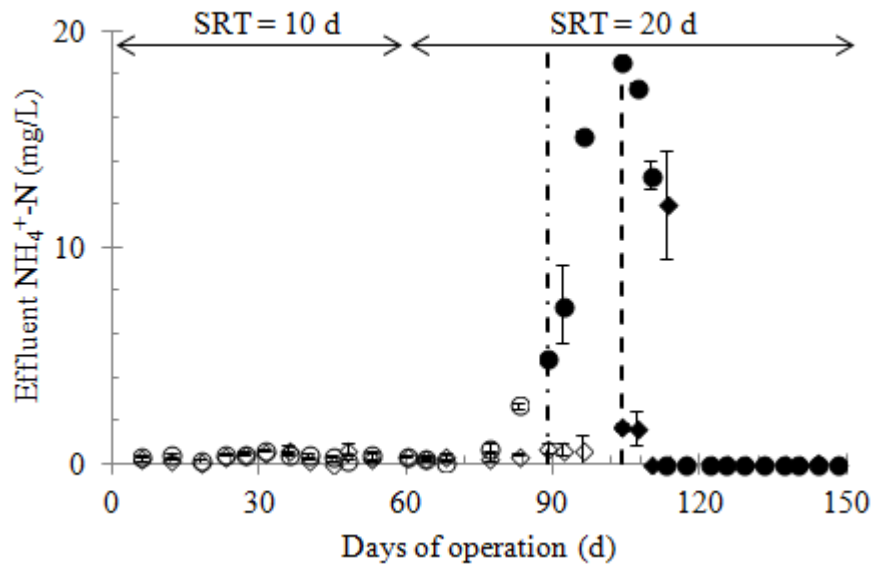
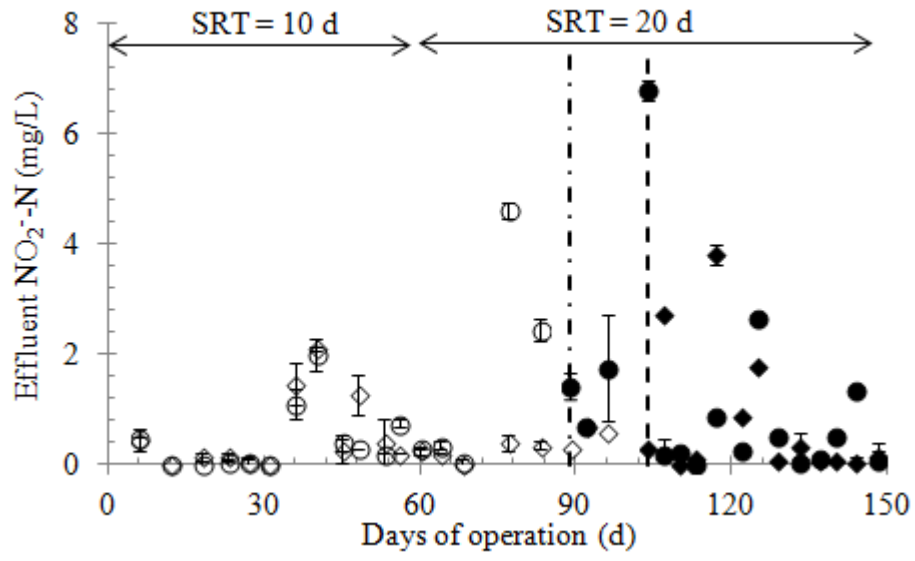


Figure 29. Effluent COD concentrations in Tank #1 (○) and Tank #2 (◇) before NZVI dosing and in Tank #1 (●) and Tank #2 (◆) after NZVI dosing on day 89 and day 104, respectively. Two vertical hashed lines show the days of NZVI addition in Tanks #1 and #2, respectively. Error bars represent the range of duplicate samples.

(a)



(b)



(c)

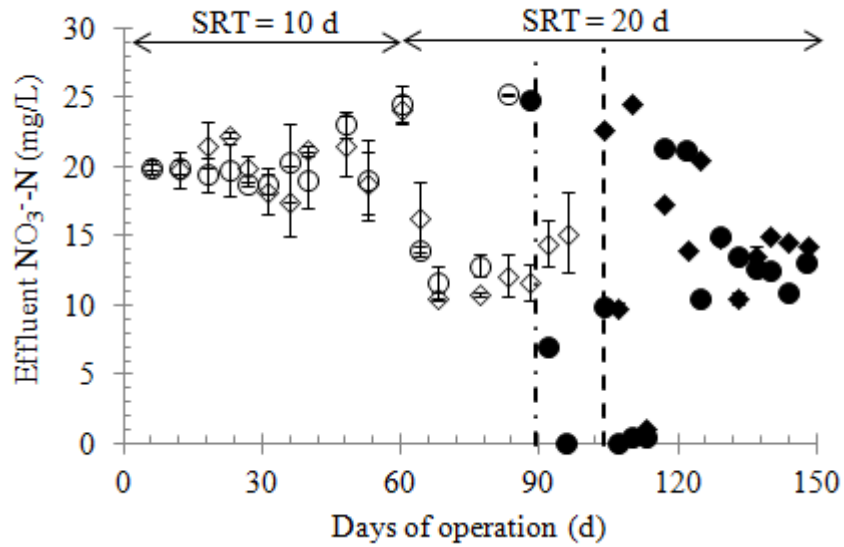


Figure 30. Effluent NH_4^+ -N (a), NO_2^- -N (b) and NO_3^- -N (c) concentrations in Tank #1 (\circ) and Tank #2 (\diamond) before NZVI dosing and in Tank #1 (\bullet) and Tank #2 (\blacklozenge) after NZVI dosing on day 89 and day 104, respectively. Error bars represent the range of duplicate samples.

4.3.2. Effectiveness of NZVI in Killing Filamentous Bacteria

Among the filamentous bacteria studied, Type 021N and *Gordonia* spp. were detected most often while *Thiothrix eikelboomii* was only detected in Tank #1 (data not shown). Type 021N bacteria were found to be excessive at the SRT of 20 d in Tank #1 on days 88 and 89 and Tank #2 on day 104 (Figure 31). The bloom of Type 021N species in Tank # 2 was delayed for about 15 days with a smaller population for unknown reasons, which was in agreement with the sludge bulking conditions observed through SVI measurements and light microscopy.

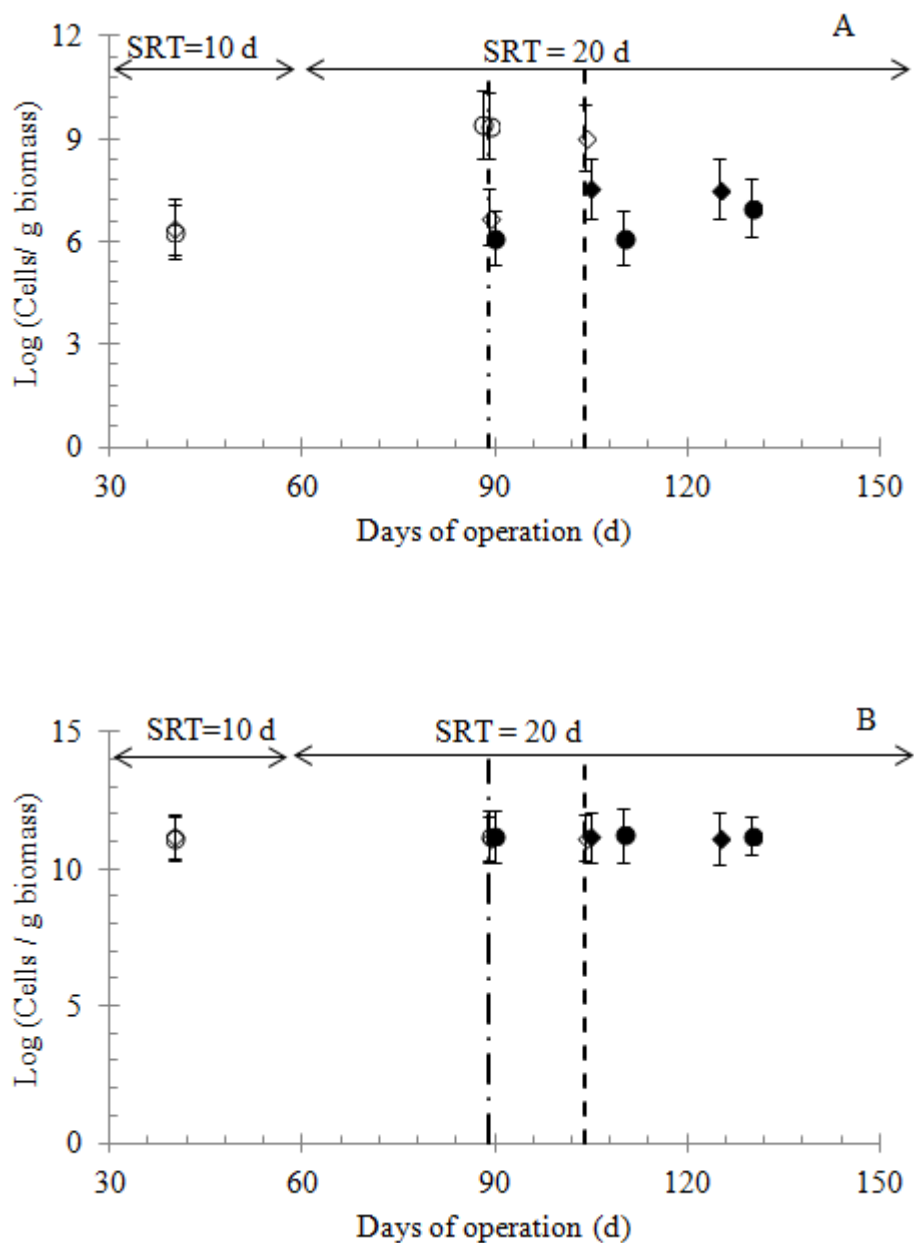


Figure 31. Type 021N (A) and total bacterial population (B) dynamics in Tank #1 and Tank #2 . A single dose of NZVI at the final concentration of 100 mg Fe/L in the mixed liquor was applied on day 89 and day 104 in Tank #1 and Tank #2, respectively. Two vertical hashed lines show the days of NZVI addition in Tanks #1 and #2, respectively. Error bars represent one standard deviation from the mean of at least triplicate samples.

In Tank #1, before NZVI dosing, the average concentration of Type 021N were increased from $(2.00 \pm 0.69) \times 10^6$ cells/g biomass on day 40 to $(2.67 \pm 0.09) \times 10^9$ cells/g biomass on day 88 and $(2.43 \pm 0.07) \times 10^9$ cells/g biomass on day 89 (Figure 31a). One day after NZVI dosing, however, Type 021N was reduced to $(1.37 \pm 0.54) \times 10^6$ cells/g biomass, a significant decrease (in 3 log units). In the following 20 and 40 days, the average concentrations of Type 021N were $(1.35 \pm 0.80) \times 10^6$ cells/g biomass and $(9.56 \pm 0.26) \times 10^6$ cells/g biomass, respectively, indicating a slight and slow recovery of the bacteria under long SRT operation. In Tank #2, Type 021N species increased from $(2.70 \pm 0.69) \times 10^6$ cells/g biomass on day 40 to $(1.09 \pm 0.01) \times 10^9$ cells/g biomass on day 104 (before NZVI dosing) (Figure 31a). One day after NZVI treatment, the number of Type 021N was reduced to $(3.58 \pm 0.20) \times 10^7$ cells/g biomass, a significant decrease (in about 2 log units or a 96.7% reduction). After 20 more days of operation at the SRT of 20 d, the number of Type 021N remained low at $(3.40 \pm 0.23) \times 10^7$ cells/g biomass. For comparison, the average concentration of total bacteria ranged from $(1.38 \pm 0) \times 10^{11}$ cells/g biomass to $(1.68 \pm 0.15) \times 10^{11}$ cells/g biomass in Tank #1 and from $(1.30 \pm 0.05) \times 10^{11}$ cells/g biomass to $(1.49 \pm 0) \times 10^{11}$ cells/g biomass in #2 throughout the study period (Figure 31b), which were generally consistent with the range of biomass concentrations in municipal

WWTPs (Harms et al., 2003). Type 021N was characterized by having extremely high SVI values (Séka et al., 2001a). The results demonstrated the successful use of NZVI in sludge bulking control by significantly reducing the number of Type 021N bacteria.

Due to its high specific surface area, it is likely that NZVI was capable of directly attaching to the cell surface thus more likely killing filamentous bacteria, which also have high surface/volume ratio (Figure 32). Interestingly, the use of NZVI did not cause significant deflocculation one hour after the dosing while the nanoparticles appeared to be agglomerated. Live/dead staining results showed that unlike the control group (Figure 33), NZVI effectively killed the filamentous bacteria in both bioreactors, while a large fraction of floc-forming species were still alive with a larger amount of dead cells for the higher NZVI to biomass ratio in Tank #1 (Figure 34), because the filamentous bacteria are not protected by the floc. NZVI was also effective in killing *Gordonia* spp. based on regular PCR analysis, as the bands associated with this species disappeared right after NZVI dosing indicating the significant bactericidal effect (Figure 35).

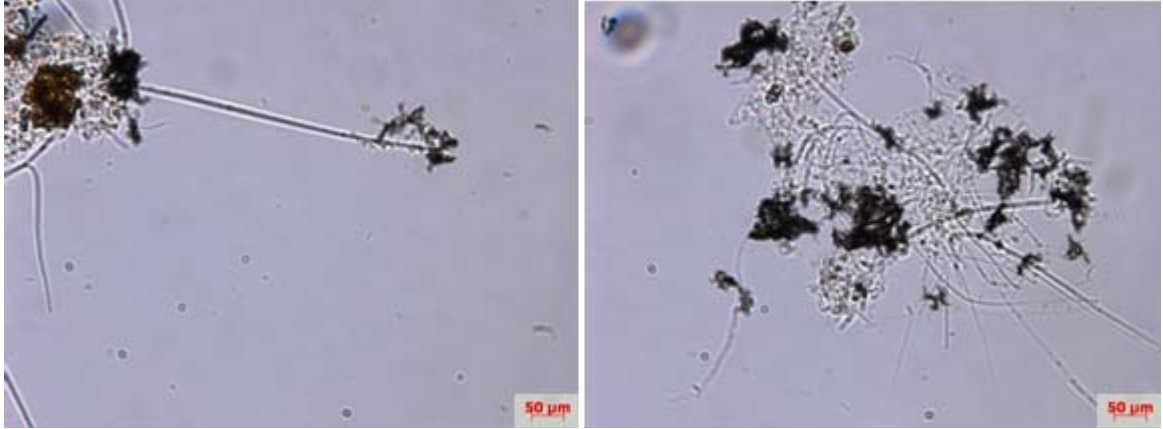


Figure 32. Micrographs of light microscopy of activated sludge samples from Tank #1 (left panel) and Tank #2 (right panel) taken 1 h after NZVI dosing in the MLE systems with agglomerated NZVI structure shown in black.

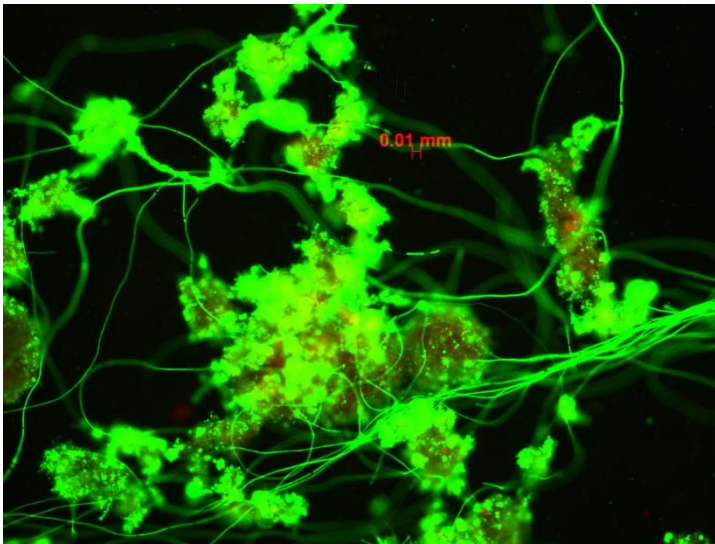


Figure 33. The viability of bulking activated sludge before NZVI treatment. Under fluorescence microscopy, living cells were stained green and dead cells were stained red.

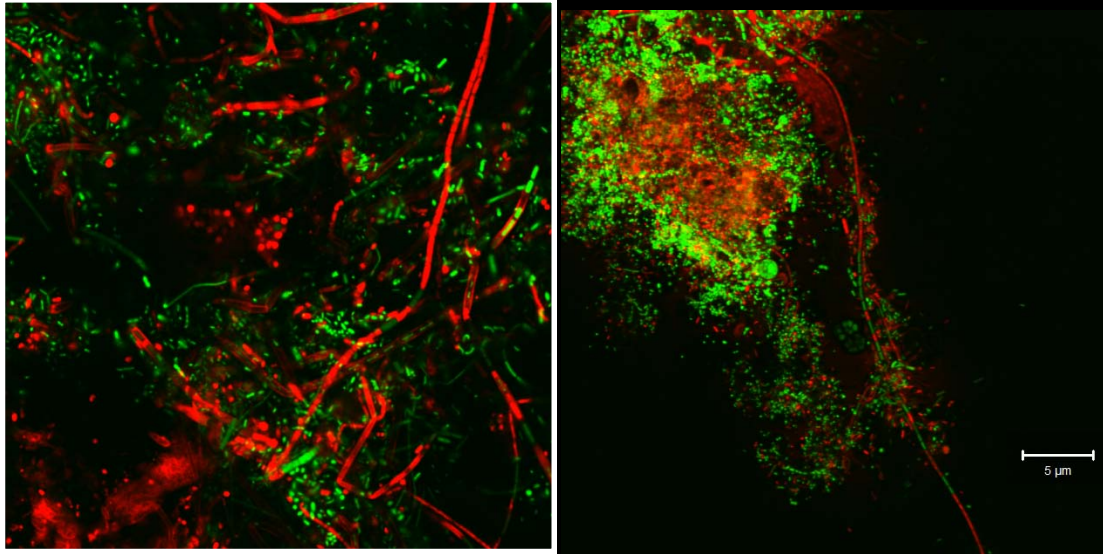


Figure 34. The viability of activated sludge from Tank #1 (with sludge bulking and significant sludge loss already, left) and Tank #2 (with the early stages of bulking, right) after the NZVI treatment on day 90 and 105, respectively. Under florescence microscopy, living cells were stained green and dead cells were stained red.

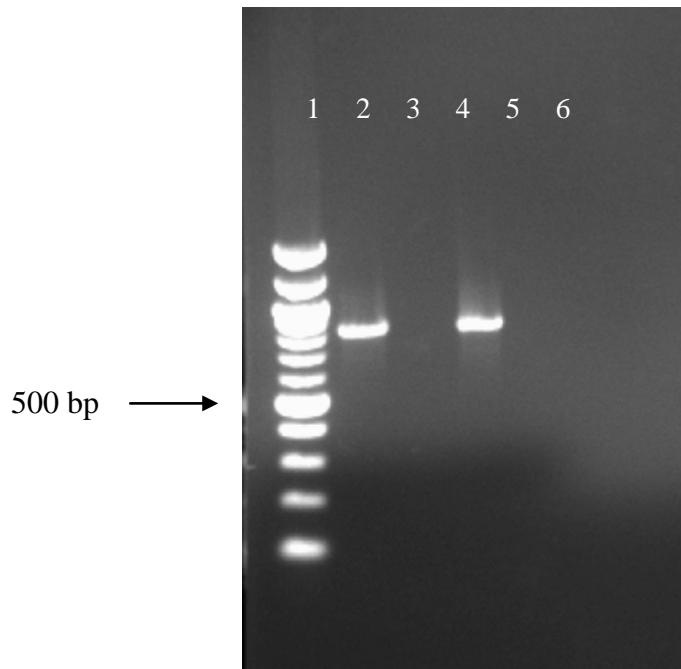
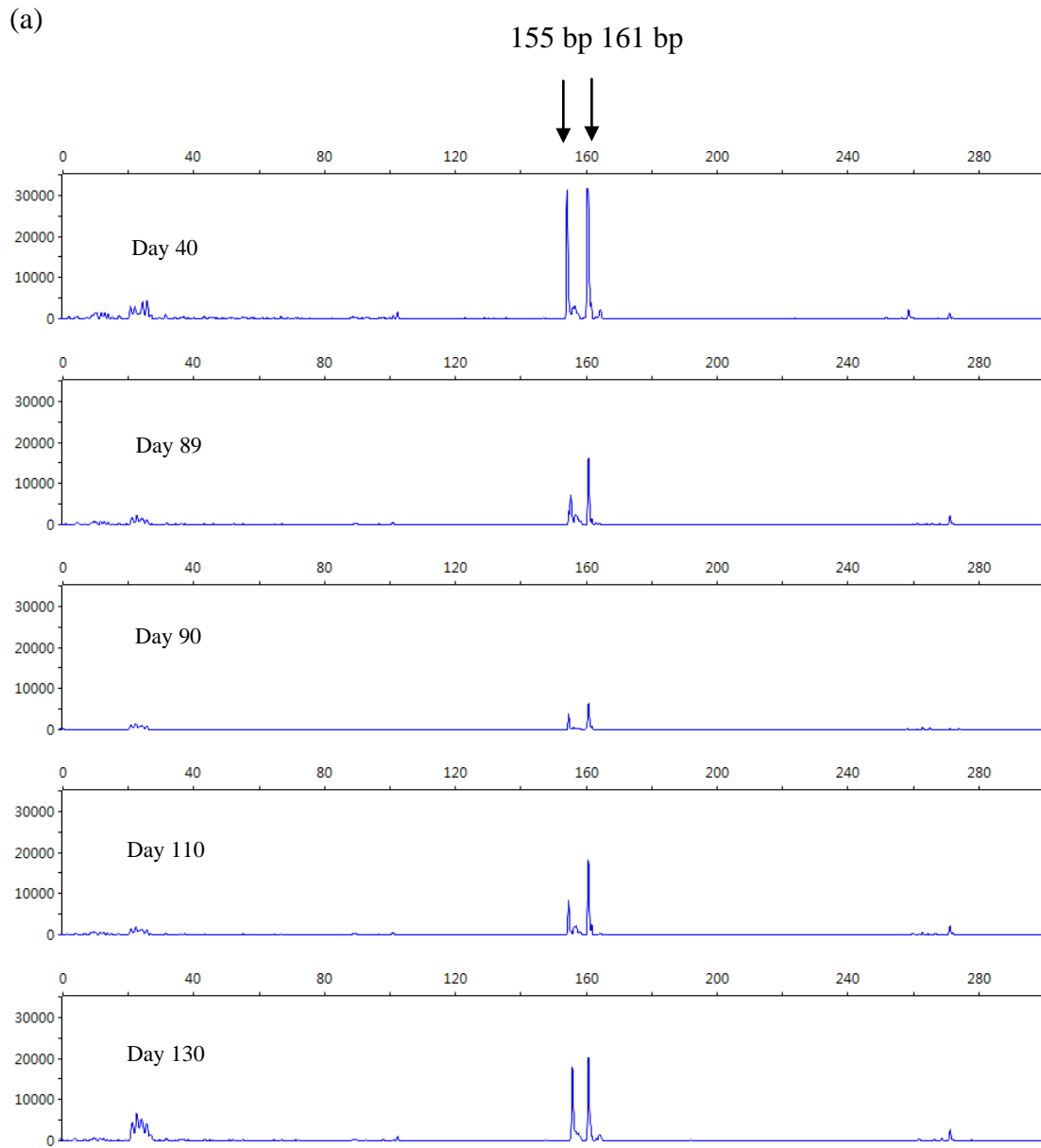


Figure 35. Conventional PCR analysis of the sludge samples targeting genomic DNA (829 bp) of *Gordonia* spp. Lane 1, molecular mass marker (100 bp plus DNA ladder); Lane 2, DNA template from Tank #1 before NZVI dosing; Lane 3, DNA template from Tank #1 one day after NZVI dosing; Lane 4, DNA template from Tank #2 before NZVI dosing; Lane 5, DNA template from Tank #2 one day after NZVI dosing; Lane 6, negative control (no DNA template).

4.3.3. Impact of Sludge Bulking and NZVI Dosing on Nitrifying Bacterial Population and Activity

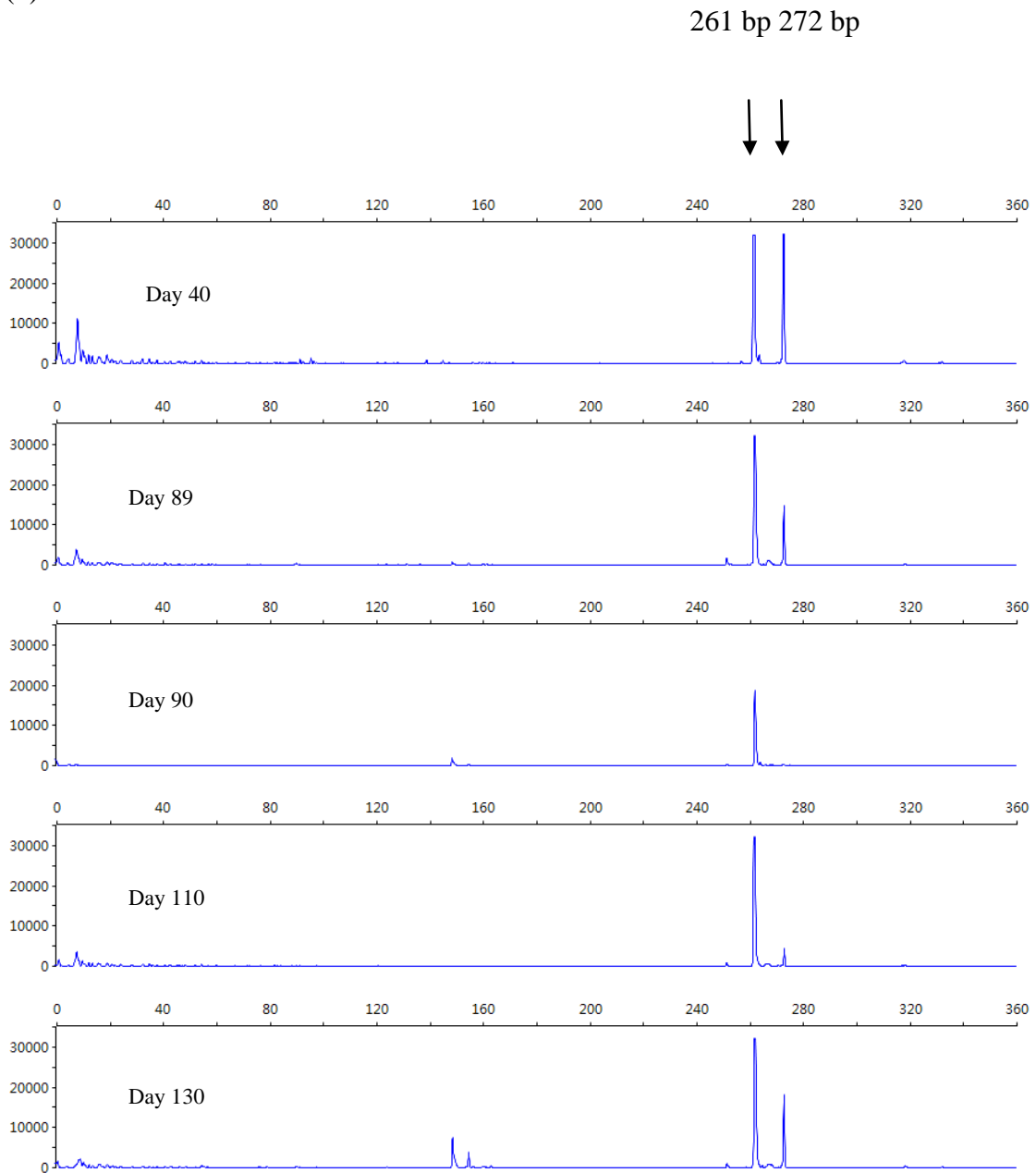
T-RFLP analysis (Figure 36) shows the change in nitrifying bacterial community structure in Tank #1 before and after NZVI dosing. On day 40, *Nitrosomonas* was the dominant genus of AOB while *Nitrospira* was dominant among NOB. With significant sludge bulking on day 89, there was a large decrease in the AOB population as indicated from the change in peak intensity (at 155 bp and 161 bp) of *Nitrosomonas*; in contrast, only one of

the *Nitrospira* peaks (272 bp) was reduced considerably. Consistent with the higher effluent NH_4^+ -N and NO_2^- -N concentrations, the decrease in *Nitrosomonas* and *Nitrospira* population was attributed to overgrowth of filamentous bacteria and associated biomass loss in the effluent. Additional decrease in the numbers of *Nitrosomonas* and *Nitrospira* species were observed one day after NZVI dosing (day 90), showing the bactericidal effect of NZVI on nitrifying bacteria. Thereafter, the peak sizes of *Nitrosomonas* and *Nitrospira* species increased gradually as indicated from the data on days 110 and 130, correlating well with the effluent water quality data (Figures 29 and 30).



Note: Arrows indicate significant T-RFLPs of AOB: 161bp for AOB Group-1 and 155 bp could belong to the uncharacterized AOB.

(b)



Note: Arrows correspond to significant T-RFLPs of *Nitrospira*, 261 bp, and 272 bp.

Figure 36. Nitrifying bacterial community composition reflected by T-RFLP profiles targeting 16S rRNA genes of *Nitrosomonas* (a) and *Nitrospira* (b) in Tank #1 before and after NZVI dosing on day 89.

Furthermore, consistent with the change in nitrifying population and the effluent water quality, the autotrophic SOUR values in Tank #1 were decreased by $46 \pm 4\%$ due to sludge bulking on day 89 (Figure 37). One day after NZVI dosing, the nitrifying bacteria activity decreased further, with the full recovery of the activated sludge system taking more than 40 days. There was also a slight decrease in nitrifying activity in Tank # 2 on day 104 followed by a significant decrease ($34 \pm 1\%$) one day after NZVI dosing. Thereafter, the nitrifying bacteria activity was fully recovered within a few days.

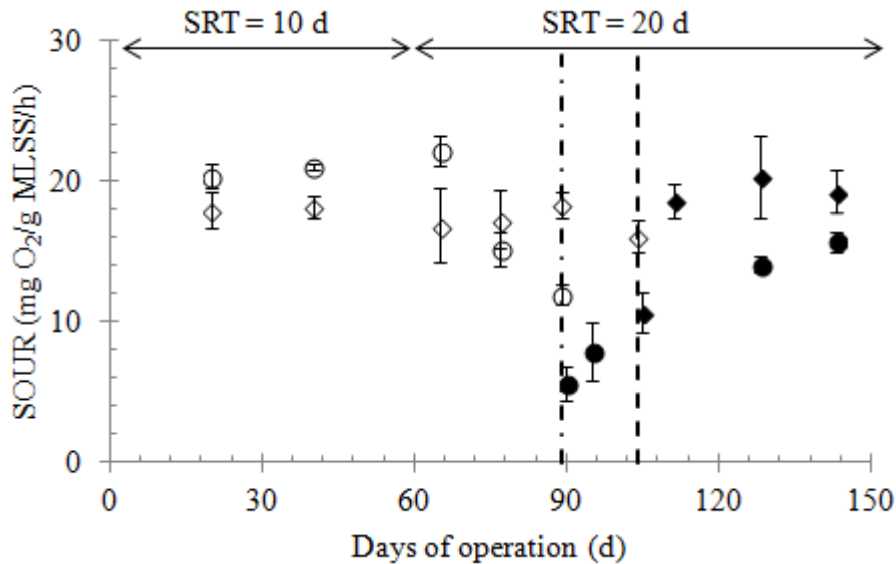


Figure 37. Autotrophic SOUR in Tank #1 (\circ) and #2 (\diamond) before NZVI dosing and in Tank #1 (\bullet) and #2 (\blacklozenge) after NZVI dosing on day 89 and day 104 and day 104, respectively. Two vertical hashed lines show the days of NZVI addition in Tanks #1 and #2, respectively.

4.3.4. Bioreactor Performance Recovery and Other Benefits Associated with NZVI Dosing

In Tank #1 with sludge bulking and sludge loss already present (average biomass concentration = $1,022 \pm 159$ COD mg/L or at the ratio of 0.098 g Fe/g biomass COD), the use of NZVI caused a significant increase in effluent COD, NH_4^+ -N and NO_2^- -N concentrations, with the full recovery of the activated sludge system taking more than 40 days (Figures 29 and 30). For comparison, in Tank #2 with the early stages of bulking and the biomass concentration of $1,799 \pm 113$ COD mg/L (at the ratio of 0.056 g Fe/g biomass COD), the effluent COD concentration was stabilized at 22 ± 1 mg/L, with the exception of NH_4^+ -N accumulation during the first week after NZVI dosing, the effluent NH_4^+ -N concentration was quickly reduced to 0.02 ± 0.03 mg/L (Figures 29 and 30). Hence, the effluent water quality and overall activated sludge bioreactor performance were only affected for a few days in Tank #2.

Additional benefits of the use of NZVI included improved phosphorus removal and sludge settling. An single dose of NZVI resulted in fast and enhanced reduction of effluent PO_4^{3-} -P concentration (Figure 38), possibly due to iron phosphate precipitates (e.g., $\text{Fe}_3(\text{PO}_4)_2$, FePO_4 , and $\text{Fe}_x(\text{OH})_y(\text{PO}_4)_3$) (Stumm and Morgan, 1996) and the formation of

iron oxides/hydroxides for P adsorption (Almeelbi and Bezbaruah, 2012). However, the effluent $\text{PO}_4^{3-}\text{-P}$ concentrations resumed to the previous level three HRTs after NZVI treatment, indicating the rapid loss of NZVI reactivity as nanoparticles were mainly associated with sludge. Nevertheless, due to the dissolution of NZVI, the oxidized forms (Fe^{2+} , Fe^{3+}) of iron could improve the sludge flocculation and settleability, as was also confirmed in this study where the SVI was generally below 100 mg/L in both bioreactors after the one-time NZVI treatment (Figure 26). Although more questions remain as to whether or how the NZVI treated sludge would affect sludge digestion, it is expected that NZVI could be converted to iron ions and their complexes through fast NZVI dissolution (within an hour, data not shown) and therefore would not pose problems.

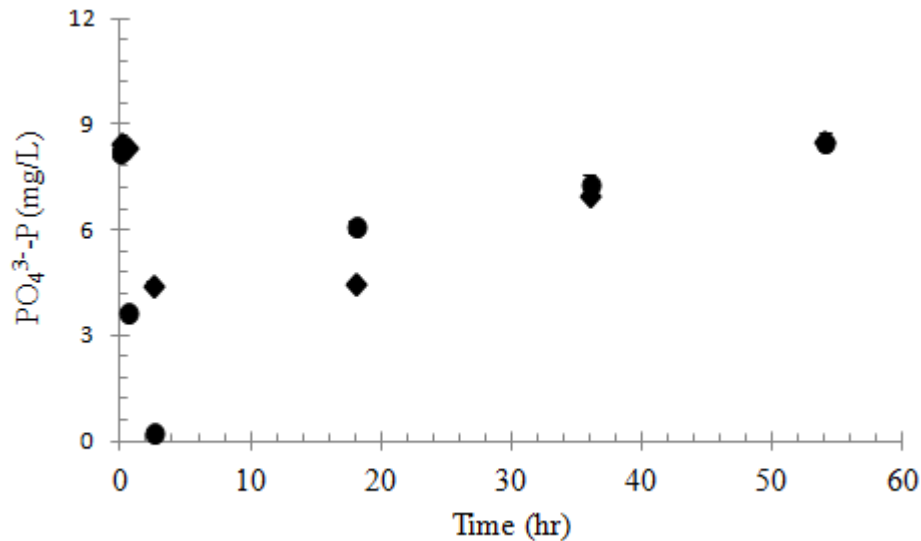


Figure 38. Effluent $\text{PO}_4^{3-}\text{-P}$ concentrations in Tank #1 (●) and Tank #2 (◆) right after NZVI dosing. Error bars represent one standard deviation from the mean of duplicate samples.

In chlorination-based bulking control, filamentous and floc-forming bacteria do not appear to largely differ in their chlorine susceptibility. Unlike chlorine, NZVI may serve as a new bulking control agent that can selectively kill filamentous organisms due to the unique fate and transport characteristics associated with NZVI dissolution and agglomeration (Figure 31). Nevertheless, the findings of this paper are more of an exploratory nature. A NZVI final concentration of 100 mg/L is very high, which shows side effects in a way that excess chlorine treatment does. More research is needed to show if there is a NZVI specific dose that can control filaments without causing nitrification inhibition by adjusting the particle size and dose of NZVI. Also there could be more complicated instances of filamentous

bulking that are much more challenging to resolve in full-scale wastewater treatment plants. Further research is needed to design and test NZVI related nanomaterials for better sludge bulking control.

4.4. Conclusions

A new approach of filamentous sludge bulking control with NZVI was proposed. NZVI is an effective biocide. A single dose of NZVI at the final concentration of 100 mg Fe/L in the mixed liquor reduced filamentous bacteria such as Type 021N by 2-3 log units. Meanwhile, the nitrification efficiency was also reduced while the side effect of the use of NZVI depended on sludge bulking conditions and sludge concentration. Because the filamentous bacteria are not protected by the floc and the agglomeration of nanoparticles in the sludge may reduce the negative effect of NZVI on floc formers, this research opens up the potential to use NZVI as a more selective sludge bulking control agent.

CHAPTER 5

5. Fate and Toxicity of Melamine in Activated Sludge Treatment Systems after a Long-Term Sludge Adaptation*

Melamine is a nitrogen-rich (67% nitrogen by mass) heterocyclic aromatic compound that could significantly increase effluent total nitrogen concentrations. In this study, we investigated the degradation of melamine and its impact on activated sludge operations by employing two common activated sludge processes, namely the Modified Ludzack-Ettinger (MLE) process and the continuous stirred tank reactor (CSTR) process. Melamine was dosed continuously from day 125 in both activated sludge treatment systems at an influent concentration of 3 mg/L for about 100 days. Even after such a long period of sludge adaptation, melamine appeared not to be easily biodegradable. The average melamine removal efficiencies in the CSTR and MLE systems were $14 \pm 10\%$ and $20 \pm 15\%$, respectively. There was no significant difference in melamine removal between the two different activated sludge processes. The long-term input of melamine resulted in a

* A research paper based on this thesis chapter has been published: Full citation in Water Research, Vol 47(2003):2307~2314

decrease in the nitrifying bacterial activities (by $82 \pm 8 \%$) and population in both systems. Short-term microtiter assay results also showed that melamine reduced activated sludge growth by 80% when supplied at a concentration of 75.6 mg/L. These results suggest that sludge adaptation plays a minimal role in melamine degradation, as the enzymes responsible for hydrolytic deamination of melamine in activated sludge are not easily induced. The insignificant biodegradation of melamine is also attributed to bacterial growth inhibition under long-term dosing conditions with melamine, resulting in a significant decrease in effluent water quality.

5.1. Objectives

Earlier studies have shown that the inherent biodegradability of melamine by unacclimated activated sludge is very low, ranging from 0 to 16% after continuous aeration at 24 °C in the dark for 28 days (UNEP). The objective of this study was to determine the fate and toxicity of melamine in activated sludge systems and to evaluate whether long-term sludge adaptation can improve melamine degradation.

5.2. Materials and Methods

5.2.1. Bioreactor Setup and Operation

Two lab-scale activated sludge systems were operated in parallel by employing two commonly used activated sludge treatment processes during this study. Each system had a working volume of 7.4 L. For the bioreactor using the Modified Ludzack-Ettinger (MLE) process, the system was composed of sequential anoxic and aerobic chambers separated by a glass baffle. The effective volumes for the anoxic, aerobic, and internal settling chambers were 1.9, 3.8 and 1.7 L, respectively. There was a recirculation from the aerobic chamber to the anoxic chamber in the MLE system at a flow rate equal to the influent flow rate. The continuous stirred tank reactor (CSTR) system was a completely mixed bioreactor with aeration and settling chamber effective volumes of 5.7 and 1.7 L, respectively. For each bioreactor, a fine bubble diffuser and a magnetic stirrer provided mixing and aeration in the aeration chamber.

The synthetic wastewater primarily contained nonfat dry milk powder with a target chemical oxygen demand (COD) concentration of 500 mg/L, 50 mg/L total N, 30 mg/L NH_4^+ -N and 6 mg/L PO_4^{3-} -P. The synthetic wastewater also contained the following micronutrients per liter: 44 mg MgSO_4 , 14 mg $\text{CaCl}_2 \cdot 2\text{H}_2\text{O}$, 2 mg $\text{FeCl}_2 \cdot 4\text{H}_2\text{O}$, 3.4 mg $\text{MnSO}_4 \cdot \text{H}_2\text{O}$, 1.2 mg $(\text{NH}_4)_6\text{Mo}_7\text{O}_{24} \cdot 4\text{H}_2\text{O}$, 0.8 mg CuSO_4 , 0.3 mg $\text{NiSO}_4 \cdot 6 \text{H}_2\text{O}$, and 1.8

mg $\text{Zn}(\text{NO}_3)_2 \cdot 6\text{H}_2\text{O}$ (Sigma Aldrich, St Louis, MO) (Liang et al., 2010a, Liang et al., 2010b).

The two bioreactors were operated with a hydraulic retention time (HRT) of 0.75 d and target solids retention time (SRT) of 15 d. At the beginning of reactor operation, a total of 2,000 mL of activated sludge taken from the aeration basin of a local municipal wastewater treatment plant (WWTP) (Columbia, MO) was added as an inoculum to each bioreactor. The bioreactors were operated and monitored for 227 days, which was divided into two phases. Phase I consisted of the first 124 days of operation before melamine dosing. Phase II started on day 125, with continuous melamine dosing at an influent concentration of 3 mg/L. This concentration was chosen considering some industrial wastewater streams containing melamine and its derivatives (e.g., melamine formaldehyde) at a concentration of about 30 mg/L (Othman, 2012) and the fact of dilution with other wastewater prior to entering the WWTP.

5.2.2. Effect of Long-term Melamine Dosing on Bioreactor Performance

Melamine (99%) was purchased from Acros Organics. From day 125 onwards, a melamine stock solution with a concentration of 122.8 mg/L was fed separately into each bioreactor

at a flow rate of 0.172 L/d. This was mixed with influent synthetic wastewater to reach an influent nominal concentration of 3 mg/L in each bioreactor. The change in HRT due to melamine addition was negligible because the flow rate of melamine stock was much lower than the influent (6.9 L/d). Wastewater effluent from each bioreactor was collected and analyzed for melamine, $\text{NH}_4^+\text{-N}$, $\text{NO}_3^-\text{-N}$, $\text{NO}_2^-\text{-N}$, and COD following the standard methods (APHA, 2002). SOUR measurement is shown in 2.2.4.

5.2.3. Batch Melamine Degradation and Adsorption Study

Batch studies were conducted to determine the potential for adsorption and degradation of melamine in activated sludge systems before melamine dosing in the continuous flow systems. The sludge samples were collected from the CSTR and the aeration chamber of the MLE system. All of the samples were washed with phosphate buffered saline (PBS) three times to remove the residual carbon and nutrients before they were resuspended in medium that had the same recipe as the feed solution with the exception of the organic matter (milk powder). Aliquots (500 mL) of the sample with a biomass concentration of about 2 g/L were poured into 1,000 mL beakers. Then 5 mL aliquots of the melamine stock solution (1,000 mg/L) were spiked into the sludge samples, to obtain a final melamine concentration of 10 mg/L. The mixed liquor in each beaker was mixed at 350 rpm with

magnetic stirrers at 25 ± 1 °C and the batch systems were run under aerobic and anoxic conditions. An aeration pump was used to supply air in addition to mixing under aerobic conditions. Excess sodium nitrate was added to the mixed liquor under anoxic conditions. After 2, 4, 6, 10, 22, 34, 46, and 70 hours, 5 mL aliquots of the mixed liquor were collected. Following 70 hours of culture time, the mixed liquor was allowed to settle for 10 min, and then the supernatant was filtered through a 0.45 µm nylon syringe filter and the filtrate was stored at 4 °C before analysis. To determine the adsorption of melamine by the sludge, two more groups of heat-inactivated biomass samples were prepared (killed by heating at 80 °C for 20 min) (Hu et al., 2005b) and the experiment was repeated under aerobic and anoxic conditions.

5.2.4. Melamine Toxicity Inferred from the Microtiter Assay

Activated sludge samples from the CSTR system at the end of phase II were washed with 1× PBS three times to remove the residual organic matter and nutrients before use. The samples were placed into sterile basal mineral medium that was modified by removing the $(\text{NH}_4)_2\text{SO}_4$ and $(\text{NH}_4)_6\text{Mo}_7\text{O}_{24} \cdot 7\text{H}_2\text{O}$ components, and replacing them with melamine (final concentration = 75.6 mg/L or 0.6 mM) as a sole nitrogen source (El-Sayed et al.,

2006). Glucose was added to the medium as the main carbon source when needed. The liquid medium was sterilized by autoclaving at 121 °C before use.

A turbidimetric microtiter assay was used to determine the growth of active sludge with different substrates (melamine only, glucose only, and a combination of glucose and melamine). Aliquots (10 µL) of sludge samples in 8 replicates were added to the microplate wells followed by the addition of 190 µL medium containing the different substrates. The absorbance of the cell culture in each microwell was measured at 600 nm every 1 hour for 72 h by a microreader (VICTOR3, PerkinElmer, Shelton, USA).

5.2.5. Effect of Melamine on Nitrifying Community Structure and Population

Activated sludge samples in the CSTR and MLE bioreactors were collected before and after the melamine dosing for DNA extraction and nitrifying community structure analysis using terminal restriction fragment length polymorphism (T-RFLP) (see 2.2.5).

5.2.6. Chemical and Statistical Analysis

The melamine concentration was determined by high-pressure liquid chromatography (HPLC) coupled with a Zorbax SB-C8 column with a dimension of 4.6 mm ID × 250 mm. In each analysis, a 5 µL sample was injected into a mobile phase consisting of 15% acetonitrile and 85% buffer solution (10 mM citric acid + 10 mM sodium octanesulphonate at pH 3) at a flow rate of 1 mL/min (Lin et al., 2008). Wastewater influent and effluent samples were collected twice a week for COD, ammonium-N, nitrite-N, and nitrate-N measurements following standard methods (APHA, 2002). The biomass concentrations of the bioreactors were measured in COD units. One-Way ANOVA analysis was conducted to assess the significance of the differences among groups, with p values less than 0.05 indicating statistical significance.

5.3. Results and Discussion

5.3.1. Biodegradation of Melamine by Activated Sludge

The sludge adaptation period lasted for 124 days and continuous melamine dosing began on day 125. The average influent melamine concentration over Phase II of testing was 2.9 ± 0.4 mg/L, while the average effluent melamine concentrations in the MLE and CSTR systems over the same period were 2.3 ± 0.5 mg/L (removal efficiency = $20 \pm 15\%$) and 2.4

± 0.4 mg/L (removal efficiency = $14 \pm 10\%$), respectively. These values were also fairly constant across all of Phase II, as seen in Figure 39. Although the removal efficiencies were not high, there were significant differences in melamine concentration between the influent and effluent samples in both the MLE and CSTR systems ($p < 0.001$). However, there was no significant difference in the effluent melamine concentration between the two activated sludge treatment processes ($p = 0.22$). This suggests that melamine is not easily removed under either aerobic conditions or anoxic/aerobic sequencing conditions. Furthermore, the results from the short-term batch studies suggest that melamine is not removed by biodegradation or adsorption either (Figures 40 and 41).

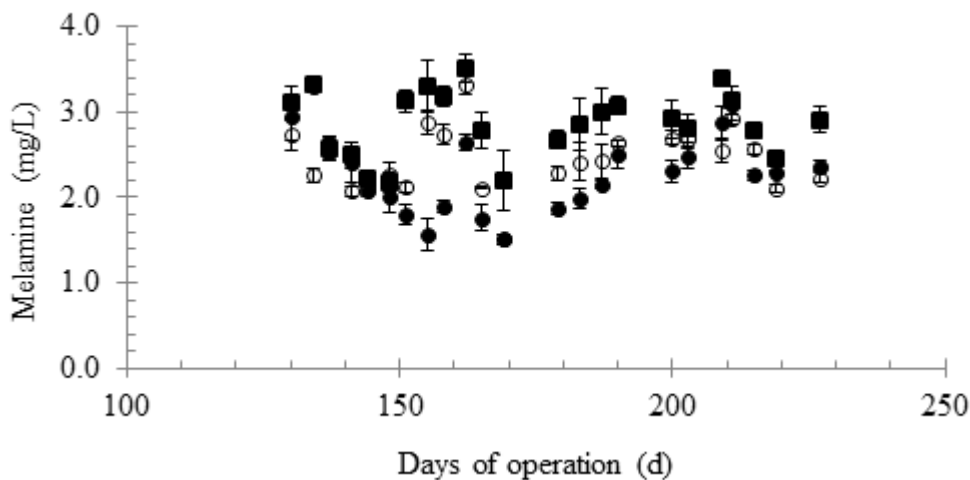


Figure 39. Influent (■) and effluent melamine concentrations in the CSTR (○) and MLE (●) systems after continuous melamine dosing starting on day 125. Error bars represent one standard deviation from the mean of triplicate samples.

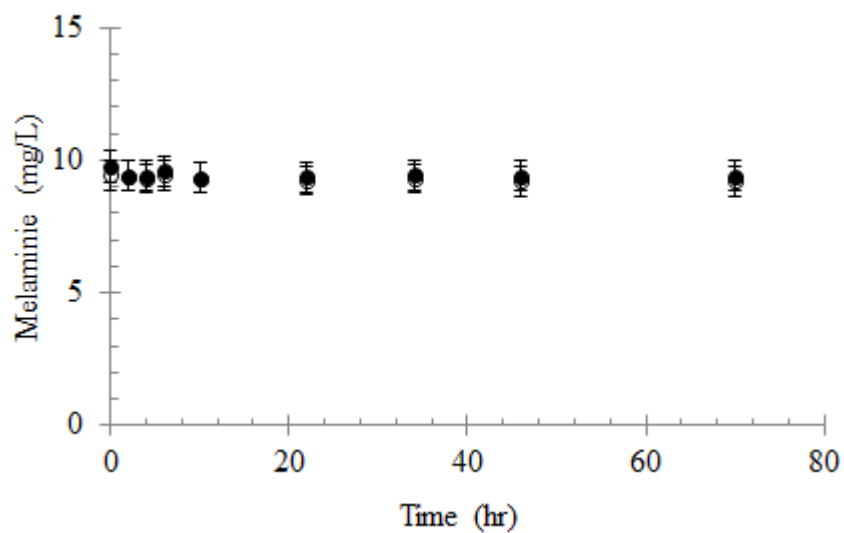


Figure 40. Change in melamine concentration due to biodegradation (●) and adsorption (○) of melamine under anoxic conditions in batch studies.

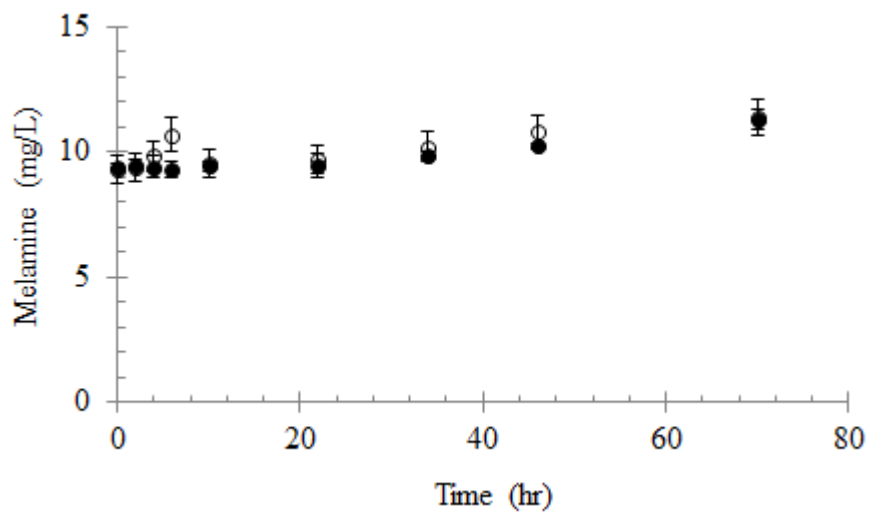


Figure 41. Change in melamine concentration due to biodegradation (●) and adsorption (○) of melamine under aerobic conditions in batch studies.

5.3.2. Bioreactor Performance before and after Melamine Exposure

The start-up period for both bioreactor systems lasted about 30 days before consistent effluent water quality was observed. At an average influent COD concentration of 503 ± 78 mg/L, the COD removal efficiencies during Phase I of operation for the MLE and CSTR systems were $94 \pm 3\%$ and $93 \pm 4\%$, respectively. The variation in the performance of both reactors over the operating period can be seen in Figure 42. The effluent ammonium removal efficiencies during Phase I of operation were $99 \pm 1\%$ and $99 \pm 0\%$ for the MLE and CSTR systems, respectively, indicating complete nitrification in both bioreactors. Variations in the ammonium removal with both reactors over the operating period can be seen in Figure 43a. There were no significant differences in COD ($p = 0.13$) or $\text{NH}_4^+\text{-N}$ ($p = 0.15$) removal efficiencies between the two types of activated sludge processes. There was also no significant difference in the effluent concentrations of $\text{NO}_2^-\text{-N}$ between the two bioreactors as seen in Figure 43b. However, during Phase I of operation, a significant difference was seen between the two reactors in the effluent concentrations of $\text{NO}_3^-\text{-N}$. The average effluent $\text{NO}_3^-\text{-N}$ concentration in the MLE system was 1.3 ± 1.1 mg/L, which was much lower than the 19.7 ± 4.9 mg/L found in the CSTR system. This result demonstrates the role of anoxic and aerobic alternation in nitrogen removal in the MLE system.

After melamine dosing (Phase II), the average effluent COD concentration in the MLE system was statistically ($p < 0.05$) higher than that in Phase I, whereas in the CSTR there was no statistically significant difference in the effluent COD concentration between the two phases. The variability in performance over Phase II is also shown in Figure 42. The average effluent NH_4^+ -N and NO_3^- -N concentrations in both the MLE and CSTR systems were statistically higher after melamine dosing, although there was high variability in the results from day to day as seen in Figure 43a and 43c. However, while there was noticeably more variability in the NO_2^- -N concentrations as shown in Figure 43b, the differences in the concentrations between the two Phases of operation were only statistically significant for the CSTR system. All of the average effluent conditions before and after melamine dosing for both reactor systems are summarized in Table 5. These results clearly demonstrate that the presence of melamine in activated sludge systems reduces effluent water quality. The COD and nitrogen species data also suggest that melamine has more of an impact on autotrophic nitrifying bacteria than on heterotrophic bacteria based on the results for the MLE system.

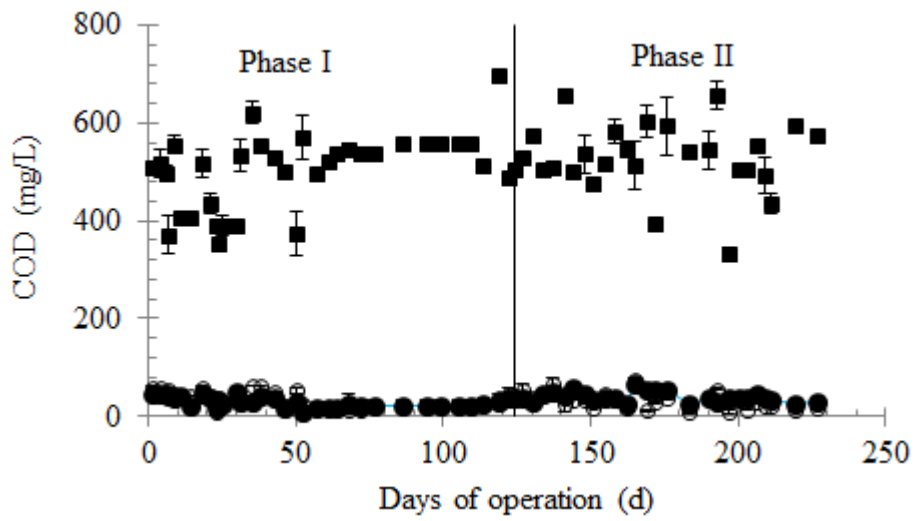
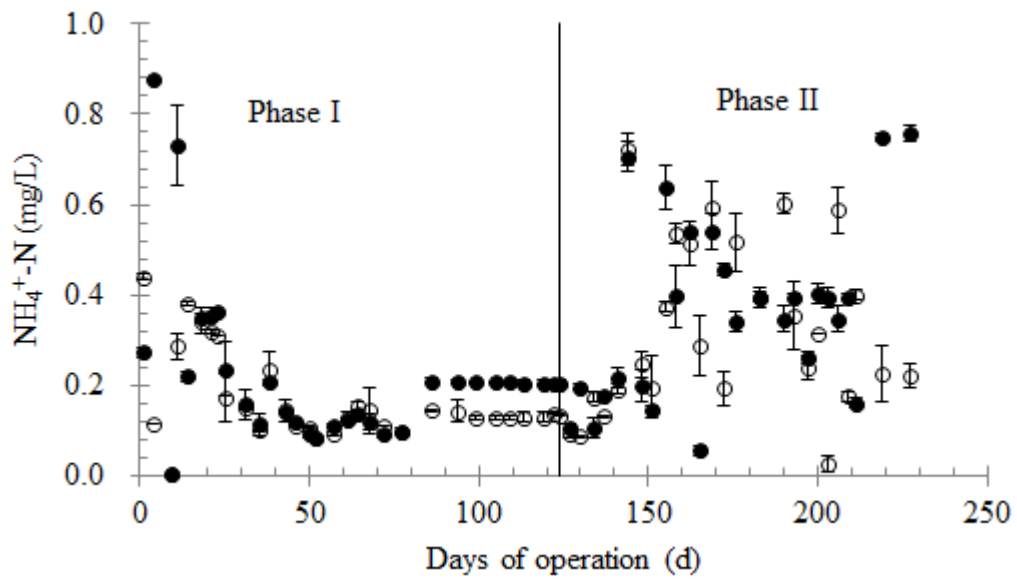
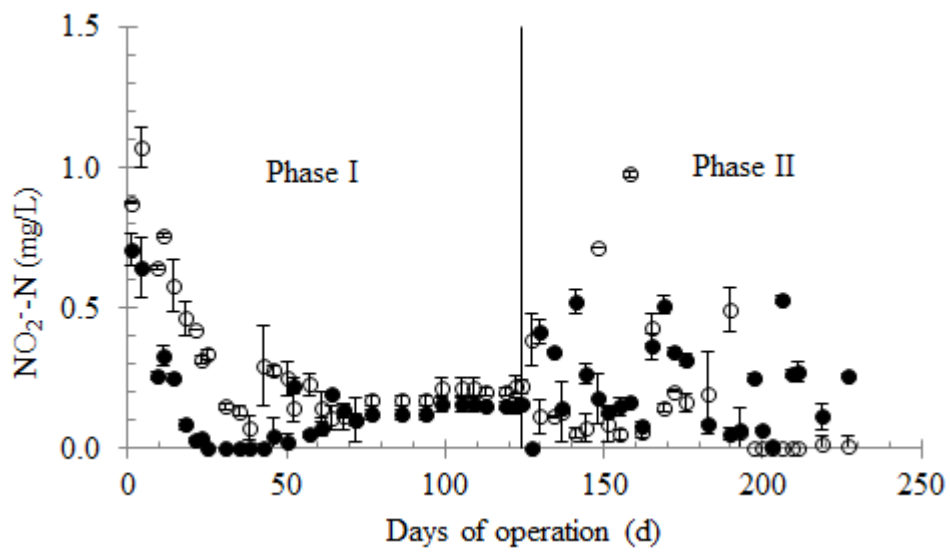


Figure 42. Influent (■) and effluent COD concentrations in the CSTR (□) and MLE (●) systems before (Phase I) and after (Phase II) melamine dosing. Error bars represent the data range of duplicate samples.

(a)



(b)



(c)

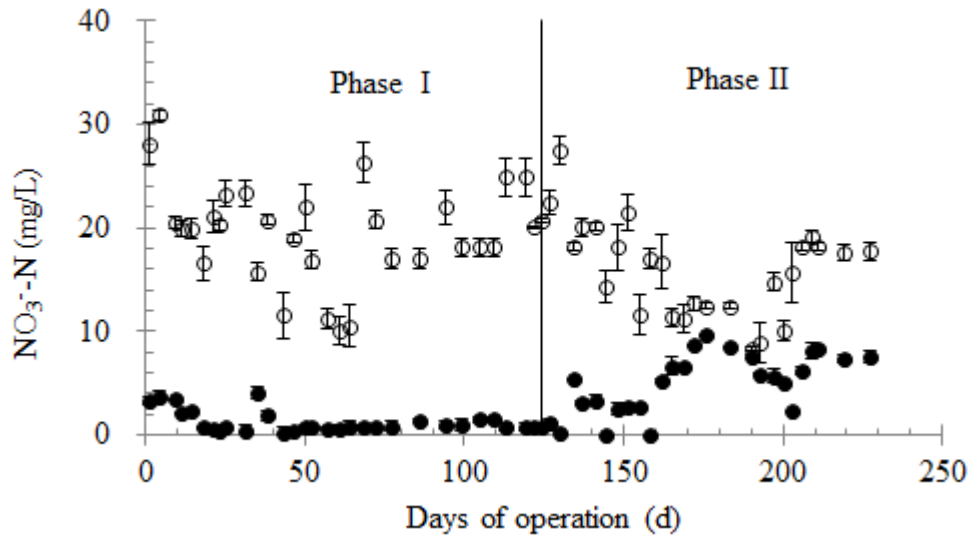


Figure 43. Effluent NH_4^+ -N (a), NO_2^- -N (b) and NO_3^- -N (c) concentrations in the CSTR (○) and MLE (●) bioreactors before (Phase I) and after (Phase II) melamine dosing. Error bars represent the data range of duplicate samples.

Table 5. One-way ANOVA analysis of the effluent water quality in the MLE and CSTR systems before (phase I) and after melamine dosing (phase II).

	Effluent COD (mg/L)	Effluent NH ₄ ⁺ -N (mg/L)	Effluent NO ₂ ⁻ -N (mg/L)	Effluent NO ₃ ⁻ -N (mg/L)
MLE, before dosing	29 ± 11	0.2 ± 0.2	0.2 ± 0.2	1.3 ± 1.1
MLE, after dosing	40 ± 11	0.4 ± 0.2	0.2 ± 0.2	5.0 ± 2.9
p value *	0.0005	0.006	0.075	1.46E-08
CSTR, before dosing	34 ± 16	0.2 ± 0.1	0.3 ± 0.3	19.7 ± 4.8
CSTR, after dosing	37 ± 19	0.3 ± 0.2	0.2 ± 0.2	16.0 ± 4.6
p value **	0.460	0.0002	0.040	0.005

*A statistical analysis of reactor performance in the MLE system before and after melamine dosing.

**A statistical analysis of reactor performance in the CSTR system before and after melamine dosing.

5.3.3. Toxicity of Melamine to Activated Sludge

The SOURs were used to determine the nitrifying bacterial activity profiles before and after melamine dosing in the bioreactors and the results are shown in Figure 44. There was a significant decrease in the nitrifying activity after melamine dosing. At the completion of Phase II, the nitrifying activities in the MLE and CSTR systems decreased by $92 \pm 5 \%$ and $82 \pm 8 \%$, respectively. The impact on the nitrifying bacterial activity happened more quickly in the CSTR system, even though both systems had similar overall reductions in activity. The rate at which the nitrifying bacterial activity drops also provides an explanation for the effluent NO₂⁻-N results seen in Figure 43.

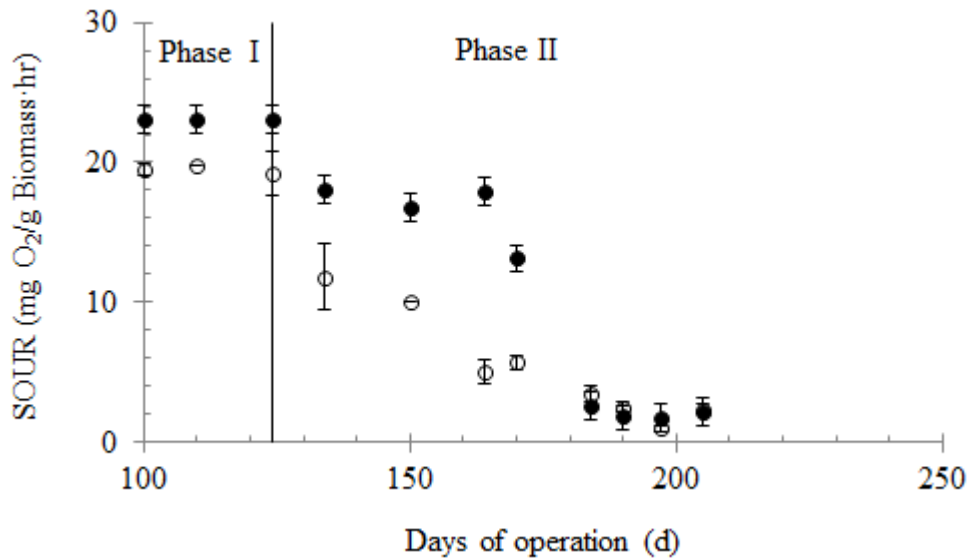


Figure 44. Change in autotrophic SOURs in the CSTR (○) and MLE (●) bioreactors before (Phase I) and after (Phase II) melamine dosing. Error bars represent the data range of duplicate samples.

The bacterial growth curves in the presence of melamine were tracked using a short-term microtiter assay and the results are shown in Figure 45. When melamine served as a sole carbon and nitrogen source, there was no growth of activated sludge. Exponential growth was observed in the presence of glucose only (positive control) with an average specific growth rate of $0.090 \pm 0.011 \text{ d}^{-1}$. The relatively low specific bacterial growth rate is attributed to the lack of an ammonia nitrogen source, which was done to see if melamine can be used as a sole nitrogen source. The presence of glucose and melamine together (75.6 mg/L melamine) resulted in a longer lag phase and a reduced specific growth rate of 0.018

$\pm 0.001 \text{ d}^{-1}$. This reduction of 80% suggests that melamine inhibits activated sludge growth when it is present at high concentrations.

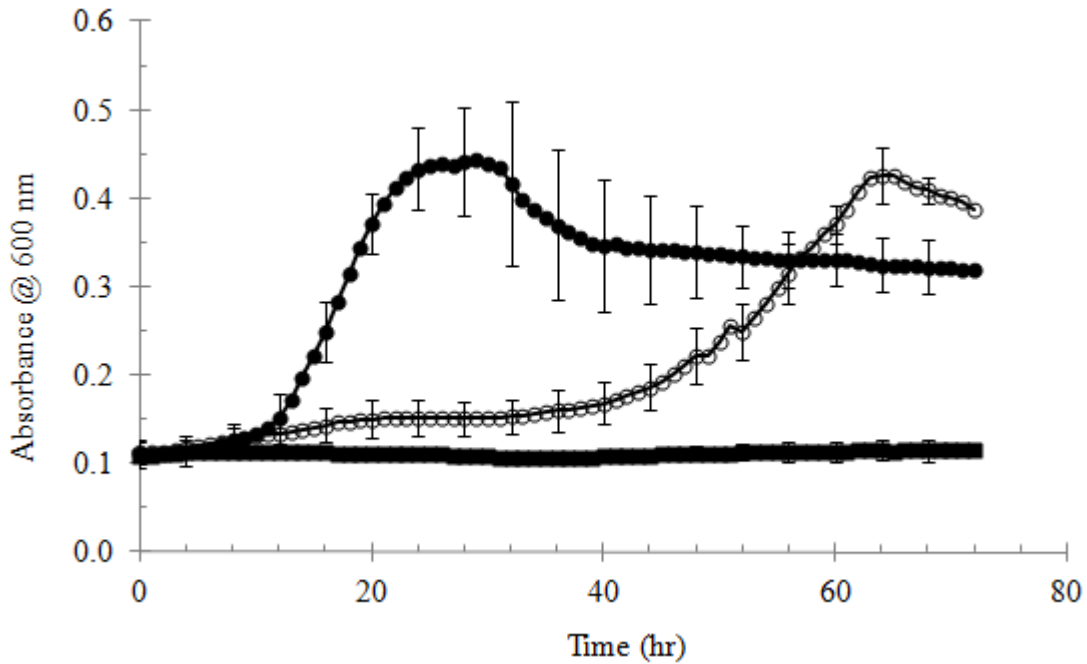


Figure 45. Aerobic bacterial growth as indicated by optical density curves at 600 nm, with different substrate concentrations: 0.6 mM (or 75.6 mg/L) melamine only (■), 14 mM glucose only (●), and a combination of 0.6 mM melamine and 14 mM glucose (○). Activated sludge from the CSTR before melamine dosing was used as a seed culture. Error bars represent one standard error of the mean (n=4).

5.3.4. Bacteria Community Structure Changes after Continuous Melamine Dosing

The T-RFLP analysis specifically targeting the AOB and NOB indicated that the AOB genera primarily consisted of *Nitrosomonas* and the NOB genera contained *Nitrospira* and

Nitrobacter in both the CSTR and MLE systems (data not shown). The peak heights in Figure 46a and 46c represent the relative abundance of each species in the CSTR and MLE systems (Luna et al., 2006, Luna et al., 2004), and before melamine dosing, both systems had almost the same AOB population. After melamine dosing, the *Nitrosomonas* population in the CSTR system was reduced, based on the reduction in the peak heights in Figure 46b as compared to those in Figure 46a. At the same time, the AOB population was decreased even more substantially in the MLE system, as evidenced by the greater reduction in peak height shown in Figure 46d. These results correlate well with the effluent water quality (Figure 43) and nitrifying bacterial activity (Figure 44) results before and after melamine dosing.

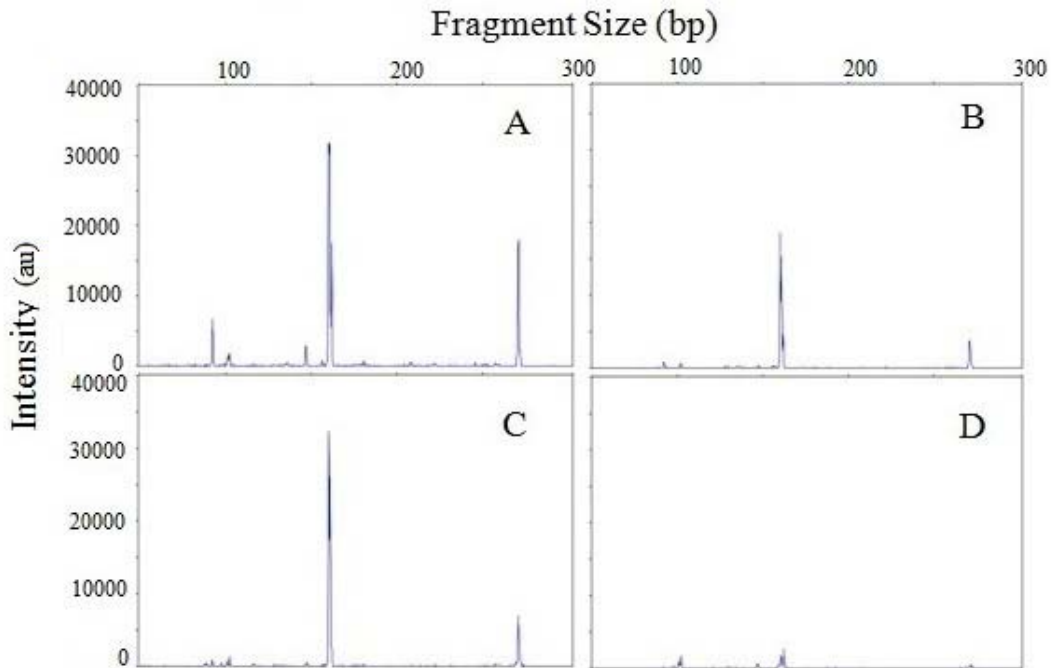


Figure 46. Ammonia-oxidizing bacterial community structure and abundance reflected by T-RFLP profiles targeting 16S rRNA genes of *Nitrosomonas* in the CSTR before melamine dosing (A), the CSTR after melamine dosing (B), the MLE before melamine dosing (C), and the MLE after melamine dosing (D). AU = arbitrary units. DNA samples were taken 1 month before melamine dosing and after 50 days of continuous melamine dosing.

5.3.5. Implications of Melamine Biodegradation and Its Toxicity to Activated Sludge

Melamine has been reported to be slowly degradable in soil with an estimated half-life between 2 and 3 years (UNEP). The results of this study demonstrate that melamine is not readily biodegradable in activated sludge processes used for domestic wastewater treatment (UNEP). Even after a prolonged exposure, activated sludge has no demonstrated

capability to degrade melamine. The melamine removal efficiencies in the CSTR and MLE systems were $14 \pm 10\%$ and $20 \pm 15\%$, respectively. These removal efficiencies were not statistically significant from each other, indicating that neither aerobic conditions nor anoxic/aerobic sequencing conditions have an impact on melamine degradation. Earlier studies have suggested that the biodegradation rates of single aromatic compounds are often highest under aerobic conditions (Hu et al., 2005b). As biochemical conditions are shifted from oxygen-respiration to nitrate respiration, to anaerobiosis, the biodegradation rates decrease or cease to occur. However, this is not the case for the biodegradation of melamine, which is a triazine derivative (Seffernick et al., 2001). Such N-heterocyclic molecules have lower electron affinities than benzene (Nenner and Schulz, 1975), which reduces their potential for electrophilic aromatic substitution. Instead, these molecules are more likely to undergo nucleophilic aromatic substitution (e.g., via hydrolyzation). Based on this degradation process and the results of this study, it appears that the enzymes responsible for hydrolytic deamination are not readily induced in activated sludge processes.

Microbial communities adapt to a chemical contaminant that is not easily biodegradable through one or more of five primary mechanisms: selective enrichment, enzyme regulation,

gene transfer (via conjugation, transformation, and transduction), inheritable genetic change through mutation and recombination, and alternation of their growth environment (Rittman and McCarty, 2001). In this study, none of the above mechanisms seemed to occur. Because the valence of carbon is +4 in $C_3H_6N_6$, melamine could not be used as a carbon source to support the growth of heterotrophs that are dominant in activated sludge systems. Therefore, selective enrichment of bacteria capable of degrading melamine was not seen as bacteria prefer to use biogenic substrate for growth. This suggests that the enzymes responsible for the hydrolytic deamination of melamine appear not to be produced by bacteria in activated sludge. This is plausible because only a few bacterial strains have been found to be capable of degrading melamine and they have only been isolated from soil (Boundy-Mills et al., 1997, Cook and Hütter, 1981, El-Sayed et al., 2006, Shelton et al., 1997), Alternatively, the competent biomass fraction (Hu et al., 2005b) or the number of bacterial specialists capable of degrading melamine may simply be too low to degrade melamine in wastewater to a significant degree. Although genetically widespread guanine deaminases have a promiscuous activity allowing them to catalyze a key reaction in the bacterial transformation of melamine to cyanuric acid (Seffernick et al., 2010), a series of deaminases are required for complete melamine degradation. Additionally, microbial adaptations occur over times from a few hours to years. In this

study, the adaptation period lasted for about 100 days. Therefore, further study is still needed to better understand the mechanisms of adaptation and its effect on melamine degradation.

Melamine toxicity may also cause insignificant biodegradation of melamine in activated sludge processes. Continuous melamine dosing, even at a relatively low concentration (3 mg/L), resulted in a significant inhibition of nitrification (Figures 42 and 44) and a decrease in the total nitrifying bacterial population (Figure 46). Melamine also inhibited heterotrophic growth at higher concentrations (Figure 45). Consequently, melamine has a negative impact on bacterial adaptation by negatively affecting the growth environment (Rittman and McCarty, 2001).

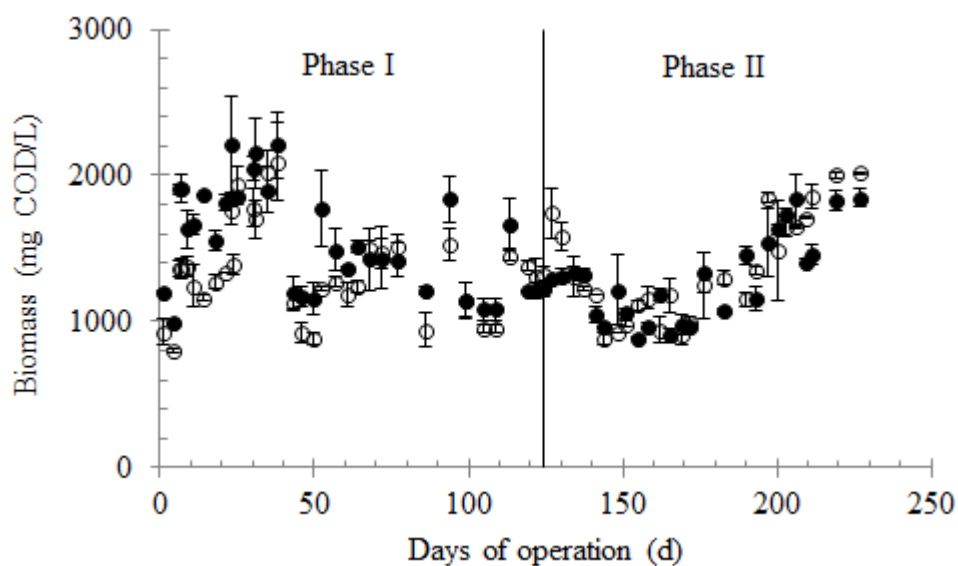


Figure 47. Biomass concentrations in the CSTR (○) and MLE (●) bioreactors before (Phase I) and after (Phase II) melamine dosing. Error bars represent data range of duplicate samples.

5.4. Conclusions

In this study, we investigated the degradation of melamine and its impact on two activated sludge treatment systems seeded with the sludge from a local municipal WWTP. Even after a long period of sludge adaptation (100 d), melamine appeared not to be easily biodegradable in these systems. Selective enrichment of activated sludge bacteria with the enzymes responsible for the hydrolytic deamination of melamine was not successful as bacteria prefer to use biogenic substrate in wastewater for growth. Furthermore,

insignificant biodegradation of melamine was also attributed to bacterial growth inhibition under long-term dosing conditions with melamine in the treatment systems.

CHAPTER 6

6. Biodegradation of Melamine in a Membrane Bioreactor with High Biomass Concentration

Melamine is recalcitrant and toxic to activated sludge in conventional activated sludge (CAS) systems. In this study, we investigated the degradation of melamine in an MBR system operated at high biomass concentrations. Melamine was dosed continuously from day 85 at an influent concentration of 3 mg/L for about 100 days. Even after such a long period of sludge adaptation, melamine appeared to not be easily biodegradable. The average melamine removal efficiency in the MBR system was $20 \pm 11\%$. For comparison, batch studies showed the acclimated sludge has higher removal efficiencies (e.g., $41 \pm 10\%$ by 10 g/L biomass) than non-acclimated sludge which has no capability for melamine degradation. Hence, the microbial specialists in the acclimated sludge were likely responsible for melamine degradation through cometabolism or fortuitous degradation. With continuous input of readily biodegradable substrate in the MBR, the population of microbial specialists capable of degrading melamine appeared not to proportionally increase as the biomass concentration increased to 10 g/L in MBR operation. Possibly because bacteria prefer to use readily biodegradable substrate for growth regardless of

acclimation, there was no significant difference in melamine removal between the MBR and the CAS systems. Furthermore, the long-term input of melamine did not affect MBR performance or the effluent water quality. These results suggest that high biomass concentrations (increased by a factor of 5 compared to that of CAS) result a significant reduction in toxicity of melamine to the activated sludge, demonstrating the significance of toxicant to biomass ratio in MBR performance.

6.1. Objectives

Although the previous chapter shows that the biodegradation of melamine was not improved after a long-term sludge adaptation in CAS systems, it has been reported that high biomass concentration may improve the biodegradation of some recalcitrant organic compounds (Boonnorat et al., 2014). In the CAS study, the competent biomass fraction (Hu et al., 2005b) or the number of bacterial specialists capable of degrading melamine may simply be too low to degrade melamine in wastewater to a significant degree. The objective of this chapter was to study the effect of long-term sludge adaptation on the biodegradation of melamine in a MBR system at high biomass concentrations (i.e., $5 \times$ biomass concentration in the CAS).

6.2. Materials and Methods

6.2.1. MBR Setup and Operation

One bench-scale submerged MLE-MBR equipped with the ZeeWeed hollow fiber membrane module (GE Water & Process Technologies, Trevose, PA) was operated during the study (Figure 48). The membrane module was made of polyvinylidene fluoride (PVDF) with a nominal pore size of 0.1 μm and a total effective surface area of 0.047 m^2 . The MLE-MBR had a total effective reactor volume of 7.2 L including anoxic (first) and aerobic chambers of 2.4 L and 4.8 L, respectively. There was a glass baffle installed to separate the anoxic and aerobic chambers and recirculation at a flow rate equal to the influent flow rate from the aerobic chamber to the anoxic chamber. The upper and lower water level sensors (Cole-Palmer, Vernon Hills, Illinois) were applied to maintain a relatively constant mixed liquor volume in the MLE-MBR. The volume difference between the upper and lower water level was less than 5% of the total mixed liquor volume in the MLE-MBR. The sensor is designed to activate an onboard solid-state relay when the sensor detects a change of water level. When the water level reaches the upper limit because of continuous feeding, the upper level sensor triggers the operation of a permeate pump. When the water level reaches the lower limit, the lower level sensor assures pump shut-down. In this study, a suction peristaltic pump after the membrane module acted as the permeate pump to produce a relative vacuum for permeate collection. An online digital

pressure gauge (Cole-Palmer) was installed to measure the transmembrane pressure (TMP). The speed of the permeate pump was set at a permeate flux higher than the influent flow rate so that the permeate pump was intermittently turned on and off by the upper and lower water level sensors, respectively, to keep the total mixed liquor volume relatively constant. An air pump supplied compressed air to the built-in orifices at the bottom of each membrane module at a constant air flow rate of 6 L/min to support aerobic biodegradation and control membrane fouling.

At a hydraulic retention time (HRT) of 1 d, the MBR was fed continuously with synthetic wastewater containing nonfat dry milk powder as the primary organic carbon source at a COD concentration of approximately 500 mg/L. The details of the synthetic wastewater were described in 5.2.1. The inoculation sludge was taken from the aerobic tank from the Columbia Wastewater Treatment Plant (Columbia, MO), which has a treatment capacity of 20 million gal per day using the CAS process. A total of 24 L of sludge was collected and fed with synthetic wastewater for 1 week before the sludge was transferred to the MLE-MBR. The starting biomass concentration in the MLE-MBR was approximately 6 g COD/L. During the start-up period of this study, there was no sludge wasted until the biomass concentration reached 10 g COD/L. Afterward, sludge was wasted daily with the

targeted SRT of approximately 130 days to maintain relatively constant biomass concentrations in MLE-MBR.

During the operating period, the TMP and permeate flux of the membrane process in the MLE-MBR were closely monitored. When the TMP increased dramatically in a short period of time or the TMP level exceeded the predefined TMP value (44.5 kPa), as suggested by the manufacturer, the membrane module was taken out of the MBR for physical cleaning. The membrane module was rinsed with tap water for about 30 min before it was submerged in the mixed liquor in the MBR for reuse.

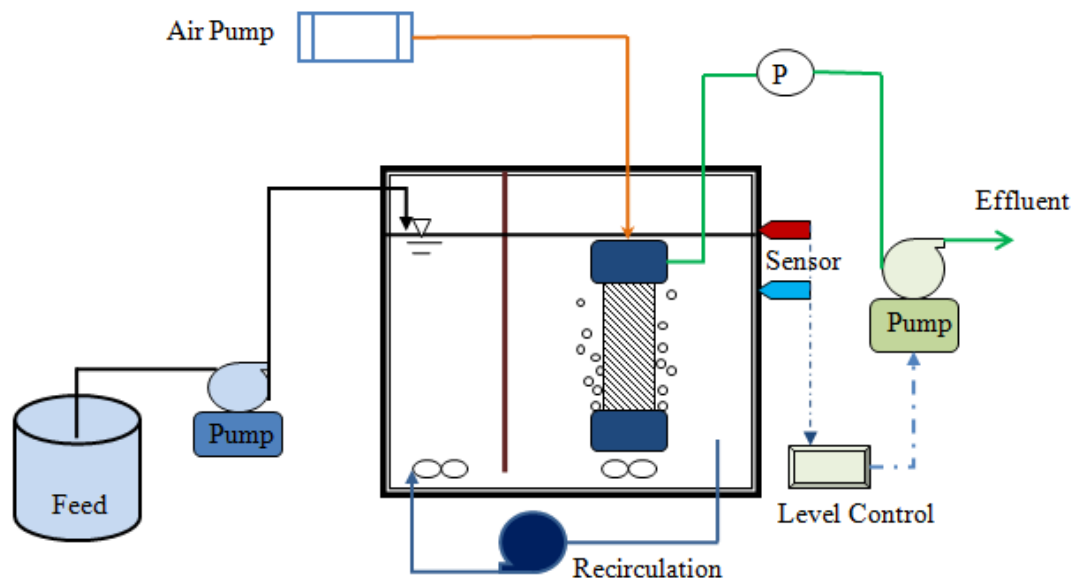


Figure 48. A schematic of a bench-scale submerged MLE-MBR. P stands for a transmembrane pressure measurement device.

6.2.2. Effect of Long-Term Melamine Dosing on Bioreactor Performance

Melamine (99%) was purchased from Acros Organics. From day 85 onwards, a melamine stock solution with a concentration of 122.8 mg/L was fed separately to the bioreactor at a flow rate of 0.172 L/d to reach a nominal influent concentration of 3 mg/L (Xu et al., 2013). The change in the HRT due to melamine addition was negligible because the flow rate of melamine stock was much lower than the influent (6.9 L/d). Wastewater effluent from the MBR system was collected and analyzed for melamine, $\text{NH}_4^+\text{-N}$, $\text{NO}_3^-\text{-N}$, $\text{NO}_2^-\text{-N}$, and COD following the standard methods (APHA, 2002).

6.2.3. Batch Melamine Adsorption and Degradation Study

Batch studies were conducted to determine the potential for adsorption of melamine by sludge in the MBR system before melamine dosing in the continuous flow system. The sludge samples were collected from the Columbia WWTP and concentrated with a final biomass concentration of about 10 g/L before use. For comparison, aliquots (500 mL) of the sludge sample were killed by heating at 80 °C for 20 min (Hu et al., 2005b). Then aliquots (5 mL) of the melamine stock solution (1,000 mg/L) were added to the sludge

samples at a final melamine concentration of 10 mg/L. The mixed liquor in each beaker was magnetically mixed at 350 rpm at 25 ± 1 °C under aerobic and anoxic conditions to evaluate the influence of different metabolic environments. An aeration pump was used to supply air in addition to mixing under aerobic conditions. Excess sodium nitrate was added to the mixed liquor under anoxic conditions. At predetermined times (4, 12, 16, 24, 36, 54, 72 h), aliquots (5 ml) of mixed liquor were collected for melamine analysis. After 10 min sedimentation, the supernatant was passed through a 0.45 μ m nylon syringe filter and the filtrate was stored at 4 °C before analysis.

Batch studies were also conducted to compare the melamine degradation behavior by the acclimated activated sludge and unacclimated sludge. The acclimated sludge samples were collected from the aeration chamber of the MBR system after 100d of continuous melamine dosing. The sludge samples with biomass concentrations of 10 g COD/L or 2 g COD/L (after dilution) were used. The activated sludge taken from the WWTP served as a control (unacclimated sludge). All of the samples were washed with distilled water three times to remove the residual carbon and nutrients before they were re-suspended in the medium that had the same recipe as the feed solution with the exception of the use acetate as a readily biodegradable substrate (~400 mg COD/L) instead of milk powder to

determine the effect of ammonia on melamine degradation. Part of the batch experiments were conducted with the medium containing no ammonia (20 mg/L). The experiment was repeated at different initial melamine concentrations (2.5, 3, 5, 10 and 20 mg/L) at the sludge concentration of 10 g biomass COD/L. All of the batch systems were set up in at least duplicate. Each study was conducted in a 250mL flask with 50 mL headspace. Each flask covered with a cotton stopper was placed on a platform shaker (Innova 2000) running at 200 rpm to ensure complete mixing of the mixed liquor inside.

6.2.4. Effect of Melamine on Nitrifying Community Structure and Microbial Activities

Activated sludge samples in the MLE-MBR bioreactor were collected before and after the melamine dosing for DNA extraction and nitrifying community structure analysis using Terminal Restriction Fragment Length Polymorphism (T-RFLP) (details shown in 2.2.5). To determine the change in heterotrophic and autotrophic microbial activities, aliquots of mixed liquor were periodically taken from the aeration chamber to determine the specific oxygen uptake rates (SOUR), with detailed procedures described in 2.2.4.

6.2.5. Chemical and Statistical Analysis

Details about the bioreactor performance monitoring are described in 5.2.6. In addition, acetic acid in the batch studies was measured by high performance liquid chromatography (HPLC) with ultraviolet detection at 210 nm. The HPLC injection volume was 10 μ L, and the mobile phase used was 0.1% o-phosphoric acid circulated at 0.8 mL/min at ambient temperature (Yang et al., 2012). Wastewater influent and effluent samples were collected twice a week for COD, ammonium-N, nitrite-N, and nitrate-N measurements following standard methods (APHA, 2002). One-Way ANOVA analysis was conducted to assess the significance of the differences among groups, with p values less than 0.05 indicating statistical significance.

6.3. Results and Discussion

6.3.1. Biodegradation of Melamine in the MBR System

After the biomass concentration in the MBR became stabilized at approximately 10 g/L (Figure 49) from day 56 to day 84 (Phase I) melamine was dosed continuously from day 85 onward (Phase II). As can be seen in Figure 50, the average influent melamine concentration over the Phase II period was 3.0 ± 0.2 mg/L, while the average permeate or effluent melamine concentrations in the MBR were 2.4 ± 0.3 mg/L (removal efficiency =

20 ± 11%). There was a significant difference in the melamine concentration between the influent and effluent samples ($p < 0.001$). Melamine removal through adsorption was not observed even at high biomass concentrations (~10 g COD/L) (Figures 51). Hence, melamine can be partially removed in activated sludge systems via biodegradation. However, the removal efficiency of melamine in the MBR remained the same as that in the CSTR or MLE systems in our previous study (Xu et al., 2013). The result suggests that high biomass concentration (10 g COD/L) in the MBR system does not improve melamine degradation.

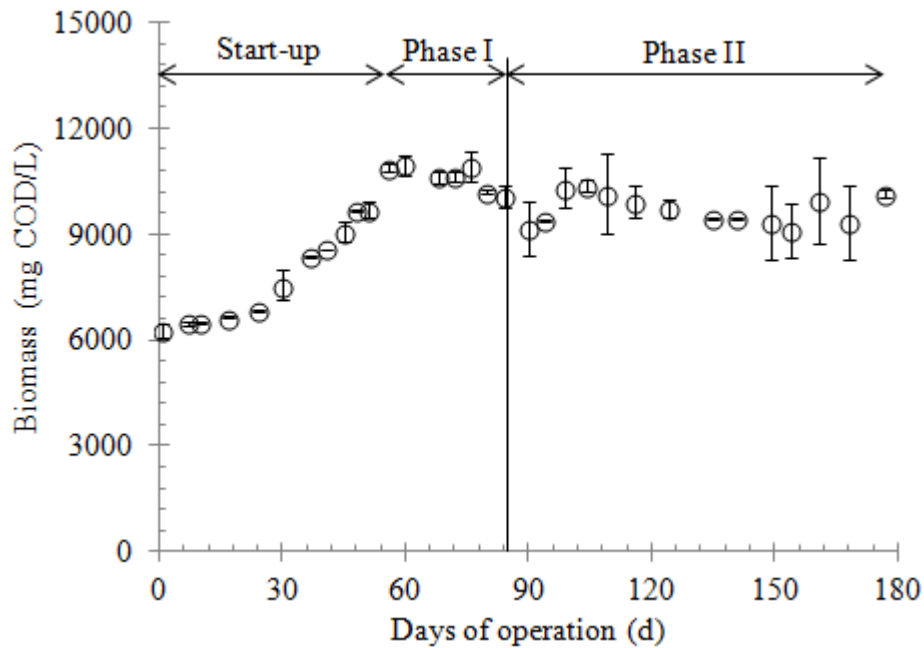


Figure 49. Change in the biomass concentration in the MBR bioreactors before (Start-up and Phase I) and after (Phase II) melamine dosing. Error bars represent data range of duplicate samples.

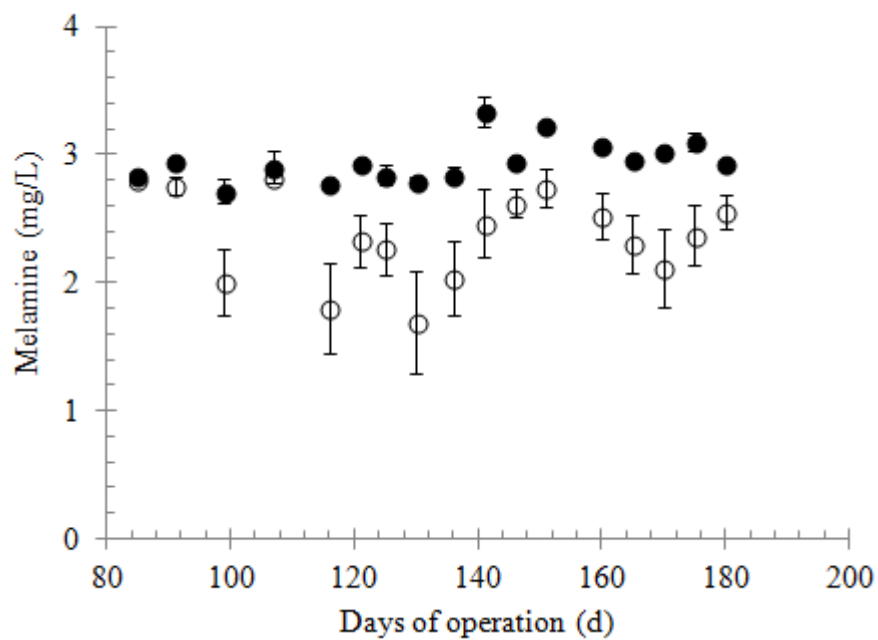
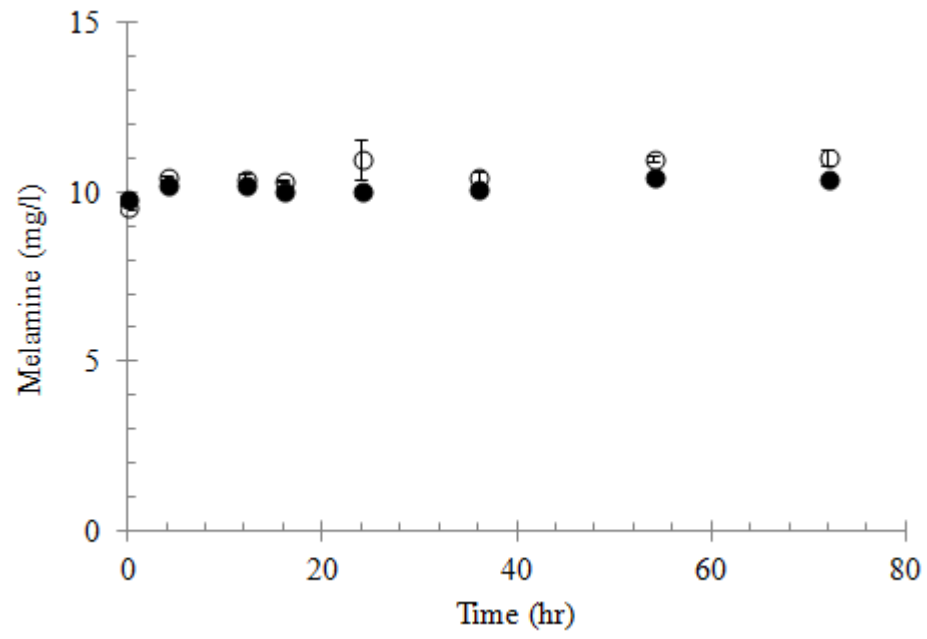


Figure 50. Influent (●) and effluent (○) melamine concentrations in the MBR system after continuous melamine dosing starting from day 85. Error bars represent one standard deviation of the mean (n = 3).

(a)



(b)

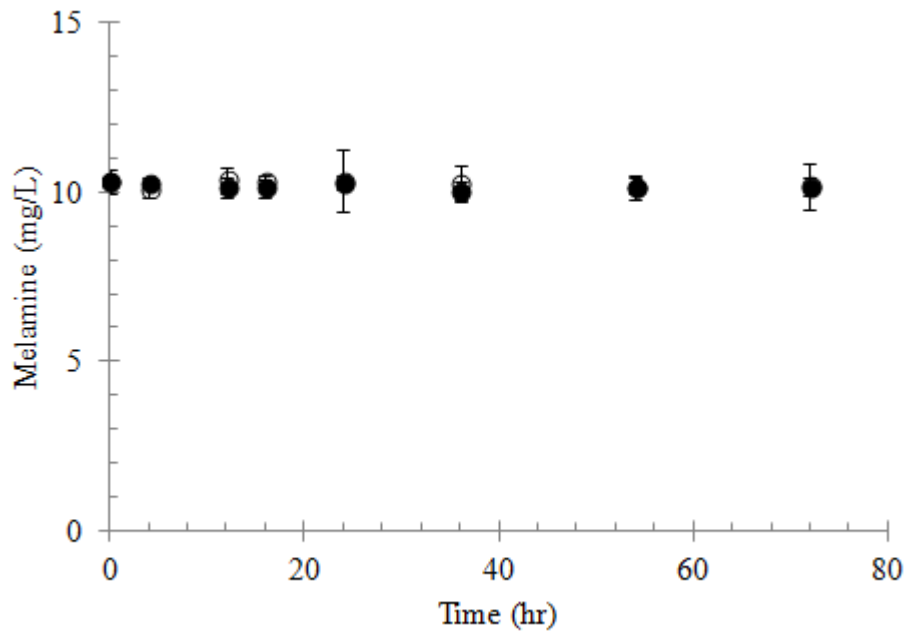


Figure 51. Change in melamine concentration in the absence of readily biodegradable substrate under aerobic (○) and anoxic (●) conditions in the mixed liquor with an average biomass concentration of 10 g COD/L in batch studies: live cells (a) and dead cells (b). Error bars represent one standard error of the mean (n = 4).

The effect of sludge acclimation on melamine degradation was further evaluated in the presence of acetate in batch studies. As shown in Figure 52, there was no removal of melamine by unacclimated activated sludge (2 g/L) during 7 d of incubation. However, acclimated sludge had higher removal efficiencies ranging from $33 \pm 6\%$ (by 2 g/L biomass) to $41 \pm 10\%$ (by 10 g/L biomass). There was a significant difference between the removal efficiencies ($p < 0.001$) possibly due to the different melamine/biomass

concentration ratios. Meanwhile, HPLC results showed that acetate was depleted in the first day (data not shown), which may drive the bacterial specialist to degrade melamine through cometabolism under stress conditions or utilize melamine as a nitrogen source. By comparing the removal efficiency in the first day with that over the rest of the days of cultivation, which were 0.1 % vs 33 ± 6 % by 2 g/L biomass and 12 ± 4 % vs 33 ± 7 % by 10 g/L biomass, the removal efficiencies after the depletion of acetate was significantly higher ($p < 0.01$ by 2 g/L biomass and $P = 0.03$ by 10 g/L biomass) than that in the presence of acetate. In fact, the significant increase in degradation started on day 4 which is probably due to bacteria doing endogenous respiration before they degrade melamine. At the same time, in the batch studies with available ammonia as a nitrogen source, the biodegradation efficiency of melamine ($= 35 \pm 8\%$) by the acclimated activated sludge (2 g/L) was not affected much even though ammonia was fully oxidized in the first day (data not shown). However, in the continuous flow systems, when the readily biodegradable organic substrate was fed continuously, the removal of melamine was limited (Figure 50). The results demonstrate the role of long-term sludge acclimation in melamine biodegradation and the impact of the readily biodegradable carbon source on melamine biodegradation. The results also suggest that the total biomass concentration plays a minimum role in melamine biodegradation. Instead, the microbial specialists capable of

degrading melamine through cometabolism or fortuitous degradation are likely responsible, but their population appeared not to proportionally increase as the biomass concentration increased from 2 g/L to 10 g/L in MBR operation.

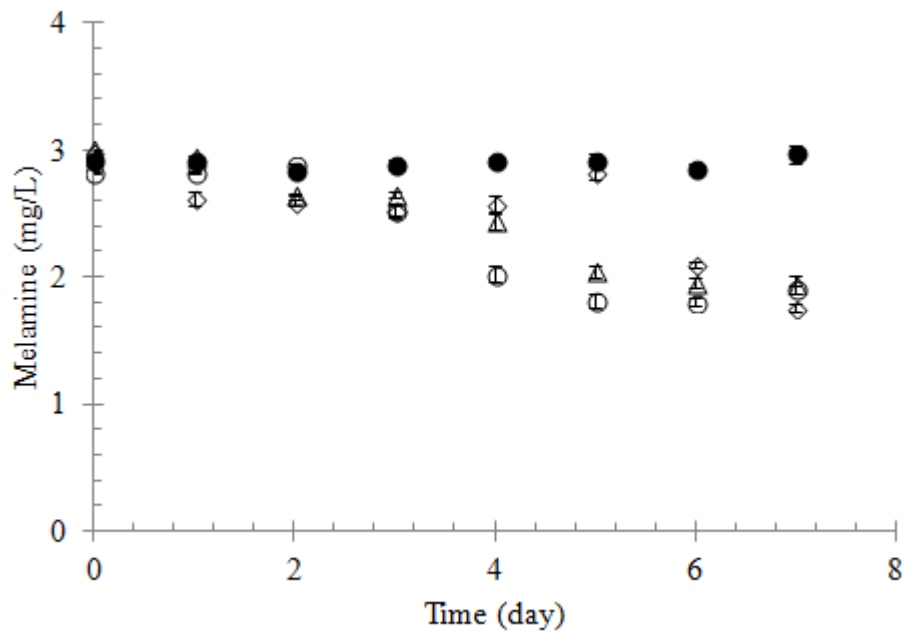


Figure 52. Change in melamine concentrations by unacclimated sludge of 2 g/L (●), acclimated sludge of 2 g/L (○), acclimated sludge of 2 g/L with ammonia substrate (20 mg/L) (△), and acclimated sludge of 10 g/L (◇) in batch studies. Error bars represent one standard error of the mean (n = 4).

Another batch experiment was conducted to investigate the effect of initial melamine concentrations on biodegradation. Regardless of initial melamine concentration (i.e., 2.5, 5,

10 and 20 mg/L), similar amounts (0.9 ~ 1.0 mg/L) of melamine were removed in one week (Figure 53), resulting in the removal efficiencies ranging from 5% (at 20 mg/L melamine) to 41% (at 2.5 mg/L melamine). This result further suggests the degradation of melamine is irrelevant to cell metabolism, but is more related to cometabolism or fortuitous degradation by some housekeeping enzymes (Gold et al., 2000).

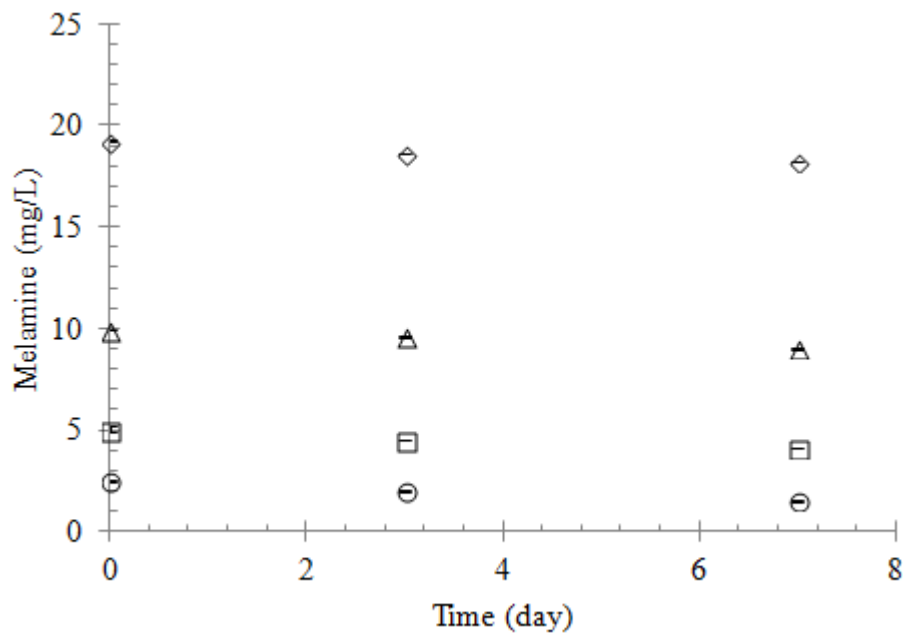


Figure 53. Change in melamine concentrations with time at initial melamine concentrations of 2.5 mg/L (○), 5 mg/L (□), 10 mg/L (△) and 20 mg/L (◇) in batch studies. Error bars represent one standard error of the mean (n = 4).

6.3.2. Bioreactor Performance before and after Melamine Exposure

During the start-up period (day 0 to 55), biomass concentrations in the MBR gradually increased from about 6 to 10 g COD/L because there was no sludge wastage. Through regular biomass wasting, the biomass concentrations leveled off and became stable between 9 and 10 g COD/L (day 56–84, Phase I) before the continuous melamine dosing began (day 85-185, Phase II). The water quality data before (Phase I) and after (Phase II) melamine dose were compared statistically. At an average influent COD concentration of 511 ± 76 mg/L, the average effluent COD concentrations during Phase I and Phase II were 17 ± 5 mg/L and 9 ± 5 mg/L respectively (Figure 54), resulting in the average removal efficiencies of 97% and 99%. The significantly lower ($p < 0.001$) effluent COD concentration in Phase II was due to the long-term MBR operation as the biomass concentration was maintained around 10 g COD/L. The continuous melamine dosing did not affect the organic matter removal, which was different from that in the CAS system (Xu et al., 2013). Meanwhile, there were no significant differences in effluent $\text{NH}_4^+\text{-N}$ ($p = 0.4$), $\text{NO}_2^-\text{-N}$ ($p = 0.8$) or $\text{NO}_3^-\text{-N}$ ($p = 0.3$) concentrations between Phase I and Phase II. The effluent $\text{NH}_4^+\text{-N}$ concentrations during Phase I and Phase II were 0.2 ± 0.1 mg/L and 0.1 ± 0.2 mg/L, respectively, with removal efficiencies of 99% and 100% respectively, indicating almost complete nitrification before and after melamine dosing (Figure 55a).

Correspondingly, the effluent NO_2^- -N concentrations during Phase I and Phase II were 0.3 ± 0.3 mg/L and 0.2 ± 0.2 mg/L, respectively, and the effluent NO_3^- -N concentrations were 11.2 ± 5.4 mg/L and 13.2 ± 4.4 mg/L, respectively (Figure 55b).

Unlike the results from CAS systems where the presence of melamine (3 mg/L) deteriorated effluent water quality (Xu et al., 2013), the continuous melamine dosing (3 mg/L) in the MBR with high biomass concentration (5 times higher than that in CAS) had no impact on organic and nitrogen removal. These results were also confirmed by the SOUR data, which indicated normal heterotrophic and autotrophic activities before and after melamine dosing (Figure 56).

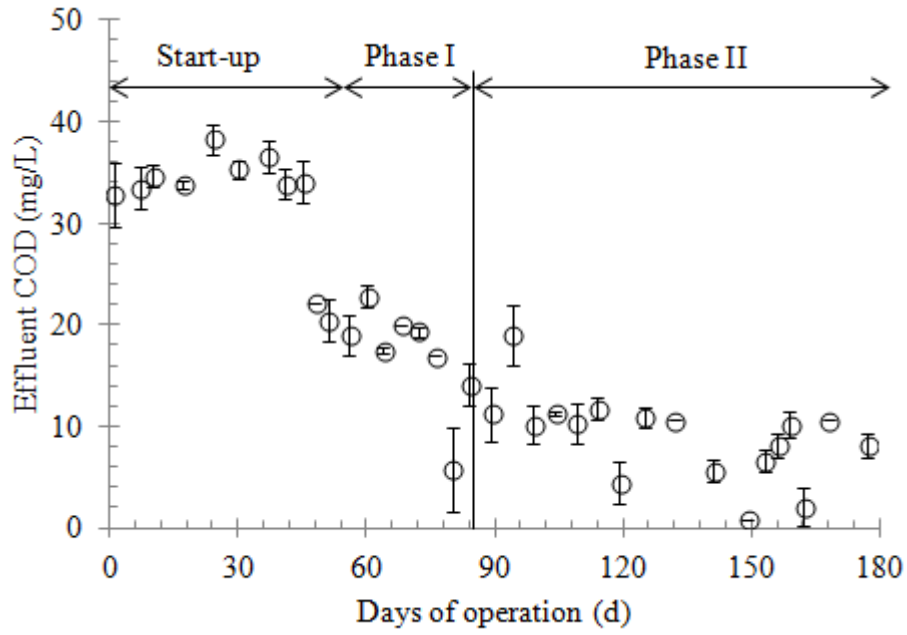
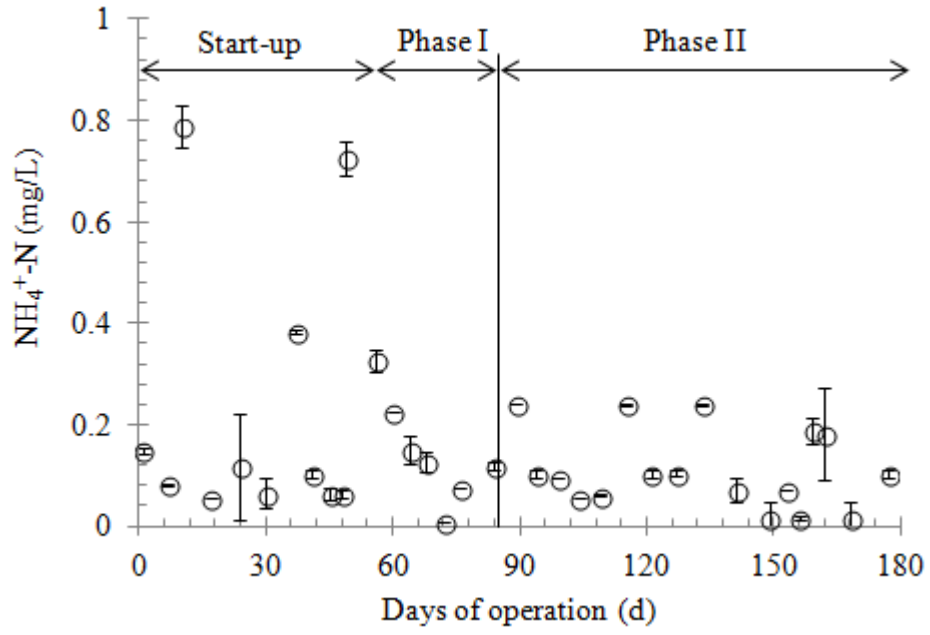
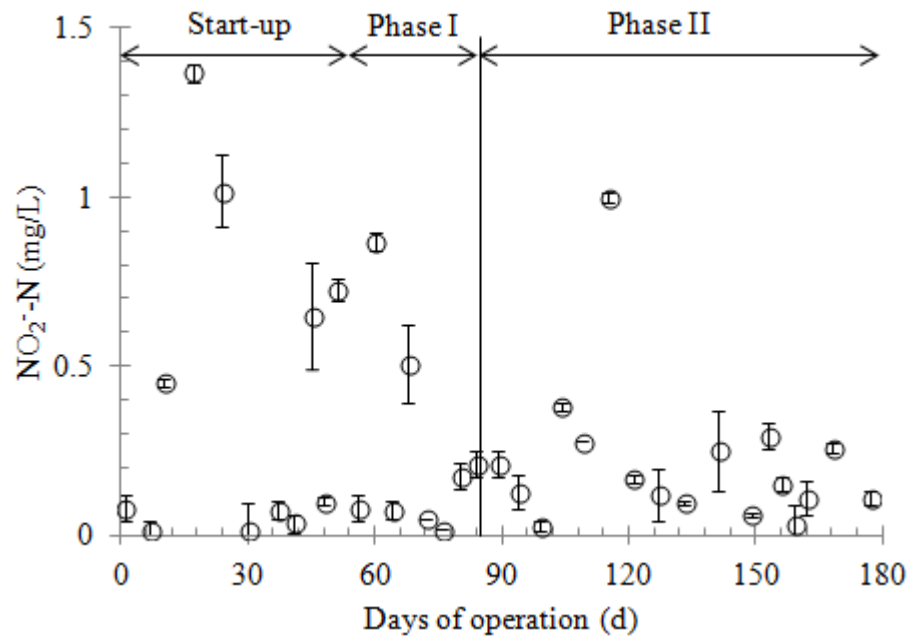


Figure 54. Effluent COD concentrations in the MBR before (Start-up and Phase I) and after (Phase II) melamine dosing. Error bars represent the data range of duplicate samples.

(a)



(b)



(c)

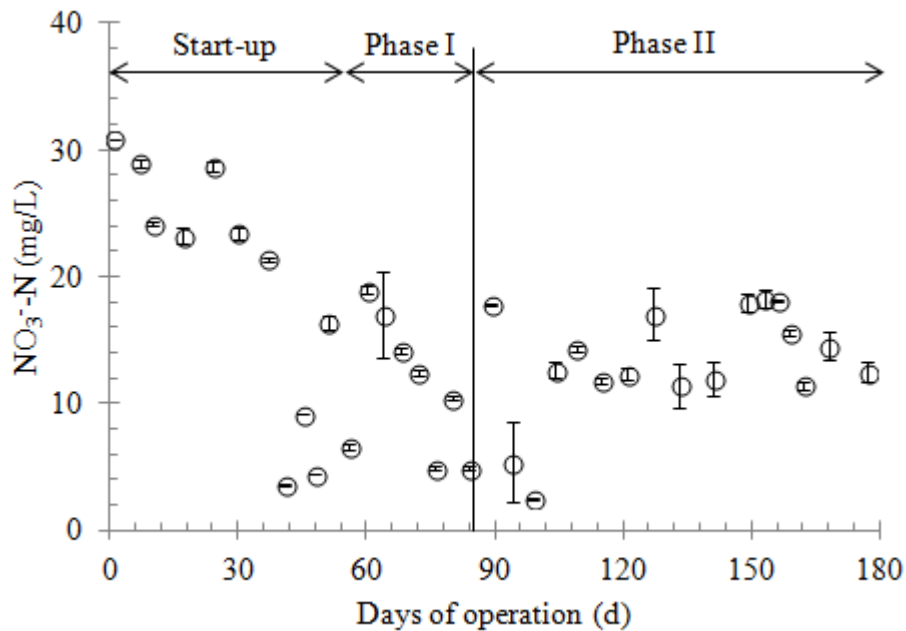


Figure 55. Effluent $\text{NH}_4^+\text{-N}$ (a), $\text{NO}_2^-\text{-N}$ (b) and $\text{NO}_3^-\text{-N}$ (c) concentrations in the MBR before (Start-up and Phase I) and after (Phase II) melamine dosing. Error bars represent the data range of duplicate samples.

6.3.3. Bacterial Activities before and after Melamine Dosing

The changes in bacterial activities in response to the continuous melamine were inferred from the extant respirometric assays as shown in Figure 56. The average heterotrophic SOUR values of the sludge before and after melamine dosing were $18.4 \pm 1.4 \text{ mg O}_2/\text{g MLSS/h}$ and $18.0 \pm 1.1 \text{ mg O}_2/\text{g MLSS/h}$, respectively. There was no significant difference ($p = 0.49$) in the heterotrophic SOUR values before and after melamine dosing. Hence, the continuous melamine dosing with an average range concentration of 3 mg/L in the sludge

did not affect heterotrophic activities, consistent with low effluent COD concentrations. A slight drop observed in heterotrophic SOUR data during the beginning of Phase II was probably due to a short and insignificant impact of melamine on the heterotrophic bacterial activity at the beginning of dosing. Similarly, the autotrophic SOUR values before and after melamine dosing were 14.8 ± 0.7 and 13.8 ± 1.5 mg O₂/g MLSS/h, respectively. There was no significant difference in autotrophic SOUR values before and after melamine dosing ($p = 0.1$).

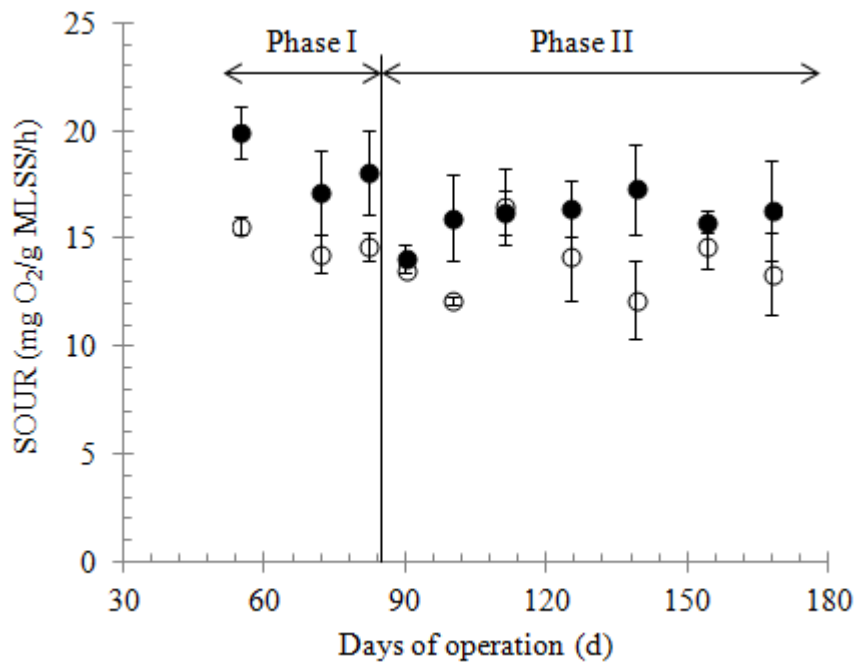


Figure 56. Changes in autotrophic (○) and heterotrophic (●) SOURs in the MBR before (Phase I) and after (Phase II) melamine dosing. Error bars represent the data range of duplicate samples.

6.3.4. Bacterial Community Structure Changes after Melamine Dosing

The T-RFLP analysis specifically targeting the AOB and NOB shows the change in nitrifying bacterial community structure in the MBR system before and after melamine dosing. The peak heights in Figure 57a and 57b represent the relative abundance of each species in the MBR system (Luna et al., 2006, Luna et al., 2004) About one week before melamine dosing, *Nitrosomonas* (Figure 57a) was the dominant genus of AOB while *Nitrospira* (Figure 57b) was dominant among NOB. About 1 month after melamine dosing, similar levels of AOB and NOB in the MBR were detected. This suggests the long-term exposure to low concentration of melamine did not affect nitrifying bacterial growth in the MBR system. These results correlate well with the effluent water quality (Figure 55) and nitrifying bacterial activity (Figure 56) results before and after melamine dosing.

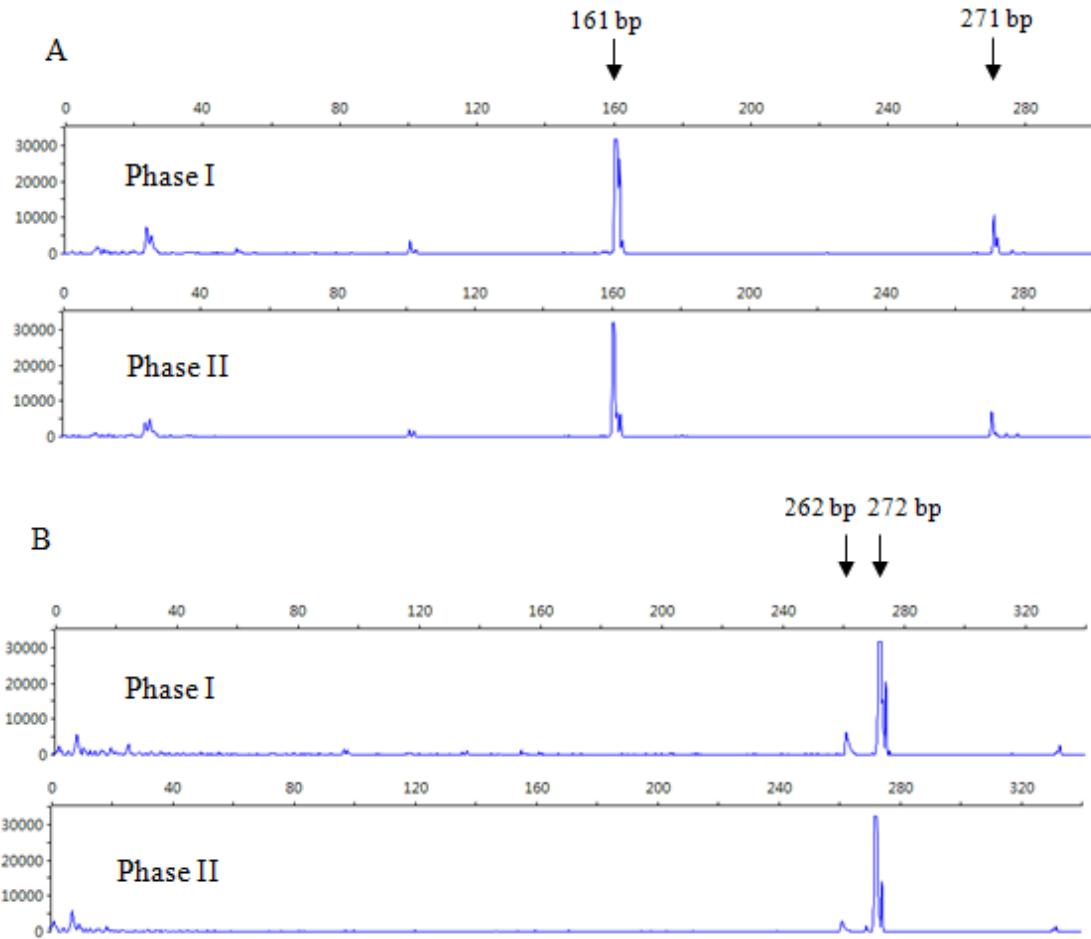


Figure 57. Nitrifying bacterial community composition reflected by T-RFLP profiles targeting 16S rRNA genes of *Nitrosomonas* (A), and *Nitrospria* (B) before (Phase I) and after (Phase II) melamine dosing.

6.3.5. Implications of Melamine Biodegradation in MBR Operated at High Biomass Concentrations

Figure 2 shows the biodegradation of melamine is mainly via hydrolysis, which occurs theoretically, according to

$$r_{\text{hyd}} = -k_{\text{hyd}}S_p \quad (9) \text{ (Rittman and McCarty, 2001)}$$

where r_{hyd} is the rate of accumulation of particulate substrate due to hydrolysis, S_p is the concentration of the particulate substrate and k_{hyd} is the first-order hydrolysis rate coefficient which is proportional to the concentration of hydrolytic enzymes. The theory suggests k_{hyd} is related to the activate biomass concentration in many cases (Rittman and McCarty, 2001). Obviously the hydrolysis of a particulate substrate cannot apply to melamine which showed no improvement in melamine degradation in the MBR system by increasing biomass concentration to about 10 g COD/L. It is believed that the competent biomass, a specific population of the microbial community that has the capacity to degrade melamine through cometabolism or fortuitous degradation, is responsible for melamine biodegradation (Cook and Hütter, 1981, Takagi et al., 2012). Acclimation of the entire microbial community to melamine in a MBR system operated at long SRT may allow a better selection of microorganisms containing enzymes and pathways or development of new catabolic pathways for recalcitrant organic chemical removal such as melamine (Boonnorat et al., 2014). So the question remains to be answered for the plateau of the melamine biodegradation efficiencies (about 20%) in both MBR and CAS systems with continuous readily biodegradable substrate. On the other hand, the water quality data showed that the MBR has a better tolerance to the variables of

influent compared to CAS systems, which is likely due to the low melamine/biomass concentration ratio or these variables (i.e. melamine) mainly responsible for triggering the shifts between functionally redundant populations (Gómez-Silván et al., 2014).

6.4. Conclusions

The degradation of melamine in the MBR with high biomass concentration (10 g COD/L) was investigated in this study. Even though acclimation appeared to improve melamine degradation in batch studies, there was no improvement of melamine degradation in the MBR even after a long period of sludge acclimation (100 d). Most likely, melamine was degraded through cometabolism or fortuitous degradation. With continuous input of readily biodegradable substrate in the MBR, the population of microbial specialists capable of degrading melamine appeared not to proportionally increase as the biomass concentration increased to 10 g/L in MBR operation. Nevertheless, compared to that in CAS systems, there was no inhibition of melamine to the activated sludge in the MBR because of operation at high biomass concentrations (with low melamine/biomass concentration ratio).

CHAPTER 7

7. Summary and Future Research Directions

Under the identical operating conditions, both the A²/O and reverse A²/O systems showed excellent organic matter and total N removal performance. The reverse A²/O process appears to be a better choice because of its higher P removal performance, and for its potentially simpler design for full-scale operation. However, how influent wastewater containing low readily biodegradable BOD or with low C/N ratio would affect P removal in the A²/O and reverse A²/O systems remains to be studied and compared. A reverse A²/O might not work properly because all biodegradable BOD can be easily consumed by denitrifiers in the anoxic tank first.

To extend its application beyond *in situ* groundwater remediation, NZVI may be used for wastewater treatment with wastewater often containing nitrate and dissolved oxygen. Such biochemical environments, particularly under anoxic conditions, are actually preferred for phosphorus removal by NZVI. It is therefore possible to dose NZVI in the anoxic or aerobic zones to improve phosphorus removal through precipitation and adsorption by iron

oxides/hydroxides along with activated sludge flocs. On the other hand, unlike ZVI powder, NZVI facilitated dissimilatory nitrate reduction to ammonium, which is unwanted in secondary wastewater effluent. Nevertheless, benefits of the use of NZVI can prevail over the risk in wastewater treatment. For instance, a single dose of NZVI can reduce the population of type 021N filamentous bacteria by 2~3 log units without causing a similar toxicity to the regular bacteria flocs, which opens up the potential to use NZVI as a more selective sludge bulking control agent. NZVI is also promising in sludge treatment for odor control (Li et al., 2007). By considering its advantages and disadvantages, NZVI may be used to address urgent operational problems in wastewater treatment such as P removal and sludge bulking control, but it is important to identify and select the appropriate dose of NZVI before use. More filamentous bacteria other than type 021N should also be tested.

The biodegradation of melamine was not improved in CAS and MBR systems through continuous dosing at an influent concentration of 3 mg/L for about 100 days. It is plausible because selective enrichment of activated sludge bacteria with the enzymes responsible for the hydrolytic deamination of melamine was very limited as bacteria prefer to use biogenic substrates in wastewater for growth. The low melamine

biodegradation efficiency through long-term exposure to melamine was more likely related to cometabolism or fortuitous degradation in these activated sludge systems. However, a significant reduction in toxicity of melamine to the activated sludge was observed in MBR systems, demonstrating the significance of MBR operation at high sludge concentrations (i.e. 10 g COD/L). More research work such as bioaugmentation or a combination use of physicochemical and biological processes should be studied to improve the biodegradation of melamine in activated sludge systems.

Appendix

Additional relevant scholar work (attached at the end)

S. Xu, D. Wu, and Z. Hu* “Impact of hydraulic retention time on organic and nutrient removal in a membrane coupled sequencing batch reactor”, **Water Research**, Vol.55 (2014): 12~20

Bibliography

Agridiotis, V., Forster, C.F. and Carliell-Marquet, C., 2007. Addition of Al and Fe salts during treatment of paper mill effluents to improve activated sludge settlement characteristics. *Bioresource Technology* 98 (15), 2926-2934.

Ahn, J., Daidou, T., Tsuneda, S. and Hirata, A., 2002. Transformation of Phosphorus and Relevant Intracellular Compounds by a Phosphorus-Accumulating Enrichment Culture in the Presence of Both the Electron Acceptor and Electron Donor. *Biotechnology and Bioengineering* 79 (1), 83-93.

Almeelbi, T. and Bezbaruah, A., 2012. Aqueous phosphate removal using nanoscale zero-valent iron. *Journal of Nanoparticle Research* 14 (7), 900.

Amann, R.I., Binder, B.J., Olson, R.J., Chisholm, S.W., Devereux, R. and Stahl, D.A., 1990. Combination of 16S rRNA-targeted Oligonucleotide Probes with Flow Cytometry for Analyzing Mixed Microbial Populations. *Applied and Environmental Microbiology* 56 (6), 1919-1925.

APHA, 2002. *Standard Methods for the Examination of Water and Wastewater*, American Public Health Association, Washington, DC.

Auffan, M., Achouak, W., Rose, J., Roncato, M.A., Chanéac, C., Waite, D.T., Masion, A., Woicik, J.C., Wiesner, M.R. and Bottero, J.Y., 2008. Relation between the redox state of iron-based nanoparticles and their cytotoxicity toward *Escherichia coli*. *Environmental science & technology* 42 (17), 6730-6735.

Beun, J.J., Verhoef, E.V., Van Loosdrecht, M.C.M. and Heijnen, J.J., 2000. Stoichiometry and Kinetics of Poly- β -Hydroxybutyrate Metabolism under Denitrifying Conditions in Activated Sludge Cultures. *Biotechnology and Bioengineering* 68 (5), 496-507.

Bhatta, C.P., Matsuda, A., Kawasaki, K. and Omori, D., 2004. Minimization of sludge production and stable operational condition of a submerged membrane activated sludge process. *Water Science and Technology* 50, 121-128.

- Boonnorat, J., Chiemchaisri, C., Chiemchaisri, W. and Yamamoto, K., 2014. Microbial adaptation to biodegrade toxic organic micro-pollutants in membrane bioreactor using different sludge sources. *Bioresource Technology* 165 (0), 50-59.
- Boundy-Mills, K.L., De Souza, M.L., Mandelbaum, R.T., Wackett, L.P. and Sadowsky, M.J., 1997. The *atzB* gene of *Pseudomonas* sp. strain ADP encodes the second enzyme of a novel atrazine degradation pathway. *Applied and Environmental Microbiology* 63 (3), 916-923.
- Carlsson, H., Aspegren, H., Lee, N. and Hilmer, A., 1997. Calcium phosphate precipitation in biological phosphorus removal systems. *Water Research* 31 (5), 1047-1055.
- Cenens, C., Smets, I.Y., Ryckaert, V.G. and Van Impe, J.F., 2000. Modeling the competition between floc-forming and filamentous bacteria in activated sludge waste water treatment systems - I. Evaluation of mathematical models based on kinetic selection theory. *Water Research* 34 (9), 2525-2534.
- Chang, N.B., Wanielista, M., Hossain, F., Zhai, L. and Lin, K.S., 2008. Integrating nanoscale zero-valent iron and titanium dioxide for nutrient removal in stormwater systems. *Nano* 3 (4), 297-300.
- Charcosset, C., 2006. Membrane processes in biotechnology: An overview. *Biotechnology Advances* 24 (5), 482-492.
- Cheng, G., Shapir, N., Sadowsky, M.J. and Wackett, L.P., 2005. Allophanate hydrolase, not urease, functions in bacterial cyanuric acid metabolism. *Applied and Environmental Microbiology* 71 (8), 4437-4445.
- Chiu, Y.C. and Chung, M.S., 2000. BNP Test to Evaluate the Influence of C/N Ratio on N₂O Production in Biological Denitrification. *Water Science and Technology* 42, 23-27.
- Choe, S., Chang, Y.Y., Hwang, K.Y. and Khim, J., 2000. Kinetics of reductive denitrification by nanoscale zero-valent iron. *Chemosphere* 41 (8), 1307-1311.
- Choi, O., Yu, C.P., Esteban Fernández, G. and Hu, Z., 2010. Interactions of nanosilver with *Escherichia coli* cells in planktonic and biofilm cultures. *Water Research* 44 (20), 6095-6103.

- Chudoba, J., Grau, P. and Ottova, V., 1973. Control of activated sludge filamentous bulking. II. Selection of microorganisms by means of a selector. *Water Research* 7 (10), 1389-1406.
- Contreras, E.M., Bertola, N.C., Giannuzzi, L. and Zaritzky, N.E., 2002. A modified method to determine biomass concentration as COD in pure cultures and in activated sludge systems. *Water SA* 28 (4), 463-467.
- Cook, A.M., 1987. Biodegradation of s-triazine xenobiotics. *FEMS Microbiology Letters* 46 (2), 93-116.
- Cook, A.M. and Hütter, R., 1981. s-triazines as nitrogen sources for bacteria. *Journal of Agricultural and Food Chemistry* 29 (6), 1135-1143.
- Costa, L. and Camino, G., 1988. Thermal behaviour of melamine. *Journal of Thermal Analysis* 34 (2), 423-429.
- Dobson, R.L.M., Motlagh, S., Quijano, M., Cambron, R.T., Baker, T.R., Pullen, A.M., Regg, B.T., Bigalow-Kern, A.S., Vennard, T., Fix, A., Reimschuessel, R., Overmann, G., Shan, Y. and Daston, G.P., 2008. Identification and characterization of toxicity of contaminants in pet food leading to an outbreak of renal toxicity in cats and dogs. *Toxicological Sciences* 106 (1), 251-262.
- Dumonceaux, T.J., Hill, J.E., Pelletier, C.P., Paice, M.G., Van Kessel, A.G. and Hemmingsen, S.M., 2006. Molecular characterization of microbial communities in Canadian pulp and paper activated sludge and quantification of a novel *Thiothrix eikelboomii*-like bulking filament. *Canadian Journal of Microbiology* 52 (5), 494-500.
- El-Sayed, W.S., El-Baz, A.F. and Othman, A.M., 2006. Biodegradation of melamine formaldehyde by *Micrococcus* sp. strain MF-1 isolated from aminoplastic wastewater effluent. *International Biodeterioration and Biodegradation* 57 (2), 75-81.
- Ersu, C.B., Ong, S.K., Arslankaya, E. and Lee, Y.W., 2010. Impact of Solids Residence Time on Biological Nutrient Removal Performance of Membrane Bioreactor. *Water Research* 44 (10), 3192-3202.
- Fang, Z., Qiu, X., Huang, R. and Li, M., 2011. Removal of chromium in electroplating wastewater by nanoscale zero-valent metal with synergistic effect of reduction and immobilization. *Desalination* 280 (1-3), 224-231.

- Fleischer, E.J., Broderick, T.A., Daigger, G.T., Fonseca, A.D., Holbrook, R.D. and Murthy, S.N., 2005. Evaluation of membrane bioreactor process capabilities to meet stringent effluent nutrient discharge requirements. *Water Environment Research* 77 (2), 162-178.
- Fu, G., Dong, B., Zhou, Z. and Gao, T., 2004. Design Characteristics and Operating Parameters of Inverted AAO Process. *China Water and Wastewater* 20 (9), 53-55.
- Gómez-Silván, C., Arévalo, J., González-López, J. and Rodelas, B., 2014. Exploring the links between population dynamics of total and active bacteria and the variables influencing a full-scale membrane bioreactor (MBR). *Bioresource Technology* 162 (0), 103-114.
- Günther, S., Trutnau, M., Kleinstauber, S., Hause, G., Bley, T., Röske, I., Harms, H. and Müller, S., 2009. Dynamics of Polyphosphate-Accumulating Bacteria in Wastewater Treatment Plant Microbial Communities Detected via DAPI (4',6'-diamidino-2-phenylindole) and Tetracycline Labeling. *Applied and Environmental Microbiology* 75 (7), 2111-2121.
- Galil, N.I. and Jacob, L., 2009. Comparative characterization of biosolids from a membrane bioreactor and from a sequencing batch reactor. *Environmental Engineering Science* 26 (5), 1001-1008.
- Gaval, G. and Pernelle, J.J., 2003. Impact of the repetition of oxygen deficiencies on the filamentous bacteria proliferation in activated sludge. *Water Research* 37 (9), 1991-2000.
- Goel, R., Mino, T., Satoh, H. and Matsuo, T., 1998. Intracellular storage compounds, oxygen uptake rates and biomass yield with readily and slowly degradable substrates. *Water Science and Technology* 38 (8-9 -9 pt 7), 85-93.
- Gold, R.S., Wales, M.E. and Grimsley, J.K.W., James R. (2000) *Enzymes in Action*, pp. 263-286.
- Grady, C.P.L., Jr., Daigger, G.T., Love, N.G. and Filipe, C., 2011. *Biological Wastewater Treatment*, 3rd Edition., CRC Press, New York.
- Gray, D.M.D., De Lange, V.P., Chien, M.H., Esquer, M.A. and Shao, Y.J., 2010. Investigating the fundamental basis for selectors to improve activated sludge settling. *Water Environment Research* 82 (6), 541-555.

- Greenlee, L.F., Torrey, J.D., Amaro, R.L. and Shaw, J.M., 2012. Kinetics of zero valent iron nanoparticle oxidation in oxygenated water. *Environmental science & technology* 46 (23), 12913-12920.
- Gu, A.Z., Liu, L., Neethling, J.B., Stensel, H.D. and Murthy, S., 2011. Treatability and Fate of Various Phosphorus Fractions in Different Wastewater Treatment Processes. *Water Science and Technology* 63 (4), 804-810.
- Gu, A.Z., Saunders, A., Neethling, J.B., Stensel, H.D. and Blackall, L.L., 2008. Functionally Relevant Microorganisms to Enhanced Biological Phosphorus Removal Performance at Full-Scale Wastewater Treatment Plants in the United States. *Water Environment Research* 80 (8), 688-698.
- Guerrero, J., Guisasola, A. and Baeza, J.A., 2011. The Nature of the Carbon Source Rules the Competition between PAO and Denitrifiers in Systems for Simultaneous Biological Nitrogen and Phosphorus Removal. *Water Research* 45 (16), 4793-4802.
- Guerrero, J., Tayà, C., Guisasola, A. and Baeza, J.A., 2012. Understanding the Detrimental Effect of Nitrate Presence on EBPR Systems: Effect of the Plant Configuration. *Journal of Chemical Technology and Biotechnology* 87 (10), 1508-1511.
- Guisasola, A., Pijuan, M., Baeza, J.A., Carrera, J., Casas, C. and Lafuente, J., 2004. Aerobic Phosphorus Release Linked to Acetate Uptake in Bio-P Sludge: Process Modeling Using Oxygen Uptake Rate. *Biotechnology and Bioengineering* 85 (7), 722-733.
- Gunnars, A., Blomqvist, S., Johansson, P. and Andersson, C., 2002. Formation of Fe(III) oxyhydroxide colloids in freshwater and brackish seawater, with incorporation of phosphate and calcium. *Geochimica et Cosmochimica Acta* 66 (5), 745-758.
- Guo, J., Peng, Y., Wang, Z., Yuan, Z., Yang, X. and Wang, S., 2012. Control filamentous bulking caused by chlorine-resistant Type 021N bacteria through adding a biocide CTAB. *Water Research* 46 (19), 6531-6542.
- Hansen, H.C.B., Koch, C.B., Nancke-Krogh, H., Borggaard, O.K. and Sørensen, J., 1996. Abiotic nitrate reduction to ammonium: Key role of green rust. *Environmental science & technology* 30 (6), 2053-2056.

Harms, G., Layton, A.C., Dionisi, H.M., Gregory, I.R., Garrett, V.M., Hawkins, S.A., Robinson, K.G. and Sayler, G.S., 2003. Real-time PCR quantification of nitrifying bacteria in a municipal wastewater treatment plant. *Environmental science & technology* 37 (2), 343-351.

Hauduc, H., Rieger, L., Oehmen, A., van Loosdrecht, M.C.M., Comeau, Y., Héduit, A., Vanrolleghem, P.A. and Gillot, S., 2013. Critical Review of Activated Sludge Modeling: State of Process Knowledge, Modeling Concepts, and Limitations. *Biotechnology and Bioengineering* 110 (1), 24-46.

He, F., Zhao, D., Liu, J. and Roberts, C.B., 2007. Stabilization of Fe - Pd nanoparticles with sodium carboxymethyl cellulose for enhanced transport and dechlorination of trichloroethylene in soil and groundwater. *Industrial & Engineering Chemistry Research* 46 (1), 29-34.

Hockenbury, M.R. and Grady Jr, C.P.L., 1977. Inhibition of nitrification: effects of selected organic compounds. *Journal of the Water Pollution Control Federation* 49 (5), 768-777.

Homhoul, P., Pengpanich, S. and Hunsom, M., 2011. Treatment of distillery wastewater by the nano-scale zero-valent iron and the supported nano-scale zero-valent iron. *Water Environment Research* 83 (1), 65-74.

Hosseini, S.M., Ataie-Ashtiani, B. and Kholghi, M., 2011. Bench-scaled nano-Fe 0 permeable reactive barrier for nitrate removal. *Groundwater Monitoring & Remediation* 31 (4), 82-94.

Hu, Z., Chandran, K., Grasso, D. and Smets, B.F., 2003. Impact of metal sorption and internalization on nitrification inhibition. *Environmental science & technology* 37 (4), 728-734.

Hu, Z., Ferraina, R.A., Ericson, J.F., MacKay, A.A. and Smets, B.F., 2005a. Biomass characteristics in three sequencing batch reactors treating a wastewater containing synthetic organic chemicals. *Water Research* 39 (4), 710-720.

Hu, Z., Ferraina, R.A., Ericson, J.F. and Smets, B.F., 2005b. Effect of long-term exposure, biogenic substrate presence, and electron acceptor conditions on the biodegradation of multiple substituted benzoates and phenolates. *Water Research* 39 (15), 3501-3510.

- Huang, C.P., Wang, H.W. and Chiu, P.C., 1998. Nitrate reduction by metallic iron. *Water Research* 32 (8), 2257-2264.
- Huang, Y.C. and Cheng, Y.W., 2012. Electrokinetic-enhanced nanoscale iron reactive barrier of trichloroethylene solubilized by Triton X-100 from groundwater. *Electrochimica Acta* 86, 177-184.
- Huang, Y.H. and Zhang, T.C., 2002. Kinetics of nitrate reduction by iron at near neutral pH. *Journal of Environmental Engineering* 128 (7), 604-611.
- Hwang, Y., Kim, D., Ahn, Y.T., Moon, C.M. and Shin, H.S., 2012. Recovery of ammonium salt from nitrate-containing water by Iron nanoparticles and membrane contactor. *Environmental Engineering Research* 17 (2), 111-116.
- Hwang, Y.H., Kim, D.G. and Shin, H.S., 2011. Effects of synthesis conditions on the characteristics and reactivity of nano scale zero valent iron. *Applied Catalysis B: Environmental* 105 (1-2), 144-150.
- In, C.L. and De Los Reyes III, F.L., 2005. Integrating decay, storage, kinetic selection, and filamentous backbone factors in a bacterial competition model. *Water Environment Research* 77 (3), 287-296.
- Iversen, V., Koseoglu, H., Yigit, N.O., Drews, A., Kitis, M., Lesjean, B. and Kraume, M., 2009. Impacts of membrane flux enhancers on activated sludge respiration and nutrient removal in MBRs. *Water Research* 43 (3), 822-830.
- Jagadevan, S., Jayamurthy, M., Dobson, P. and Thompson, I.P., 2012. A novel hybrid nano zerovalent iron initiated oxidation - Biological degradation approach for remediation of recalcitrant waste metalworking fluids. *Water Research* 46 (7), 2395-2404.
- Jenkins, D., Richard, M.G. and Daigger, G.T., 2004. *Manual on the causes and control of activated sludge bulking, foaming, and other solids separation problems*, 3rd Edition, IWA Publishing, London.
- Juang, Y.C., Aday, S.S., Lee, D.J. and Lai, J.Y., 2010. Influence of internal biofilm growth on residual permeability loss in aerobic granular membrane bioreactors. *Environmental Science and Technology* 44 (4), 1267-1273.

- Kanagawa, T., Kamagata, Y., Aruga, S., Kohno, T., Horn, M. and Wagner, M., 2000. Phylogenetic analysis of and oligonucleotide probe development for Eikelboom type 021N filamentous bacteria isolated from bulking activated sludge. *Applied and Environmental Microbiology* 66 (11), 5043-5052.
- Kang, X.S., Liu, C.Q., Zhang, B., Bi, X.J., Zhang, F. and Cheng, L.H., 2011. Application of Reversed A2/O Process on Removing Nitrogen and Phosphorus from Municipal Wastewater in China. *Water Science and Technology* 63 (10), 2138-2142.
- Kappeler, J. and Gujer, W., 1994. Verification and applications of a mathematical model for 'aerobic bulking'. *Water Research* 28 (2), 311-322.
- Kim, B.C., Kim, S., Shin, T., Kim, H. and Sang, B.I., 2013. Comparison of the Bacterial Communities in Anaerobic, Anoxic, and Oxic Chambers of a Pilot A2O Process Using Pyrosequencing Analysis. *Current Microbiology* 66 (6), 555-565.
- Kim, J.Y., Lee, C., Love, D.C., Sedlak, D.L., Yoon, J. and Nelson, K.L., 2011. Inactivation of MS2 coliphage by ferrous ion and zero-valent iron nanoparticles. *Environmental science & technology* 45 (16), 6978-6984.
- Kim, J.Y., Park, H.J., Lee, C., Nelson, K.L., Sedlak, D.L. and Yoon, J., 2010. Inactivation of escherichia coli by nanoparticulate zerovalent iron and ferrous ion. *Applied and Environmental Microbiology* 76 (22), 7668-7670.
- Kishida, N., Kim, J., Tsuneda, S. and Sudo, R., 2006. Anaerobic/Oxic/Anoxic Granular Sludge Process as an Effective Nutrient Removal Process Utilizing Denitrifying Polyphosphate-Accumulating Organisms. *Water Research* 40 (12), 2303-2310.
- Kishida, N., Kim, J.H., Kimochi, Y., Nishimura, O., Sasaki, H. and Sudo, R., 2004. Effect of C/N Ratio on Nitrous Oxide Emission from Swine Wastewater Treatment Process. *Water Science and Technology* 49, 359-365.
- Kotay, S.M., Datta, T., Choi, J. and Goel, R., 2011. Biocontrol of biomass bulking caused by *Haliscomenobacter hydrossis* using a newly isolated lytic bacteriophage. *Water Research* 45 (2), 694-704.
- Kumari, S.K.S., Marrengane, Z. and Bux, F., 2009. Application of quantitative RT-PCR to determine the distribution of *Microthrix parvicella* in full-scale activated sludge treatment systems. *Applied Microbiology and Biotechnology* 83 (6), 1135-1141.

- Leahy, J.G. and Colwell, R.R., 1990. Microbial degradation of hydrocarbons in the environment. *Microbiological Reviews* 54 (3), 305-315.
- Lee, C., Jee, Y.K., Won, I.L., Nelson, K.L., Yoon, J. and Sedlak, D.L., 2008. Bactericidal effect of zero-valent iron nanoparticles on *Escherichia coli*. *Environmental science & technology* 42 (13), 4927-4933.
- Lee, H., Han, J. and Yun, Z., 2009. Biological Nitrogen and Phosphorus Removal in UCT-Type MBR Process. *Water Science and Technology* 59 (11), 2093-2099.
- Li, X.Q., Brown, D.G. and Zhang, W.X., 2007. Stabilization of biosolids with nanoscale zero-valent iron (nZVI). *Journal of Nanoparticle Research* 9 (2), 233-243.
- Li, X.Q., Elliott, D.W. and Zhang, W.X., 2006. Zero-valent iron nanoparticles for abatement of environmental pollutants: Materials and engineering aspects. *Critical Reviews in Solid State and Material Sciences* 31 (4), 111-122.
- Li, Z., Greden, K., Alvarez, P.J.J., Gregory, K.B. and Lowry, G.V., 2010. Adsorbed polymer and NOM limits adhesion and toxicity of nano scale zerovalent iron to *E. coli*. *Environmental science & technology* 44 (9), 3462-3467.
- Liang, Z., Das, A., Beerman, D. and Hu, Z., 2010a. Biomass Characteristics of Two Types of Submerged Membrane Bioreactors for Nitrogen Removal from Wastewater. *Water Research* 44 (11), 3313-3320.
- Liang, Z., Das, A. and Hu, Z., 2010b. Bacterial response to a shock load of nanosilver in an activated sludge treatment system. *Water Research* 44 (18), 5432-5438.
- Lin, M., He, L., Awika, J., Yang, L., Ledoux, D.R., Li, H. and Mustapha, A., 2008. Detection of melamine in gluten, chicken feed, and processed foods using surface enhanced Raman spectroscopy and HPLC. *Journal of Food Science* 73 (8), T129-T134.
- Lin, Y.H., Tseng, H.H., Wey, M.Y. and Lin, M.D., 2010. Characteristics of two types of stabilized nano zero-valent iron and transport in porous media. *Science of the Total Environment* 408 (10), 2260-2267.
- Liou, Y.H., Lo, S.L. and Lin, C.J., 2007. Size effect in reactivity of copper nanoparticles to carbon tetrachloride degradation. *Water Research* 41 (8), 1705-1712.

- Littleton, H.X., Daigger, G.T., Strom, P.F. and Cowan, R.A., 2003. Simultaneous Biological Nutrient Removal: Evaluation of Autotrophic Denitrification, Heterotrophic Nitrification, and Biological Phosphorus Removal in Full-Scale Systems. *Water Environment Research* 75 (2), 138-150.
- Liu, H., Chen, T., Zou, X., Xie, Q., Qing, C., Chen, D. and Frost, R.L., 2013. Removal of phosphorus using NZVI derived from reducing natural goethite. *Chemical Engineering Journal* 234, 80-87.
- Lou, I.C. and De Los Reyes III, F.L., 2008. Clarifying the roles of kinetics and diffusion in activated sludge filamentous bulking. *Biotechnology and Bioengineering* 101 (2), 327-336.
- Luna, G.M., Dell'Anno, A. and Danovaro, R., 2006. DNA extraction procedure: A critical issue for bacterial diversity assessment in marine sediments. *Environmental Microbiology* 8 (2), 308-320.
- Luna, G.M., Dell'Anno, A., Giuliano, L. and Danovaro, R., 2004. Bacterial diversity in deep Mediterranean sediments: Relationship with the active bacterial fraction and substrate availability. *Environmental Microbiology* 6 (7), 745-753.
- Münch, E.v. and Pollard, P.C., 1997. Measuring bacterial biomass-COD in wastewater containing particulate matter. *Water Research* 31 (10), 2550-2556.
- Ma, L. and Zhang, W.X., 2008. Enhanced biological treatment of industrial wastewater with bimetallic zero-valent iron. *Environmental science & technology* 42 (15), 5384-5389.
- Madoni, P., Davoli, D. and Gibin, G., 2000. Survey of filamentous microorganisms from bulking and foaming activated-sludge plants in Italy. *Water Research* 34 (6), 1767-1772.
- Marsalek, B., Jancula, D., Marsalkova, E., Mashlan, M., Safarova, K., Tucek, J. and Zboril, R., 2012. Multimodal action and selective toxicity of zerovalent iron nanoparticles against cyanobacteria. *Environmental science & technology* 46 (4), 2316-2323.
- Martins, A.M.P., Heijnen, J.J. and Van Loosdrecht, M.C.M., 2003. Effect of feeding pattern and storage on the sludge settleability under aerobic conditions. *Water Research* 37 (11), 2555-2570.

- Martins, A.M.P., Pagilla, K., Heijnen, J.J. and Van Loosdrecht, M.C.M., 2004. Filamentous bulking sludge - A critical review. *Water Research* 38 (4), 793-817.
- Mascarenhas, T., Mikkelsen, L.H. and Nielsen, P.H., 2004. Effects of chlorination on the adhesion strength and deflocculation of activated sludge flocs. *Water Environment Research* 76 (4), 327-333.
- Maurer, M. and Gujer, W., 1998. Dynamic Modelling of Enhanced Biological Phosphorus and Nitrogen Removal in Activated Sludge Systems. *Water Science and Technology* 38, 203-210.
- Metcalf and Eddy, 2003. *Wastewater Engineering: Treatment and Reuse*, 4th Edition., McGraw-Hill Higher Education, New York.
- Mobarry, B.K., Wagner, M., Urbain, V., Rittmann, B.E. and Stahl, D.A., 1996. Phylogenetic Probes for Analyzing Abundance and Spatial Organization of Nitrifying Bacteria. *Applied and Environmental Microbiology* 62 (6), 2156-2162.
- Monclús, H., Sipma, J., Ferrero, G., Rodriguez-Roda, I. and Comas, J., 2010. Biological nutrient removal in an MBR treating municipal wastewater with special focus on biological phosphorus removal. *Bioresource Technology* 101 (11), 3984-3991.
- Moreau, J.W., Weber, P.K., Martin, M.C., Gilbert, B., Hutcheon, I.D. and Banfield, J.F., 2007. Extracellular proteins limit the dispersal of biogenic nanoparticles. *Science* 316 (5831), 1600-1603.
- Mutamim, N.S.A., Noor, Z.Z., Hassan, M.A.A. and Olsson, G., 2012. Application of membrane bioreactor technology in treating high strength industrial wastewater: A performance review. *Desalination* 305, 1-11.
- Mutamim, N.S.A., Noor, Z.Z., Hassan, M.A.A., Yuniarto, A. and Olsson, G., 2013. Membrane bioreactor: Applications and limitations in treating high strength industrial wastewater. *Chemical Engineering Journal* 225, 109-119.
- Nenner, I. and Schulz, G.J., 1975. Temporary negative ions and electron affinities of benzene and N-heterocyclic molecules: Pyridine, pyridazine, pyrimidine, pyrazine, and s-triazine. *The Journal of Chemical Physics* 62 (5), 1747-1758.

- Nielsen, J.L. and Nielsen, P.H., 1998. Microbial nitrate-dependent oxidation of ferrous iron in activated sludge. *Environmental science & technology* 32 (22), 3556-3561.
- Nielsen, P.H., Kragelund, C., Seviour, R.J. and Nielsen, J.L., 2009. Identity and ecophysiology of filamentous bacteria in activated sludge. *FEMS Microbiology Reviews* 33 (6), 969-998.
- Nielsen, P.H., Thomsen, T.R. and Nielsen, J.L., 2004. Bacterial composition of activated sludge - Importance for floc and sludge properties, pp. 51-58.
- Nishimura, K., Yamamoto, M., Nakagomi, T., Takiguchi, Y., Naganuma, T. and Uzuka, Y., 2002. Biodegradation of triazine herbicides on polyvinylalcohol gel plates by the soil yeast *Lipomyces starkeyi*. *Applied Microbiology and Biotechnology* 58 (6), 848-852.
- Noutsopoulos, C., Mamais, D. and Andreadakis, A., 2006. Effect of solids retention time on *Microthrix parvicella* growth. *Water SA* 32 (3), 315-321.
- Nurmi, J.T., Tratnyek, P.G., Sarathy, V., Baer, D.R., Amonette, J.E., Pecher, K., Wang, C., Linehan, J.C., Matson, D.W., Penn, R.L. and Driessen, M.D., 2005. Characterization and properties of metallic iron nanoparticles: Spectroscopy, electrochemistry, and kinetics. *Environmental science & technology* 39 (5), 1221-1230.
- Oehmen, A., Lemos, P.C., Carvalho, G., Yuan, Z., Keller, J., Blackall, L.L. and Reis, M.A.M., 2007. Advances in Enhanced Biological Phosphorus Removal: From Micro to Macro Scale. *Water Research* 41 (11), 2271-2300.
- Onnis-Hayden, A., Majed, N., Schramm, A. and Gu, A.Z., 2011. Process Optimization by Decoupled Control of Key Microbial Populations: Distribution of Activity and Abundance of Polyphosphate-Accumulating Organisms and Nitrifying Populations in a Full-Scale IFAS-EBPR Plant. *Water Research* 45 (13), 3845-3854.
- Peng, Y. and Ge, S., 2011. Enhanced Nutrient Removal in Three Types of Step Feeding Process from Municipal Wastewater. *Bioresource Technology* 102 (11), 6405-6413.
- Phenrat, T., Cihan, A., Kim, H.J., Mital, M., Illangasekare, T. and Lowry, G.V., 2010. Transport and deposition of polymer-modified Fe₀ nanoparticles in 2-D heterogeneous porous media: effects of particle concentration, Fe₀ content, and coatings. *Environmental science & technology* 44 (23), 9086-9093.

- Pijuan, M., Guisasola, A., Baeza, J.A., Carrera, J., Casas, C. and Lafuente, J., 2005. Aerobic Phosphorus Release Linked to Acetate Uptake: Influence of PAO Intracellular Storage Compounds. *Biochemical Engineering Journal* 26 (2-3), 184-190.
- Puschner, B., Poppenga, R.H., Lowenstine, L.J., Filigenzi, M.S. and Pesavento, P.A., 2007. Assessment of melamine and cyanuric acid toxicity in cats. *Journal of Veterinary Diagnostic Investigation* 19 (6), 616-624.
- Qi, R., Yu, T., Li, Z., Li, D., Mino, T., Shoji, T., Fujie, K. and Yang, M., 2012. Comparison of conventional and inverted A2/O processes: phosphorus release and uptake behaviors. *Journal of Environmental Sciences* 24 (4), 571-578.
- Qu, X., Alvarez, P.J.J. and Li, Q., 2013. Applications of nanotechnology in water and wastewater treatment. *Water Research* 47 (12), 3931-3946.
- Ramphao, M., Wentzel, M.C., Merritt, R., Ekama, G.A., Young, T. and Buckley, C.A., 2005. Impact of Membrane Solid-Liquid Separation on Design of Biological Nutrient Removal Activated Sludge Systems. *Biotechnology and Bioengineering* 89 (6), 630-646.
- Regan, J.M., Harrington, G.W. and Noguera, D.R., 2002. Ammonia- and nitrite-oxidizing bacterial communities in a pilot-scale chloraminated drinking water distribution system. *Applied and Environmental Microbiology* 68 (1), 73-81.
- Reinsch, B.C., Forsberg, B., Penn, R.L., Kim, C.S. and Lowry, G.V., 2010. Chemical transformations during aging of zerovalent iron nanoparticles in the presence of common groundwater dissolved constituents. *Environmental science & technology* 44 (9), 3455-3461.
- Rittman, B.E. and McCarty, P.L., 2001. *Environmental Biotechnology: Principles and Applications*, McGraw-Hill Science Engineering, New York.
- Rosenberger, S., Laabs, C., Lesjean, B., Gnirss, R., Amy, G., Jekel, M. and Schrotter, J.C., 2006. Impact of colloidal and soluble organic material on membrane performance in membrane bioreactors for municipal wastewater treatment. *Water Research* 40 (4), 710-720.
- Ruangchainikom, C., Liao, C.H., Anotai, J. and Lee, M.T., 2006. Characteristics of nitrate reduction by zero-valent iron powder in the recirculated and CO₂-bubbled system. *Water Research* 40 (2), 195-204.

Séka, M.A., Cabooter, S. and Verstraete, W., 2001a. A test for predicting propensity of activated sludge to acute filamentous bulking. *Water Environment Research* 73 (2), 237-242.

Séka, M.A., Kalogo, Y., Hammes, F., Kielemoes, J. and Verstraete, W., 2001b. Chlorine-Susceptible and Chlorine-Resistant Type 021N Bacteria Occurring in Bulking Activated Sludges. *Applied and Environmental Microbiology* 67 (3-12), 5303-5307.

Saeedi, M., Li, L.Y. and Moradi Gharehtapeh, A., 2013. Effect of alternative electrolytes on enhanced electrokinetic remediation of hexavalent chromium in clayey soil. *International Journal of Environmental Research* 7 (1), 39-50.

Salaün, F., Lewandowski, M., Vroman, I., Bedek, G. and Bourbigot, S., 2011. Development and characterisation of flame-retardant fibres from isotactic polypropylene melt-compounded with melamine-formaldehyde microcapsules. *Polymer Degradation and Stability* 96 (1), 131-143.

Scheer, H. and Seyfried, C.F., 1997. Enhanced Biological Phosphate Removal: Modelling and Design in Theory and Practice. *Water Science and Technology* 35, 43-52.

Scherer, M.M., Richter, S., Valentine, R.L. and Alvarez, P.J.J., 2000. Chemistry and microbiology of permeable reactive barriers for in situ groundwater clean up. *Critical Reviews in Environmental Science and Technology* 30 (3), 363-411.

Schon, G., Geywitz, S. and Mertens, F., 1993. Influence of Dissolved Oxygen and Oxidation-Reduction Potential on Phosphate Release and Uptake by Activated Sludge from Sewage Plants with Enhanced Biological Phosphorus Removal. *Water Research* 27 (3), 349-354.

Seffernick, J.L., De Souza, M.L., Sadowsky, M.J. and Wackett, L.P., 2001. Melamine deaminase and atrazine chlorohydrolase: 98 percent identical but functionally different. *Journal of Bacteriology* 183 (8), 2405-2410.

Seffernick, J.L., Dodge, A.G., Sadowsky, M.J., Bumpus, J.A. and Wackett, L.P., 2010. Bacterial ammeline metabolism via guanine deaminase. *Journal of Bacteriology* 192 (4), 1106-1112.

- Seffernick, J.L., Johnson, G., Sadowsky, M.J. and Wackett, L.P., 2000. Substrate specificity of atrazine chlorohydrolase and atrazine-catabolizing bacteria. *Applied and Environmental Microbiology* 66 (10), 4247-4252.
- Shariatmadari, N., Weng, C.H. and Daryaei, H., 2009. Enhancement of hexavalent chromium [Cr(VI)] remediation from clayey soils by electrokinetics coupled with a nano-sized zero-valent iron barrier. *Environmental Engineering Science* 26 (6), 1071-1079.
- Shelton, D.R., Karns, J.S., McCarty, G.W. and Durham, D.R., 1997. Metabolism of melamine by *Klebsiella terrigena*. *Applied and Environmental Microbiology* 63 (7), 2832-2835.
- Shin, K.H. and Cha, D.K., 2008. Microbial reduction of nitrate in the presence of nanoscale zero-valent iron. *Chemosphere* 72 (2), 257-262.
- Sims, A., Gajaraj, S. and Hu, Z., 2013. Nutrient removal and greenhouse gas emissions in duckweed treatment ponds. *Water Research* 47 (3), 1390-1398.
- Siripong, S. and Rittmann, B.E., 2007. Diversity Study of Nitrifying Bacteria in Full-Scale Municipal Wastewater Treatment Plants. *Water Research* 41 (5), 1110-1120.
- Smith, C.J., Nedwell, D.B., Dong, L.F. and Osborn, A.M., 2007. Diversity and abundance of nitrate reductase genes (*narG* and *napA*), nitrite reductase genes (*nirS* and *nrfA*), and their transcripts in estuarine sediments. *Applied and Environmental Microbiology* 73 (11), 3612-3622.
- Smolders, G.J.F., Van der Meij, J., Van Loosdrecht, M.C.M. and Heijnen, J.J., 1994. Model of the Anaerobic Metabolism of the Biological Phosphorus Removal Process: Stoichiometry and pH Influence. *Biotechnology and Bioengineering* 43 (6), 461-470.
- Solley, D. and Armstrong, M., 2003. Phased Upgrading for Nitrogen Removal - A Low Cost Approach. *Water Science and Technology* 47 (11), 157-163.
- Stumm, W. and Morgan, J.J., 1996. *Aquatic Chemistry*, John Wiley & Sons, New York.
- Takagi, K., Fujii, K., Yamazaki, K.I., Harada, N. and Iwasaki, A., 2012. Biodegradation of melamine and its hydroxy derivatives by a bacterial consortium containing a novel *Nocardioides* species. *Applied Microbiology and Biotechnology* 94 (6), 1647-1656.

- Tang, S.C.N. and Lo, I.M.C., 2013. Magnetic nanoparticles: Essential factors for sustainable environmental applications. *Water Research* 47 (8), 2613-2632.
- Teng, F., Guan, Y. and Zhu, W., 2008. A simple and effective method to overcome the inhibition of Fe to PCR. *Journal of Microbiological Methods* 75 (2), 362-364.
- Tyrovola, K., Nikolaidis, N.P., Veranis, N., Kallithrakas-Kontos, N. and Koulouridakis, P.E., 2006. Arsenic removal from geothermal waters with zero-valent iron-Effect of temperature, phosphate and nitrate. *Water Research* 40 (12), 2375-2386.
- UNEP, Melamine, OECD Screening Information Data Set (SIDS).
- Van Loosdrecht, M.C.M., Hooijmans, C.M., Brdjanovic, D. and Heijnen, J.J., 1997a. Biological Phosphate Removal Processes. *Applied Microbiology and Biotechnology* 48 (3), 289-296.
- Van Loosdrecht, M.C.M., Pot, M.A. and Heijnen, J.J., 1997b. Importance of bacterial storage polymers in bioprocesses. *Water Science and Technology* 35, 41-47.
- Van Veldhuizen, H.M., Van Loosdrecht, M.C.M. and Heijnen, J.J., 1999. Modelling Biological Phosphorus and Nitrogen Removal in a Full Scale Activated Sludge Process. *Water Research* 33 (16), 3459-3468.
- Vance, D.B., 2005. Nanoscale iron colloids the maturation of the technology for field scale applications. *Pollution Engineering* 37 (7), 16-18.
- Vargas, M., Casas, C. and Baeza, J.A., 2009. Maintenance of Phosphorus Removal in an EBPR System under Permanent Aerobic Conditions Using Propionate. *Biochemical Engineering Journal* 43 (3), 288-296.
- Vervaeren, H., De Wilde, K., Matthys, J., Boon, N., Raskin, L. and Verstraete, W., 2005a. Quantification of an Eikelboom type 021N bulking event with fluorescence in situ hybridization and real-time PCR. *Applied Microbiology and Biotechnology* 68 (5), 695-704.
- Vervaeren, H., De Wilde, K., Matthys, J., Boon, N., Raskin, L. and Verstraete, W., 2005b. Quantification of an Eikelboom type 021N bulking event with fluorescence in situ hybridization and real-time PCR. *Appl. Microbiol. Biotechnol.* 68 (5), 695-704.

- Wachtmeister, A., Kuba, T., Van Loosdrecht, M.C.M. and Heijnen, J.J., 1997. A Sludge Characterization Assay for Aerobic and Denitrifying Phosphorus Removing Sludge. *Water Research* 31 (3), 471-478.
- Wagner, M., Rath, G., Amann, R., Koops, H.P. and Schleifer, K.H., 1995. In Situ Identification of Ammonia-Oxidizing Bacteria. *Systematic and Applied Microbiology* 18 (2), 251-264.
- Wang, W., Jin, Z.h., Li, T.l., Zhang, H. and Gao, S., 2006. Preparation of spherical iron nanoclusters in ethanol-water solution for nitrate removal. *Chemosphere* 65 (8), 1396-1404.
- Wanner, J., 1994. *Activated sludge bulking and foaming control.*, Technomic Publishing, Pennsylvania, USA.
- Wilén, B.M., Keiding, K. and Nielsen, P.H., 2004. Flocculation of activated sludge flocs by stimulation of the aerobic biological activity. *Water Research* 38 (18), 3909-3919.
- Wimmer, R.F. and Love, N.G., 2004. Activated sludge deflocculation in response to chlorine addition: The potassium connection. *Water Environment Research* 76 (3), 213-219.
- Wu, D., Shen, Y., Ding, A., Qiu, M., Yang, Q. and Zheng, S., 2013. Phosphate removal from aqueous solutions by nanoscale zero-valent iron. *Environmental Technology (U. K.)* 34 (18), 2663-2669.
- Xiu, Z.m., Jin, Z.h., Li, T.l., Mahendra, S., Lowry, G.V. and Alvarez, P.J.J., 2010. Effects of nano-scale zero-valent iron particles on a mixed culture dechlorinating trichloroethylene. *Bioresource Technology* 101 (4), 1141-1146.
- Xu, S., Zhang, Y., Sims, A., Bernards, M. and Hu, Z., 2013. Fate and toxicity of melamine in activated sludge treatment systems after a long-term sludge adaptation. *Water Research* 47 (7), 2307-2314.
- Yan, W., Lien, H.L., Koel, B.E. and Zhang, W.X., 2013. Iron nanoparticles for environmental clean-up: Recent developments and future outlook. *Environmental Science: Processes & Impacts* 15 (1), 63-77.

Yang, G.C.C. and Lee, H.-L., 2005. Chemical reduction of nitrate by nanosized iron: kinetics and pathways. *Water Research* 39 (5), 884-894.

Yang, Y., Guo, J. and Hu, Z., 2013. Impact of nano zero valent iron (NZVI) on methanogenic activity and population dynamics in anaerobic digestion. *Water Research* 47 (17), 6790-6800.

Yang, Y., Xu, M., Wall, J.D. and Hu, Z., 2012. Nanosilver impact on methanogenesis and biogas production from municipal solid waste. *Waste Management* 32 (5), 816-825.

Yoon, S.H., Kim, H.S. and Yeom, I.T., 2004. The optimum operational condition of membrane bioreactor (MBR): Cost estimation of aeration and sludge treatment. *Water Research* 38 (1), 37-46.

Zhang, B. and Gao, T.Y., 1997. Enhancement of Nitrogen and Phosphorus Removal by Reversal of Anaerobic and Anoxic Zones Sequence. *China Water and Wastewater* 13 (3), 7-9.

Zhang, J., Hao, Z., Zhang, Z., Yang, Y. and Xu, X., 2010. Kinetics of nitrate reductive denitrification by nanoscale zero-valent iron. *Process Safety and Environmental Protection* 88 (6), 439-445.

Zhang, Q.X., Yang, G.Y., Li, J.T., Li, W.X., Zhang, B. and Zhu, W., 2011. Melamine induces sperm DNA damage and abnormality, but not genetic toxicity. *Regulatory Toxicology and Pharmacology* 60 (1), 144-150.

Zhang, W.-X. and Elliott, D.W., 2006. Applications of iron nanoparticles for groundwater remediation. *Remediation* 16 (2), 7-21.

Zhaunerchyk, V., Geppert, W.D., Rośn, S., Vigren, E., Hamberg, M., Kamińska, M., Kashperka, I., Af Ugglas, M., Semaniak, J., Larsson, M. and Thomas, R.D., 2009. Investigation into the vibrational yield of OH products in the OH+H+H channel arising from the dissociative recombination of H₃O⁺. *The Journal of Chemical Physics* 130 (21), 214302.

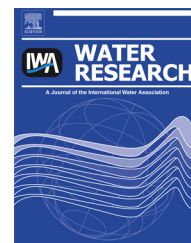
Zhou, Z., Wu, Z., Wang, Z., Tang, S., Gu, G., Wang, L., Wang, Y. and Xin, Z., 2011. Simulation and Performance Evaluation of the Anoxic/Anaerobic/Aerobic Process for Biological Nutrient Removal. *Korean Journal of Chemical Engineering* 28 (5), 1233-1240.

VITA

Shengnan Xu was born on December 8th, 1983 in Henan, China. She earned her bachelor and master degree of Environmental Engineering in 2006 and 2009, respectively, from Tongji University, Shanghai, China. She came to the U.S. in January 2010 and attended the University of Missouri, pursuing a Ph.D degree in Civil and Environmental Engineering. She studied the process improvements in biological nutrient removal systems, completing this degree in July 2014. She hopes to continue working in environmental engineering and pursue her career in academia or industry in the future.

Available online at www.sciencedirect.com

ScienceDirect

journal homepage: www.elsevier.com/locate/watres

Impact of hydraulic retention time on organic and nutrient removal in a membrane coupled sequencing batch reactor

Shengnan Xu^a, Donglei Wu^{b,*}, Zhiqiang Hu^{a,**}

^a Department of Civil and Environmental Engineering, University of Missouri, E2509 Lafferre Hall, Columbia, MO 65211, USA

^b Department of Environmental Engineering, Zhejiang University, China

ARTICLE INFO

Article history:

Received 9 September 2013

Received in revised form

17 January 2014

Accepted 24 January 2014

Available online 4 February 2014

Keywords:

Hydraulic retention time

Biological nutrient removal

Sequencing batch reactor

Membrane bioreactor

Phosphorus release and uptake

ABSTRACT

Although solids retention time (SRT) is the key parameter in wastewater treatment design and operation, this study determined the effect of hydraulic retention time (HRT) on biological nutrient removal in a membrane coupled sequencing batch reactor (MSBR) at the fixed SRT of 10 days. During more than 200 days of operation, the HRT of the MSBR were decreased from 24 to 12 and to 6 h while the volumetric exchange ratio in each operating cycle was fixed at 50%. The decrease of HRT led to a proportional increase in biomass concentration at the fixed SRT. The system demonstrated excellent removal of organic matter with the highest COD removal efficiency (97%) achieved at the shortest HRT of 6 h. As HRT was reduced from 24 to 12 h, the total nitrogen removal efficiency improved from $68 \pm 5\%$ to $80 \pm 4\%$, but there was no further improvement when HRT decreased to 6 h. Coincidentally, similar and higher abundance of nitrifying bacteria was observed in the MSBR operated at the HRTs of 6 and 12 h than that at the HRT of 24 h. The total phosphorus removal efficiencies were $62 \pm 15\%$, $77 \pm 4\%$ and $85 \pm 3\%$ at the HRTs of 24, 12 and 6 h, respectively. The maximum P release rates for activated sludge at the HRTs of 24, 12 and 6 h were 3.7 ± 0.5 , 6.4 ± 0.2 and 8.7 ± 0.1 mg P/h, respectively, while the maximum P uptake rates were 3.2 ± 0.1 , 8.6 ± 0.2 and 15.2 ± 0.2 mg P/h, respectively. Contradictory to the theory that effluent water quality is solely SRT dependent, the results suggest that it is also affected by HRT and resultant biomass concentration possibly due to factors such as change in hydrolysis of particulate organic matter, the unique microenvironment and transition between anaerobic and aerobic metabolism at high biomass concentrations in MSBR operation.

© 2014 Elsevier Ltd. All rights reserved.

1. Introduction

Wastewater treatment is evolving from the traditional activated sludge process to biological nutrient removal (BNR).

A combination of anaerobic, anoxic and aerobic processes in BNR systems results in simultaneous nitrogen (N) and phosphorus (P) removal. Biological N removal is typically achieved by autotrophic nitrification under aerobic conditions followed by heterotrophic denitrification under anoxic conditions

* Corresponding author.

** Corresponding author. Tel.: +1 573 884 0497; fax: +1 573 882 4784.

E-mail addresses: wudl@zju.edu.cn (D. Wu), huzh@missouri.edu (Z. Hu).

(Grady et al., 2011; Metcalf and Eddy, 2003). Phosphorus accumulating organisms (PAOs) are essential to enhanced biological phosphorus removal (EBPR). By taking readily biodegradable organic matter from wastewater and storing it as polyhydroxyalkanoates (PHAs) under anaerobic conditions, PAOs are able to use stored PHAs as an energy source to remove inorganic P from wastewater and convert into intracellular poly-P (Grady et al., 2011; Wu et al., 2006) under subsequent aerobic conditions or anoxic conditions (for denitrifying PAOs). Consequently, P in wastewater can be significantly accumulated in mixed liquor suspended solids (MLSS) and then removed by sludge wasting (Grady et al., 2011; Metcalf and Eddy, 2003).

The activated sludge wastewater treatment performance can be optimized with various BNR processes and configurations, such as the selection of proper volumes of anaerobic/anoxic/aerobic chambers and the flow rates of internal mixed liquor recirculation (MLR) and return activated sludge (RAS) (Grady et al., 2011; Metcalf and Eddy, 2003). These requirements often make it difficult to retrofit and upgrade existing troubled wastewater treatment systems. One option to overcome this obstacle is the use of sequencing batch reactor (SBR) technology, which does not require RAS and MLR operations and allows all complex processes to occur in a single bioreactor by performing cyclic events such as fill, react, settle, draw and idle steps in sequence (Grady et al., 2011). SBR can mimic various types of continuous flow systems by changing the cycle format and the time associated with each step (Metcalf and Eddy, 2003). Due to its flexibility in operation, control and small footprint feature, SBR is preferred in small-scale treatment plants (with flow rates < 19,000 m³/d or 5 million gallons per day) (Dubber and Gray, 2011; Lee et al., 2001). However, the risk in poor settlement and the consequently turbid effluent are concerns in SBR operation (Kang et al., 2003).

On the other hand, membrane bioreactor (MBR) systems are excellent in solid–liquid separation and offer higher effluent quality than conventional activated sludge systems (Ersu et al., 2010; Metcalf and Eddy, 2003). Additional benefits can be achieved through MBR operation, such as higher volumetric loading rates and thus shorter hydraulic retention times (HRTs) for economical operation, and longer solid retention times (SRTs) and thus less sludge production (Bhatta et al., 2004; Metcalf and Eddy, 2003). The biomass concentration in MBR systems can therefore be 10 times that of the conventional activated sludge systems (Galil and Jacob, 2009), resulting in more efficient pollutant removal (Fleischer et al., 2005; Monclús et al., 2010). Although membrane fouling is still a problem in its operation (Charcosset, 2006), MBR is increasingly used in wastewater treatment for wastewater reuse (Iversen et al., 2009; Juang et al., 2010; Mutamim et al., 2012; Rosenberger et al., 2006; Yoon et al., 2004).

Since both SBR and MBR are widely used (Shannon et al., 2008), combining a membrane process with SBR to have a membrane coupled sequencing batch reactor (MSBR) may offer a better solution for wastewater treatment. MSBR can provide engineering flexibility in organic and nutrient removal more than conventional BNR processes. The use of membranes eliminates settling and decanting steps reducing the SBR cycle length. Meanwhile, the SBR operation allows a feast-

famine environment that favors biogranulation of activated sludge to mitigate membrane fouling (Tu et al., 2010). Not surprisingly, MSBR technique has been employed for industrial wastewater treatment to effectively remove organics and toxic compounds from wastewater (Fakhru'l-Razi et al., 2010; Kaewsuk et al., 2010; Moreno-Andrade and Buitrón, 2012; Serrano et al., 2011; Vargas et al., 2008). With prolonged SRTs (e.g., >360 d), the technique has also shown to be capable of treating greywater with improved nitrogen removal at reduced HRTs (Scheumann and Kraume, 2009). However, long SRT results in poor phosphorus removal because P is only removed through sludge wasting (Metcalf and Eddy, 2003). Since HRT is another important operating parameter which affects biomass concentration and separation by membrane filtration (Tay et al., 2003), the objective of this study was to determine the impact of HRT on MSBR wastewater treatment performance at a fixed SRT (10 d). During more than 200 days of operation, a lab-scale MSBR was operated and monitored to investigate and compare the biomass concentration, organic and nutrient removal efficiency, P release and uptake behaviors and nitrifying community structure at different HRTs.

2. Materials and methods

2.1. MSBR set-up and operation

An 8-L glass vessel (length × width × height = 0.12 m × 0.11 m × 0.61 m) was employed for MSBR operation with an effective working volume of 7.2 L. Two identical ZeeWeed hollow fiber membrane modules (GE Water & Process Technologies, Trevose, PA) were submerged in the MSBR. The membrane module was made of polyvinylidene fluoride (PVDF) with a nominal pore size of 0.1 μm, a total effective filtration area of 0.047 m², and a maximum membrane flux of 15.0 L/m²·h. The MSBR was operated at room temperature (24 ± 2 °C) with a short start-up period lasting about 10 days. Activated sludge (obtained from the Columbia Wastewater Treatment Plant, Columbia, MO) was seeded at an initial biomass concentration of approximately 2000 mg COD/L. The MSBR was fed with synthetic wastewater that was mainly composed of nonfat dry milk powder. The wastewater contained about 400 mg/L of chemical oxygen demand (COD), 40 mg/L total N (TN), 25 mg/L NH₄⁺-N, and 10 mg/L total P (TP). The synthetic wastewater also contained the following macro- and micro-nutrients per liter: 44 mg MgSO₄, 14 mg CaCl₂·2H₂O, 2 mg FeCl₂·4H₂O, 3.4 mg MnSO₄·H₂O, 1.2 mg (NH₄)₆Mo₇O₂₄·4H₂O, 0.8 mg CuSO₄, 0.3 mg NiSO₄·6H₂O, and 1.8 mg Zn(NO₃)₂·6H₂O (Sigma Aldrich, St Louis, MO) (Liang et al., 2010). A magnetic stirrer ensured homogeneous mixing continuously while compressed air was supplied to the built-in orifices at the bottom of the membrane module to control membrane fouling and support aeration and mixing. Peristaltic pumps (Cole–Parmer, Vernon Hills, Illinois) were used for the influent filling and effluent drawing (Fig. 1).

A standard four-circuit programmable timer (Cole–Parmer, Vernon Hills, Illinois) was used to control the operating cycles of the MSBR. During each cycle a total of 3.6 L feed solution was added, which led to a volumetric exchange ratio (defined as the ratio between the influent volume added

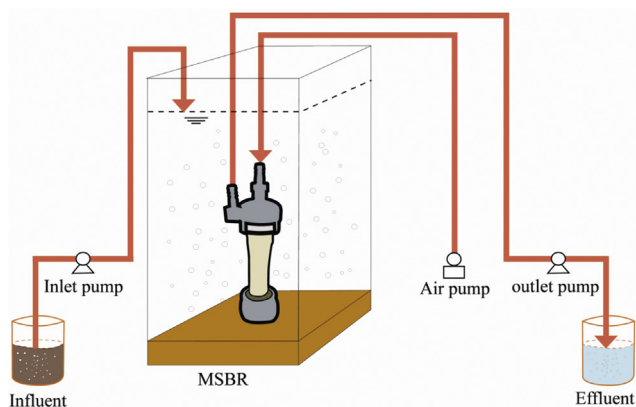


Fig. 1 – A schematic diagram of the MSBR process.

per cycle and the effective working volume (7.2 L) of 50%. Since HRT used in SBR operation ranges from 20 to 30 h while for many BNR facilities HRT ranges from 4 to 18 h (Metcalf and Eddy, 2003), three HRTs (24, 12, and 6 h) were selected for evaluation. As shown in Supporting Information (Table S1), in Phase I (HRT = 24 h), the MSBR cycle consisted of a 4-h anaerobic reaction including a 10-min influent filling at the beginning and then an 8-h aerobic reaction including a 20–30-min effluent drawing at the end. Thus two cycles were running each day giving an HRT of 24 h. On day 91, the MSBR operation was shifted to Phase II (HRT = 12 h), when the operating cycle consisted of a 2-h anaerobic reaction (including a 10-min influent filling at the beginning) and then a 4-h aerobic reaction (including a 20-min effluent drawing at the end). The HRT was reduced to 12 h by running four cycles per day. Starting from day 151 (Phase III), an HRT of 6 h was chosen by running eight cycles each day. Each cycle consisted of a 1-h anaerobic reaction (including a 10-min influent filling) and then a 2-h aerobic reaction (including a 20-min effluent drawing). The SRT was maintained at about 10 days throughout the study period by wasting 0.72 L mixed liquor before the start of effluent drawing in the last cycle each day according to the Garrett wastage strategy (Grady et al., 2011). The transmembrane pressure (TMP) was closely monitored while the membrane flux was set at maximum. When the TMP level exceeded the maximum value (45.5 kPa), the membrane module was taken out of the MSBR for physical cleaning (Liang and Hu, 2012). The module was rinsed with distilled water for 30-min before it was submerged back to the bioreactor. The influent and effluent quality was monitored twice a week during the whole operation period.

2.2. P release/uptake kinetics and sludge phosphorus content

The phosphorus release and uptake kinetics of the sludge at different HRTs were determined directly from the MSBR by sampling the sludge mixed liquor at a predetermined time interval and then measuring the supernatant TP concentration of the samples. The maximum P release and uptake rates were calculated according to the procedures described elsewhere (Wachtmeister et al., 1997). The sludge P content at the anaerobic and aerobic stages in the MSBR was calculated by

subtracting the supernatant phosphorus concentration from the TP concentration of the MLSS, and then divided by the MLSS concentration.

2.3. Analysis of nitrifying communities in the MSBR

Two distinct groups of nitrifying bacteria, ammonia oxidizing bacteria (AOB) and nitrite oxidizing bacteria (NOB), are responsible for the ammonia and nitrite oxidation, respectively. To analyze the nitrifying community structure in the MSBR, Terminal Restriction Fragment Length Polymorphism (T-RFLP) was used by targeting 16S rRNA genes of ammonia-oxidizing bacteria (AOB) (Amann et al., 1990; Mobarry et al., 1996) and nitrite-oxidizing bacteria (NOB) including *Nitrospira* spp. (Regan et al., 2002) and *Nitrobacter* spp. (Wagner et al., 1995). DNA was extracted from a 1.0 mL sample of mixed liquor taken directly from the aerobic phase of the MSBR using an Ultraclean Soil DNA Isolation Kit (Carlsbad, CA). The concentration and purity of DNA were analyzed with a NanoDrop instrument (ND-1000 NanoDrop Technologies, Wilmington, DE). All of the primers (Supporting Information, Table S2) were synthesized by Integrated DNA Technologies (Coralville, IA). A fluorescent dye, 6-FAM, was incorporated at the 5' end of the labeled oligonucleotides.

Polymerase chain reactions (PCRs) were conducted in a PCR DNA thermocycler (Eppendorf, Westbury, NY). The thermal profiles used for each PCR amplification have been described elsewhere (Siripong and Rittmann, 2007). The PCR amplification products were purified and digested with *MspI* restriction endonuclease (Promega, Madison, WI) at 37 °C for 3 h. After digestion, the DNA products were diluted 10 times and run through an ABI 3730 DNA Analyzer (Applied Biosystems, Carlsbad, CA) at the University of Missouri DNA Core Facility. An internal lane standard ranging from 20 to 600 bases (Genescan 600 LIZ) was added to each sample for precise sizing of each fragment by adjusting for lane to lane loading variation. All experiments were performed in triplicates per sample and all PCR runs included control reactions without the DNA template.

2.4. Chemical and statistical analysis

The water quality parameters such as COD, TN, ammonium-N, nitrite-N, nitrate-N, TP, orthophosphorus in the MSBR were measured in duplicate following the standard methods (APHA, 1998). Biomass concentration was measured in COD units (Contreras et al., 2002; Münch and Pollard, 1997). One-way ANOVA analysis was conducted to assess the statistical significance of the differences among groups, with *p* values less than 0.05 indicating statistical significance.

3. Results and discussion

3.1. Effect of HRT on reactor biomass concentration and COD removal

At the fixed SRT (10 d), the biomass COD concentration experienced a proportional increase as the HRT decreased, which were 1717 ± 436 mg/L, 3502 ± 1082 mg/L and

6093 ± 1064 mg/L at the HRTs of 24, 12 and 6 h, respectively (Fig. 2). The results confirmed the theory that biomass concentration in the bioreactor depends on HRT although the product of biomass concentration and HRT is constant at a fixed SRT (Grady et al., 2011; Metcalf and Eddy, 2003). The rate of biomass increase by decreasing the HRT from 12 h to 6 h was relatively lower than that from 24 h to 12 h. This was attributed to the loss of biomass because more frequent rinsing and washing of the membrane module was required at the HRT of 6 h. It is also possibly due to biomass loss by more endogenous respiration at high biomass concentrations because of oxygen transfer limitation within the biological flocs (Yoon et al., 2004).

Meanwhile, at the influent COD concentration of 410 ± 11 mg/L, the effluent COD concentrations were 34 ± 22 , 32 ± 23 and 12 ± 12 mg/L at the HRTs of 24, 12 and 6 h, respectively, with COD removal efficiencies of 92%, 92% and 97%, respectively (Fig. 3). There was no significant difference in COD removal efficiency between the operation at HRTs of 24 h and 12 h ($p = 0.82$) while the difference was significant between HRTs of 12 h and 6 h ($p = 0.008$). It seems that the COD removal efficiency was increased as the biomass concentration increased in the MSBR, as was also reported elsewhere in MBR operation (Liang and Hu, 2012).

3.2. Nitrogen removal performance and community structure of nitrifiers

At the influent TN concentration of 39.9 ± 2.6 mg/L, the average effluent TN concentrations at the HRTs of 24, 12 and 6 h were 12.9 ± 2.5 , 8.0 ± 1.6 and 7.8 ± 1.4 mg/L, respectively (Fig. 3), with average nitrogen removal efficiencies of $68 \pm 5\%$, $80 \pm 4\%$ and $80 \pm 2\%$, respectively. The nitrogen removal efficiency of the MSBR operated at the HRT of 12 h was significantly higher than that at the HRT of 24 h ($p < 0.001$) while there was no significant difference between the operation at HRTs of 12 h and 6 h ($p = 0.70$).

For detailed nitrogen species performance analysis the effluent NH_4^+-N , NO_2^--N and NO_3^--N concentrations at

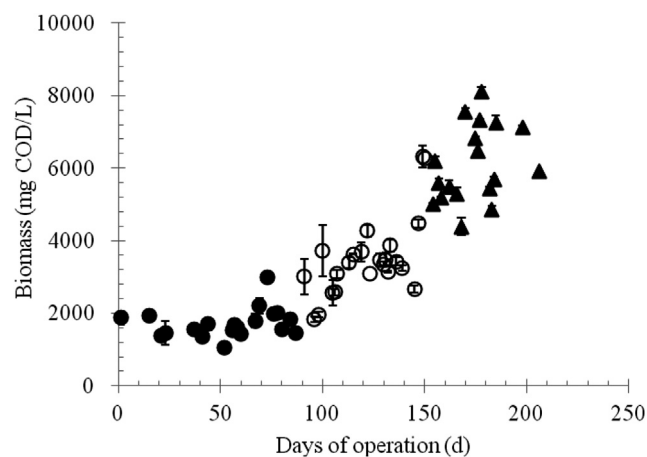


Fig. 2 – Biomass concentrations of the MSBR operated at the HRTs of 6 (▲), 12 (○), and 24 h (●), respectively. Error bars represent data range of duplicate samples.

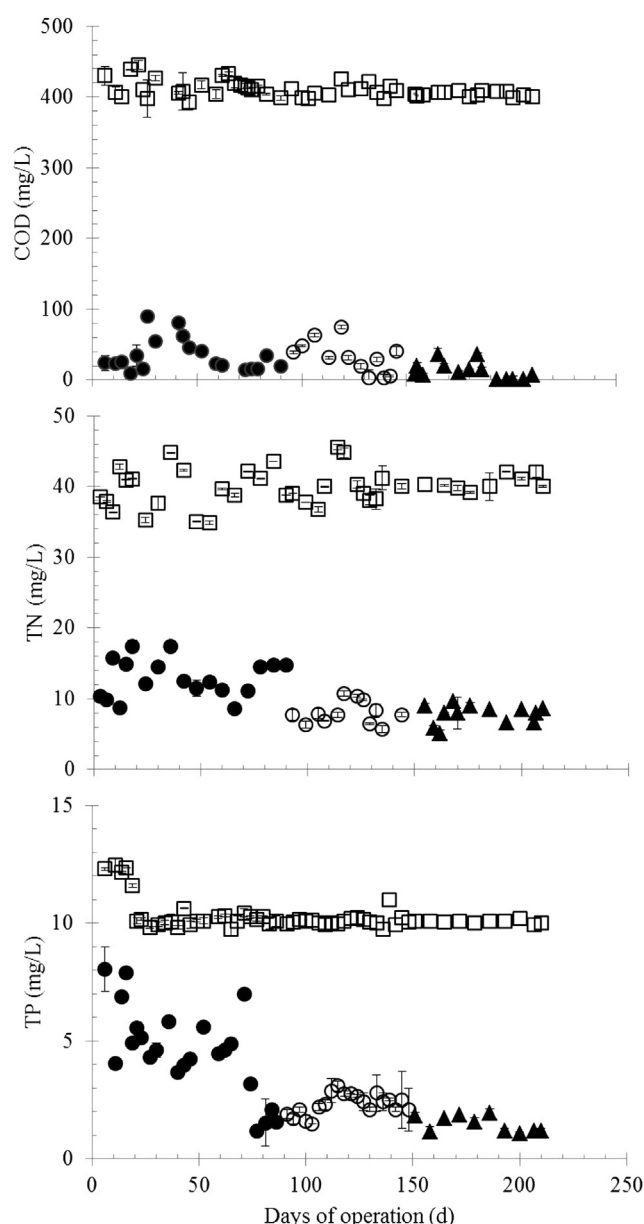


Fig. 3 – Influent (□) and effluent COD, TN and TP concentrations in the MSBR operated at the HRTs of 6 (▲), 12 (○), and 24 h (●), respectively. Error bars represent the data range of duplicate samples.

different HRTs were relatively stable (Fig. S1) despite a temporary ammonia spike on day 78 and an obvious NO_2^--N accumulation on day 48 due to mixing failure. The effluent NH_4^+-N concentration at the HRT of 12 h (0.1 ± 0.1 mg/L) was lower than that at the HRT of 24 h (0.2 ± 0.1 mg/L) ($p = 0.03$) whereas there was no significant difference ($p = 0.99$) in effluent NH_4^+-N concentration between the operation at HRTs of 12 h and 6 h. Similarly, effluent NO_3^--N concentration at HRT of 12 h (7.2 ± 1.4 mg/L) was significantly lower than that at HRT of 24 h (11.8 ± 2.4 mg/L) ($p < 0.001$) whereas there was no significant difference ($p = 0.82$) in effluent NO_3^--N concentration between operation at the HRTs of 12 h and 6 h (7.2 ± 1.6 mg/L). There were no significant differences in

effluent NO_2^- -N concentration among operations at HRTs of 24, 12 and 6 h, which were all at an average of 0.1 mg/L.

The change in nitrogen removal efficiency with HRT was consistent with the change in nitrifying bacterial population. As shown in Fig. 4, the T-RFLP profiles specifically targeting

AOB and NOB indicated that the AOB genera primarily consisted of *Nitrosomonas* spp. and the NOB genera contained both *Nitrospira* and *Nitrobacter* in the MSBR. As peak height represents the relative abundance of each bacterial species (Regan et al., 2002), both *Nitrosomonas* (AOB) and *Nitrobacter* (NOB) at

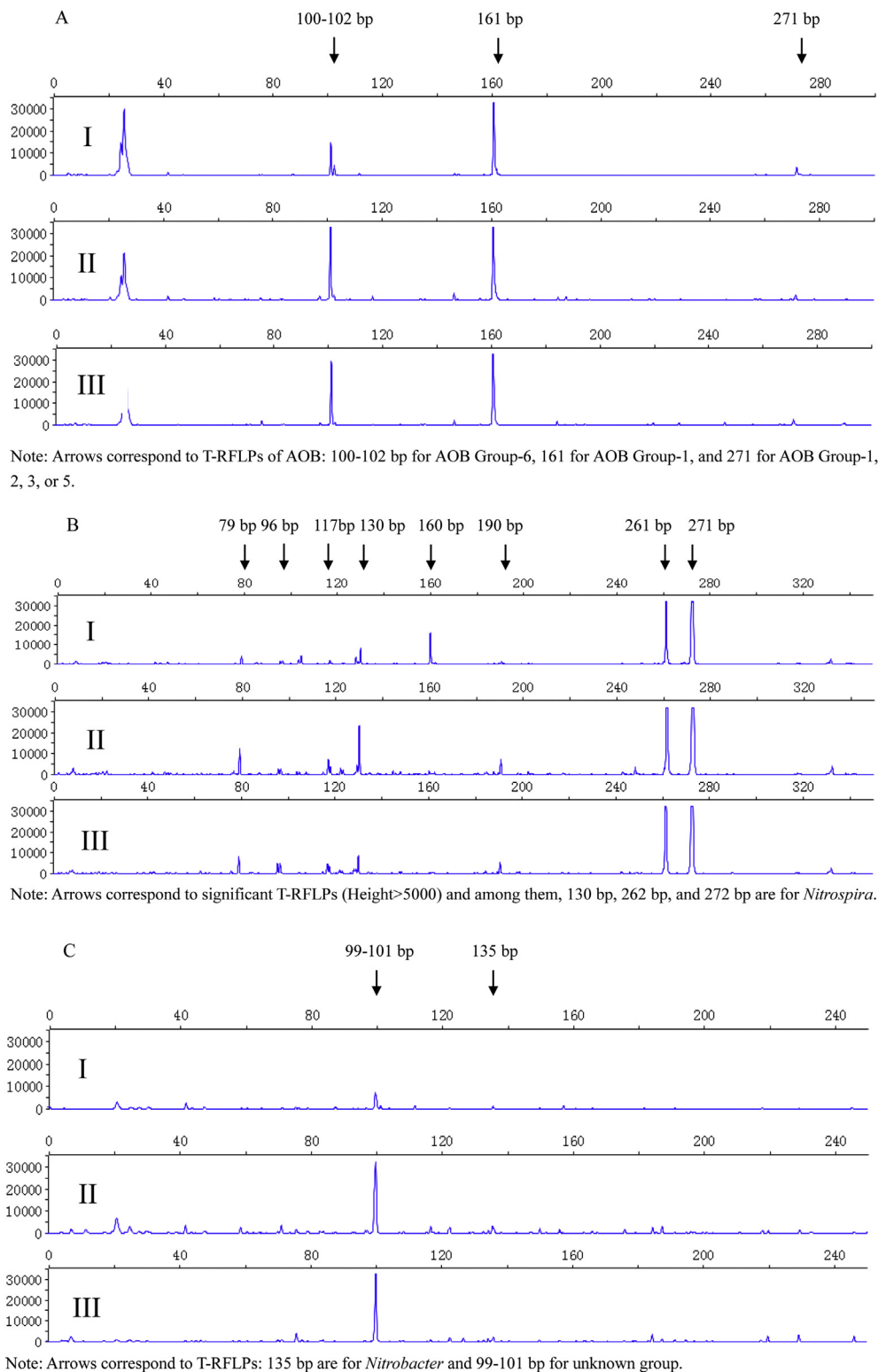


Fig. 4 – Nitrifying bacterial community composition reflected by T-RFLP profiles targeting 16S rRNA genes of *Nitrosomonas* (A), *Nitrospira* (B) and *Nitrobacter* (C) in the Phases I, II, III with HRTs of 24, 12, and 6 h, respectively.

the HRTs of 12 h and 6 h appeared to exhibit higher population abundance than those at the HRT of 24 h (Fig. 4A and C). Higher biomass concentration in MBR operation could provide better retention of slowly growing AOB and NOB (Holakoo et al., 2007) because of potentially beneficial interactions between heterotrophic and autotrophic bacteria (Grady et al., 2011), while the nitrifiers formed in clusters and in frequently close contact with each other in sludge flocs (Mobarry et al., 1996; Ni et al., 2008). Remarkably, the population abundance of AOB and NOB in the MSBR was similar at the HRTs of 12 h and 6 h (Fig. 4A and C). The growth of AOB and NOB could be susceptible to mass transfer (e.g., ammonium and oxygen diffusion) at high biomass concentrations which could result in more aggregation of suspended cells and sludge floc formation (Huang et al., 2001). *Nitrospira* (NOB), on the other hand, was detected at the same population abundance at different HRTs (Fig. 4B).

3.3. Effect of HRT on phosphorus removal

The effluent TP (Fig. 3) and $\text{PO}_4^{3-}\text{-P}$ data (Fig. S2) showed that there was significant difference in P removal efficiency at different HRTs. At the influent TP concentration of 10.3 ± 0.6 mg/L, the effluent TP concentrations at the HRTs of 24, 12 and 6 h were 3.9 ± 1.7 mg/L, 2.3 ± 0.4 mg/L and 1.5 ± 0.3 mg/L, respectively (Fig. 3). The average TP removal efficiency at the HRT of 12 h ($77 \pm 4\%$) was significantly higher ($p < 0.001$) than that at the HRT of 24 h ($62 \pm 5\%$), and furthermore, the TP removal efficiency at the HRT of 6 h ($85 \pm 3\%$) was significantly higher than that at the HRT of 12 h ($p < 0.001$). Correspondingly, at the influent $\text{PO}_4^{3-}\text{-P}$ concentration of 8.2 ± 0.5 mg/L, the effluent $\text{PO}_4^{3-}\text{-P}$ concentrations at the HRTs of 24, 12 and 6 h were 3.5 ± 1.6 mg/L, 2.2 ± 0.1 mg/L and 1.3 ± 0.1 mg/L, respectively (Fig. S2), with average removal efficiencies of $56 \pm 20\%$, $73 \pm 7\%$ and $83 \pm 3\%$, respectively.

3.4. P release/uptake kinetics and sludge P content

As shown in Fig. 5, significant P release in the anaerobic stage and P uptake in the aerobic stage was observed at different HRTs. The maximum P release rates from the sludge at the HRTs of 24, 12 and 6 h were 3.7 ± 0.5 , 6.4 ± 0.2 and 8.7 ± 0.1 mg P/h, respectively, with significant differences (p values < 0.001). Longer anaerobic HRT led to more complete P release but with lower P release rates, which is similar to the scenario of the continuous flow system whereas the anaerobic zone decreases, the PAOs release P less completely (Grady et al., 2011). Long anaerobic HRT might lead to a depletion of volatile fatty acids (VFAs) which could negatively impact P release (Coats et al., 2011). Meanwhile, the maximum phosphorus uptake rates at the HRTs of 24, 12 and 6 h were 3.2 ± 0.1 , 8.6 ± 0.2 and 15.2 ± 0.2 mg P/h, respectively, with significant differences (p values < 0.002). Hence, the incomplete P release under anaerobic conditions at shorter HRTs (Fig. 5) did not affect the subsequent P uptake under aerobic conditions. This result is in agreement with a recent study where the shortened anaerobic HRT actually induced PAOs to store more PHAs and then drive them to take up more P aerobically (Liu et al., 2013).

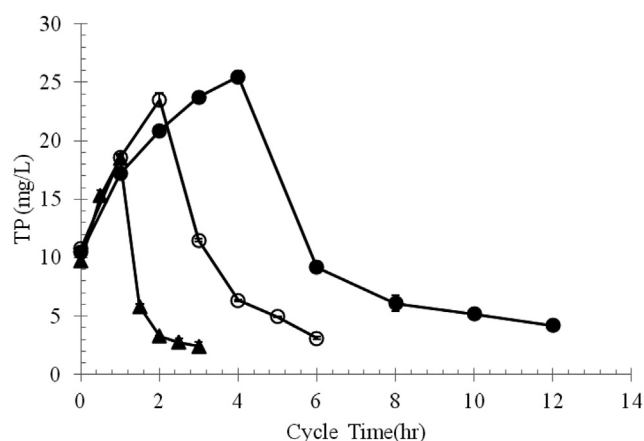


Fig. 5 – Phosphorus release and uptake by the sludge from the MSBR operated at the HRTs of 6 (▲), 12 (○), and 24 h (●), respectively. Error bars represent one standard error of the mean ($n = 6$).

As shown in Fig. 6, the P contents of the sludge collected from the anaerobic stage at the HRTs of 24, 12 and 6 h were $2.2 \pm 0.3\%$, $3.5 \pm 0.1\%$ and $3.4 \pm 0.2\%$, respectively. In comparison, the P contents were $3.3 \pm 0.7\%$, $4.0 \pm 0.2\%$ and $3.6 \pm 0.1\%$ for the sludge from the aerobic stage at the HRTs of 24 h, 12 h and 6 h, respectively. The higher sludge P content in the MSBR than that in conventional activated sludge processes (ranging from 1 to 3%) indicates luxury P uptake by PAOs (Qi et al., 2012). There were significant differences in anaerobic ($p = 0.002$) and aerobic ($P = 0.01$) sludge P content between the operation at HRTs of 24 h and 12 h because of the characteristics of P release and uptake under anaerobic and aerobic conditions, respectively. However, such difference was not significant between the operation at HRTs of 12 h and 6 h due to sludge loss through more frequently membrane cleaning at the HRT of 6 h.

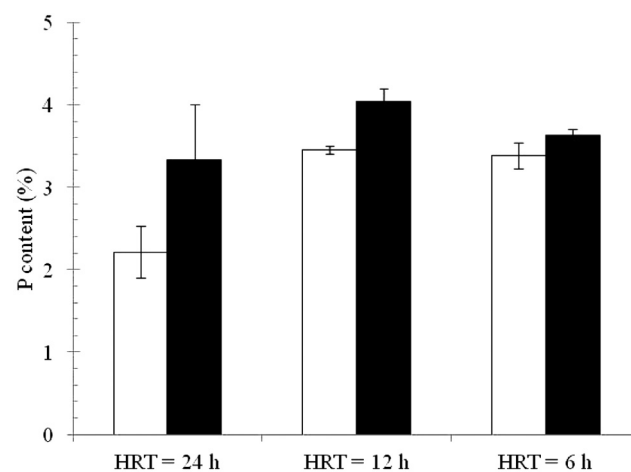


Fig. 6 – Sludge phosphorus content at the anaerobic (□) and aerobic (■) stages of each SBR cycle in the MSBR operated at the HRTs of 6, 12, and 24 h. Error bars represent one standard error of the mean ($n = 6$).

3.5. Implication for wastewater treatment in MSBRs and MBRs

For nutrient removal in wastewater that requires aerobic/anoxic/anaerobic environments, operating parameters and conditions such as SRT, HRT, volumetric exchange ratio and biomass concentration are crucial factors affecting treatment performance. In this study, at the same SRT (10 d) and fixed volumetric exchange ratio (50%), biomass concentration increased almost inversely proportional to the decrease in HRT (Fig. 2). The reduced HRT and corresponding increased volumetric organic loading rate provided more available organic carbon for denitrification (Grady et al., 2011; McCarty and Bremner, 1992; Zumft, 1997) resulting in higher nitrogen removal at the HRTs of 12 h and 6 h. However, higher MLSS concentrations could result in more aggregation of suspended cells and sludge floc formation (Huang et al., 2001), which limit oxygen and substrate (such as ammonia) diffusion, while the nitrifiers formed in clusters and in frequently close contact with each other in sludge flocs are more susceptible to inhibition at low dissolved oxygen concentrations (Mobarry et al., 1996; Ni et al., 2008). Therefore, further improvement of nitrogen removal was not observed at the HRT of 6 h (Fig. 3B). Coincidentally, similar levels of AOB and NOB were observed in the sludge operated at the HRTs of 6 h and 12 h (Fig. 4A and C).

The increasing P removal efficiency with decreasing HRT at the fixed SRT was possibly related to the higher biomass concentration that contributes higher hydrolysis and fermentation ability to supply VFAs for PAO growth (Grady et al., 2011). P removal can be also improved at higher biomass concentrations due to sludge-assisted adsorption and precipitation (Adam et al., 2003; De-Bashan and Bashan, 2004; Huang et al., 2010; Wang et al., 2013). However, the lower than expected content of sludge P at the HRT of 6 h (Fig. 6) suggested that P removal due to sludge loss and membrane cleaning, which was difficult to quantify, should be taken into account. More frequent maintenance was necessary due to rapid membrane fouling at the HRT of 6 h.

Contradictory to the theory that the effluent water quality is solely SRT dependent, the results suggest that effluent quality is also affected by HRT and resultant biomass concentration in MSBR operation. At the fixed SRT of 10 days in this study, the shorter HRT consistently led to better P removal. Unlike organic carbon and nitrogen removal processes, biological P removal process is mainly achieved by the growth of PAOs and sludge wastage (Monclús et al., 2010). A shorter anaerobic HRT was reported to be the key parameter for PAOs to obtain more PHA storage as the energy source that is needed for P release. Hence, as the anaerobic HRT decreased the P release rate was increased (Valentino et al., 2013). The study further confirmed that the incomplete P release at the short HRT did not negatively impact the P uptake under subsequent aerobic conditions (Fig. 5). The intermittent aeration in MSBR or general MBR operation also provides anaerobic and aerobic sequencing conditions with possibly more favorable change in oxidation-reduction potential during the transition between anaerobic and aerobic metabolism under higher biomass concentrations. As a result, the EBPR process could be enhanced under low HRTs or high biomass concentrations.

The intermittent feeding further creates a feast-famine environment to microorganisms, which could enhance the hydrophobic characteristic of sludge cells to resist starvation and facilitate biogranulation (Bossier and Verstraete, 1996; Liu et al., 2004; Watanabe et al., 2000). Coincidentally, the COD removal efficiency was also the highest at the shortest HRT (6 h) from this study. Hence, a selection of an appropriate range of SRT and HRT and their ratio along with anaerobic/aerobic sequencing is required to ensure that the highest organic and nutrient removal can be achieved in MSBR or general MBR operation with minimal fouling. The results suggest that it is preferred to maintain high biomass concentrations (e.g., >6000 mg/L) and high ratios of SRT/HRT (e.g., >40) in the MSBR or general MBR systems for maximum organic and nutrient removal.

4. Conclusions

The effect of HRT on MSBR performance at a fixed SRT (10 days) was determined in this study. The following conclusions were drawn from the data obtained:

- A decrease in HRT led to a proportionally inverse increase in biomass concentration in the MSBR.
- COD and phosphorus removal efficiencies in the MBSR were highest at the shortest HRT (6 h).
- When HRT was reduced from 24 to 12 h, nitrogen removal efficiency increased significantly, which was accompanied by an increase of nitrifying bacterial population. There was no improvement of nitrogen removal when HRT was further reduced to 6 h.
- Activated sludge wastewater treatment principles show that effluent COD is solely SRT dependent. Under the same anaerobic and aerobic SRTs and similar biochemical environment, the effluent nutrient (N and P) concentration is fixed as well. In this MSBR operation at the constant SRT of 10 days, however, the highest organic and nutrient removal efficiencies were achieved at the shortest HRT (6 h), suggesting that operating conditions at high biomass concentrations or high ratios of SRT/HRT are necessary for better wastewater treatment performance.

Appendix A. Supplementary data

Supplementary data related to this article can be found at <http://dx.doi.org/10.1016/j.watres.2014.01.046>.

REFERENCES

- Adam, C., Kraume, M., Gnirss, R., Lesjean, B., 2003. Membrane bioreactor configurations for enhanced biological phosphorus removal. *Water Sci. Technol. Water Supply* 3, 237–244.
- Amann, R.I., Binder, B.J., Olson, R.J., Chisholm, S.W., Devereux, R., Stahl, D.A., 1990. Combination of 16S rRNA-targeted oligonucleotide probes with flow cytometry for analyzing

- mixed microbial populations. *Appl. Environ. Microbiol.* 56 (6), 1919–1925.
- APHA (Ed.), 1998. *Standard Methods for the Examination of Water and Wastewater*, twentieth ed. American Public Health Association, Washington, DC.
- Bhatta, C.P., Matsuda, A., Kawasaki, K., Omori, D., 2004. Minimization of sludge production and stable operational condition of a submerged membrane activated sludge process. *Water Sci. Technol.* 50, 121–128.
- Bossier, P., Verstraete, W., 1996. Triggers for microbial aggregation in activated sludge? *Appl. Microbiol. Biotechnol.* 45 (1–2), 1–6.
- Charcosset, C., 2006. Membrane processes in biotechnology: an overview. *Biotechnol. Adv.* 24 (5), 482–492.
- Coats, E.R., Watkins, D.L., Brinkman, C.K., Loge, F.J., 2011. Effect of anaerobic HRT on biological phosphorus removal and the enrichment of phosphorus accumulating organisms. *Water Environ. Res.* 83 (5), 461–469.
- Contreras, E.M., Bertola, N.C., Giannuzzi, L., Zaritzky, N.E., 2002. A modified method to determine biomass concentration as COD in pure cultures and in activated sludge systems. *Water SA* 28 (4), 463–467.
- De-Bashan, L.E., Bashan, Y., 2004. Recent advances in removing phosphorus from wastewater and its future use as fertilizer (1997–2003). *Water Res.* 38 (19), 4222–4246.
- Dubber, D., Gray, N.F., 2011. The effect of anoxia and anaerobia on ciliate community in biological nutrient removal systems using laboratory-scale sequencing batch reactors (SBRs). *Water Res.* 45 (6), 2213–2226.
- Ersu, C.B., Ong, S.K., Arslankaya, E., Lee, Y.W., 2010. Impact of solids residence time on biological nutrient removal performance of membrane bioreactor. *Water Res.* 44 (10), 3192–3202.
- Fakhru'l-Razi, A., Pendashteh, A., Abidin, Z.Z., Abdullah, L.C., Biak, D.R.A., Madaeni, S.S., 2010. Application of membrane-coupled sequencing batch reactor for oilfield produced water recycle and beneficial re-use. *Bioresour. Technol.* 101 (18), 6942–6949.
- Fleischer, E.J., Broderick, T.A., Daigger, G.T., Fonseca, A.D., Holbrook, R.D., Murthy, S.N., 2005. Evaluation of membrane bioreactor process capabilities to meet stringent effluent nutrient discharge requirements. *Water Environ. Res.* 77 (2), 162–178.
- Galil, N.I., Jacob, L., 2009. Comparative characterization of biosolids from a membrane bioreactor and from a sequencing batch reactor. *Environ. Eng. Sci.* 26 (5), 1001–1008.
- Grady Jr., C.P.L., Daigger, G.T., Love, N.G., Filipe, C., 2011. *Biological Wastewater Treatment*, third ed. CRC Press, New York.
- Holakoo, L., Nakhla, G., Bassi, A.S., Yanful, E.K., 2007. Long term performance of MBR for biological nitrogen removal from synthetic municipal wastewater. *Chemosphere* 66 (5), 849–857.
- Huang, X., Gui, P., Qian, Y., 2001. Effect of sludge retention time on microbial behaviour in a submerged membrane bioreactor. *Process Biochem.* 36 (10), 1001–1006.
- Huang, X., Xiao, K., Shen, Y., 2010. Recent advances in membrane bioreactor technology for wastewater treatment in China. *Front. Environ. Sci. Eng. China* 4 (3), 245–271.
- Iversen, V., Koseoglu, H., Yigit, N.O., Drews, A., Kitis, M., Lesjean, B., Kraume, M., 2009. Impacts of membrane flux enhancers on activated sludge respiration and nutrient removal in MBRs. *Water Res.* 43 (3), 822–830.
- Juang, Y.C., Adav, S.S., Lee, D.J., Lai, J.Y., 2010. Influence of internal biofilm growth on residual permeability loss in aerobic granular membrane bioreactors. *Environ. Sci. Technol.* 44 (4), 1267–1273.
- Kaewsuk, J., Thorasampan, W., Thanuttamavong, M., Seo, G.T., 2010. Kinetic development and evaluation of membrane sequencing batch reactor (MSBR) with mixed cultures photosynthetic bacteria for dairy wastewater treatment. *J. Environ. Manag.* 91 (5), 1161–1168.
- Kang, I.J., Lee, C.H., Kim, K.J., 2003. Characteristics of microfiltration membranes in a membrane coupled sequencing batch reactor system. *Water Res.* 37 (5), 1192–1197.
- Lee, D.S., Jeon, C.O., Park, J.M., 2001. Biological nitrogen removal with enhanced phosphate uptake in a sequencing batch reactor using single sludge system. *Water Res.* 35 (16), 3968–3976.
- Liang, Z., Das, A., Beerman, D., Hu, Z., 2010. Biomass characteristics of two types of submerged membrane bioreactors for nitrogen removal from wastewater. *Water Res.* 44 (11), 3313–3320.
- Liang, Z., Hu, Z., 2012. Start-up performance evaluation of submerged membrane bioreactors using conventional activated sludge process and modified Luzack-Ettinger process. *J. Environ. Eng.* 138 (9), 932–939 (United States).
- Liu, G., Xu, X., Zhu, L., Xing, S., Chen, J., 2013. Biological nutrient removal in a continuous anaerobic-aerobic-anoxic process treating synthetic domestic wastewater. *Chem. Eng. J.* 225, 223–229.
- Liu, Y., Yang, S.F., Tay, J.H., Liu, Q.S., Qin, L., Li, Y., 2004. Cell hydrophobicity is a triggering force of biogranulation. *Enzyme Microb. Technol.* 34 (5), 371–379.
- Münch, E.v., Pollard, P.C., 1997. Measuring bacterial biomass-COD in wastewater containing particulate matter. *Water Res.* 31 (10), 2550–2556.
- McCarty, G.W., Bremner, J.M., 1992. Availability of organic carbon for denitrification of nitrate in subsoils. *Biol. Fertil. Soil.* 14 (3), 219–222.
- Metcalf, Eddy, 2003. *Wastewater Engineering: Treatment and Reuse*, fourth ed. McGraw-Hill Higher Education, New York.
- Mobarry, B.K., Wagner, M., Urbain, V., Rittmann, B.E., Stahl, D.A., 1996. Phylogenetic probes for analyzing abundance and spatial organization of nitrifying bacteria. *Appl. Environ. Microbiol.* 62 (6), 2156–2162.
- Monclús, H., Sipma, J., Ferrero, G., Rodriguez-Roda, I., Comas, J., 2010. Biological nutrient removal in an MBR treating municipal wastewater with special focus on biological phosphorus removal. *Bioresour. Technol.* 101 (11), 3984–3991.
- Moreno-Andrade, I., Buitrón, G., 2012. Comparison of the performance of membrane and conventional sequencing batch reactors degrading 4-chlorophenol. *Water Air Soil Pollut.* 223 (5), 2083–2091.
- Mutamim, N.S.A., Noor, Z.Z., Hassan, M.A.A., Olsson, G., 2012. Application of membrane bioreactor technology in treating high strength industrial wastewater: a performance review. *Desalination* 305, 1–11.
- Ni, B.J., Yu, H.Q., Sun, Y.J., 2008. Modeling simultaneous autotrophic and heterotrophic growth in aerobic granules. *Water Res.* 42 (6–7), 1583–1594.
- Qi, R., Yu, T., Li, Z., Li, D., Mino, T., Shoji, T., Fujie, K., Yang, M., 2012. Comparison of conventional and inverted A2/O processes: phosphorus release and uptake behaviors. *J. Environ. Sci.* 24 (4), 571–578.
- Regan, J.M., Harrington, G.W., Noguera, D.R., 2002. Ammonia- and nitrite-oxidizing bacterial communities in a pilot-scale chloraminated drinking water distribution system. *Appl. Environ. Microbiol.* 68 (1), 73–81.
- Rosenberger, S., Laabs, C., Lesjean, B., Gnirss, R., Amy, G., Jekel, M., Schrotter, J.C., 2006. Impact of colloidal and soluble organic material on membrane performance in membrane bioreactors for municipal wastewater treatment. *Water Res.* 40 (4), 710–720.
- Scheumann, R., Kraume, M., 2009. Influence of hydraulic retention time on the operation of a submerged membrane

- sequencing batch reactor (SM-SBR) for the treatment of greywater. *Desalination* 246 (1–3), 444–451.
- Serrano, D., Suárez, S., Lema, J.M., Omil, F., 2011. Removal of persistent pharmaceutical micropollutants from sewage by addition of PAC in a sequential membrane bioreactor. *Water Res.* 45 (16), 5323–5333.
- Shannon, M.A., Bohn, P.W., Elimelech, M., Georgiadis, J.G., Mariñas, B.J., Mayes, A.M., 2008. Science and technology for water purification in the coming decades. *Nature* 452 (7185), 301–310.
- Siripong, S., Rittmann, B.E., 2007. Diversity study of nitrifying bacteria in full-scale municipal wastewater treatment plants. *Water Res.* 41 (5), 1110–1120.
- Tay, J.H., Luhai Zeng, J., Sun, D.D., 2003. Effects of hydraulic retention time on system performance of a submerged membrane bioreactor. *Sep. Sci. Technol.* 38 (4), 851–868.
- Tu, X., Zhang, S., Xu, L., Zhang, M., Zhu, J., 2010. Performance and fouling characteristics in a membrane sequence batch reactor (MSBR) system coupled with aerobic granular sludge. *Desalination* 261 (1–2), 191–196.
- Valentino, F., Brusca, A.A., Beccari, M., Nuzzo, A., Zanaroli, G., Majone, M., 2013. Start up of biological sequencing batch reactor (SBR) and short-term biomass acclimation for polyhydroxyalkanoates production. *J. Chem. Technol. Biotechnol.* 88 (2), 261–270.
- Vargas, A., Moreno-Andrade, I., Buitrón, G., 2008. Controlled backwashing in a membrane sequencing batch reactor used for toxic wastewater treatment. *J. Membr. Sci.* 320 (1–2), 185–190.
- Wachtmeister, A., Kuba, T., Van Loosdrecht, M.C.M., Heijnen, J.J., 1997. A sludge characterization assay for aerobic and denitrifying phosphorus removing sludge. *Water Res.* 31 (3), 471–478.
- Wagner, M., Rath, G., Amann, R., Koops, H.P., Schleifer, K.H., 1995. In situ identification of ammonia-oxidizing bacteria. *Syst. Appl. Microbiol.* 18 (2), 251–264.
- Wang, Y., Guo, G., Wang, H., Stephenson, T., Guo, J., Ye, L., 2013. Long-term impact of anaerobic reaction time on the performance and granular characteristics of granular denitrifying biological phosphorus removal systems. *Water Res.* 47 (14), 5326–5337.
- Watanabe, K., Miyashita, M., Harayama, S., 2000. Starvation improves survival of bacteria introduced into activated sludge. *Appl. Environ. Microbiol.* 66 (9), 3905–3910.
- Wu, Q., Bishop, P.L., Keener, T.C., 2006. Biological phosphate uptake and release: effect of pH and magnesium ions. *Water Environ. Res.* 78 (2), 196–201.
- Yoon, S.H., Kim, H.S., Yeom, I.T., 2004. The optimum operational condition of membrane bioreactor (MBR): cost estimation of aeration and sludge treatment. *Water Res.* 38 (1), 37–46.
- Zumft, W.G., 1997. Cell biology and molecular basis of denitrification? *Microbiol. Mol. Biol. Rev.* 61 (4), 533–616.